UNIVERSITÀ DEGLI STUDI DI CATANIA

DIPARTIMENTO DI MEDICINA CLINICA E SPERIMENTALE

Dottorato di ricerca in Biomedicina Traslazionale - XXXI ciclo

MATILDE CIRNIGLIARO

Profiling of circulating microRNAs in body fluids from Autism Spectrum Disorder patients

Doctoral thesis

Supervisor:

PROF. MICHELE PURRELLO

Coordinator:

PROF. LORENZO MALATINO

2018

"... The willingness to risk failure is an essential component of most successful initiatives. The unwillingness to face the risks of failure -or an excessive zeal to avoid all risks- is, in the end, an acceptance of mediocrity and an abdication of leadership. To use a sports metaphor, if you do not come to bat at all, or, when at bat, wait hopefully for a walk, you cannot hit a home run. At best, you can get to first base. Major leaguers can decide to play in the minor leagues, and they may have more hits and fewer failures there, but their impact on the game and on society would be very much diminished. The risk of failure is intrinsic to significant accomplishment. Even the great Babe Ruth struck out almost twice as often as he hit home runs. Successful change depends on experimentation with uncertain results. A willingness to occupy new ground always involves the risk of losing your footing along the way. We must also beware of raising the flag of failure too quickly. The world too often calls it failure if we do not immediately reach our goals; true failure lies, rather, in giving up on our goals. ..."

Shapiro HT. The willingness to risk failure. Science. 1990;250(4981):609. doi: 10.1126/science.250.4981.609.

Abstract

Autism Spectrum Disorder (ASD) is the name for a heterogeneous group of complex neurodevelopmental conditions, which are clinically defined by: (1) defects in social interaction and communication; (2) fixed interests and repetitive behaviors. Given its prevalence and social impact, ASD is drawing much interest.

Molecular basis of ASD is heterogeneous and only partially known. In particular, ASD is genetically highly heterogeneous. ASD-associated variants have been characterized in hundreds of genes and separate transcriptome studies have identified points of convergence among these loci, proving that common biological processes play an essential role in this disorder. However, no common ASD-associated variants with large effect size, that would be appropriate for its molecular diagnosis, have been identified to date, and therefore, diagnosis just relies on clinical assessment and confirmation. Many factors, including disorders comorbid with ASD, like Tourette syndrome (TS), complicate ASD behavior-based diagnosis and make it vulnerable to bias.

Since their identification and characterization in serum and plasma of humans and other animals, extracellular microRNAs (miRNAs) have attracted researchers for their potential as new non-invasive tools for diagnosis, prognosis, and treatment evaluation of many human diseases and disorders. Circulating miRNAs can be detected, associated with extracellular vesicles, like exosomes and macrovesicles, or conjugated to RNA-binding proteins and lipoproteins, in all mammalian body fluids, from serum to saliva. Stability and general consistency of levels among individuals, along with the existence of specific expression signatures in association with both physiological and pathological conditions, make circulating miRNAs appropriate biomarkers: their convenient features also suggest the prospective alternative use of liquid biopsies as sources of biomarkers in the clinic.

To further investigate ASD heterogeneous etiology and to identify potential biomarkers to support its precise (even differential) diagnosis, we used TLDA (TaqMan Low Density Array) technology to profile serum miRNAs from ASD, TS, and TS+ASD patients and NCs (unaffected controls). Through validation assays, we demonstrated that miR-140-3p is upregulated in ASD vs: NC, TS, and TS+ASD. We found that ΔCt values for miR-140-3p and YGTSS (Yale Global Tic Severity Scale) scores are positively correlated and show a linear relationship. Our network functional analysis showed that nodes controlled by miR-140-3p, especially CD38 (CD38 molecule) and NRIP1 (nuclear receptor interacting protein 1) that are its validated targets, are involved in processes convergingly dysregulated in ASD, such as synaptic plasticity, immune response, and chromatin binding. Through biomarker analysis, we proved that serum miR-140-3p can discriminate among (1) ASD and NC, (2) ASD and TS, and (3) ASD and TS+ASD, showing that it could be particularly useful to strengthen the behavior-based diagnosis of either ASD or TS+ASD, which can be challenging in some clinical cases.

Among all body fluids, saliva represents the most accessible and complete source of different types of molecules that could reflect genetic, epigenetic, environmental, metabolic, emotional, and behavioral alterations in ASD. For this reason, we also used NanoString nCounter technology to profile supernatant saliva circulating miRNAs from ASD patients and NCs. Through validation assays, we demonstrated that both miR-29a-3p and miR-141-3p are upregulated in ASD saliva compared to NC one. We observed that ΔCt values for both miRNAs are correlated with overlapping neuropsychiatric scores evaluating ASD defects in social interaction and verbal communication. Target genes of miR-29a-3p and miR-141-3p, in particular the well-documented ASD susceptibility gene PTEN (phosphatase and tensin homolog), represent main components and regulators of pathways and processes known to be dysregulated in ASD (i.e., PI3K-Akt-mTOR signaling pathway, neuronal differentiation, synaptic function, and methionine metabolism). Through biomarker performance evaluation, we proved that saliva miR-29a-3p and miR-141-3p when used in combination could be useful and non-invasive tools for discriminating ASD patients from NCs. In particular, these miRNAs could be used as supportive means for the recognition of ASD verbal and social defects.

Overall, our findings suggest that profiling of circulating microRNAs in body fluids can represent an easy and innovative approach to address and solve important biomedical issues, such as the need for molecular biomarkers and the necessity to further investigate neurodevelopmental and psychiatric disorders through more accessible patient biopsies. In fact, through the characterization of circulating miRNAs in serum and saliva from ASD patients, we identified three miRNAs that could facilitate ASD clinical assessment and confirmation and that are worth being further investigated for their potential central role in neurodevelopment.

Table of contents

List of Figures and Tables

Chapter 1. Autism Spectrum Disorder

1.1. Autism Spectrum Disorder (ASD): clinical definition and epidemiology

Autism Spectrum Disorder (ASD) is the name for a heterogeneous group of complex neurodevelopmental conditions, which are clinically defined by: (1) defects in social interaction and communication; (2) fixed interests and repetitive behaviors. Typically, ASD symptoms become fully manifest during school age and have a lifelong impact on everyday functions (American Psychiatric Association, 2013).

The broadening of the autism concept and the resulting changes in ASD categorization have increased ASD awareness and improved its diagnostic surveillance in health and educational care. This has led to an alarming rise in the number of milder cases of ASD, without co-occurring intellectual disability, in developed countries around the world. Prevalence estimates under new ASD classification (American Psychiatric Association, 2013) are not available yet.

According to the Centers for Disease Control and Prevention (CDC) surveillance, approximately 1.5% of eight-year-old US children were affected by ASD in 2012: it clearly represents a major public health concern. In addition, 1% of English adults had ASD in 2007 (Lyall et al., 2016). Recently, it has been reported that ASD affects one in sixty-eight US children and that four males suffer from ASD for every female (Christensen et al., 2016).

Comorbid neuropsychiatric and neurodevelopmental disorders contribute to ASD impairment, being common (70.8%) and frequently multiple (57%) in ASD children (Simonoff et al., 2008). Such conditions include social anxiety disorder (simultaneously diagnosed in 29.2% of ASD cases), attention-deficit/hyperactivity disorder (ADHD) (in 28.2% of ASD cases), oppositional defiant disorder (ODD) (in 28.1% of ASD cases), chronic tic disorder (in 9% of ASD cases), obsessive-compulsive disorder (OCD) (in 8.2% of ASD cases), and Tourette syndrome (TS) (in 4.8% of ASD cases) (Figure 1.1) (Simonoff et al., 2008).

Prevalence of *DSM-IV* Disorders

Disorder	3-Mo Point Prevalence/100	95% CI
Any disorder	70.8	58.2–83.4
Any main disorder[a]	62.8	49.8–75.9
Any emotional disorder[b]	44.4	30.2–58.7
Any anxiety or phobic disorders[c]	41.9	26.8–57.0
Generalized anxiety disorder	13.4	0–27.4
Separation anxiety disorder	0.5	0–1.6
Panic disorder	10.1	0–24.8
Agoraphobia	7.9	3.0–12.9
Social anxiety disorder	29.2	13.2–45.1
Simple phobia	8.5	2.8–14.1
Obsessive-compulsive disorder	8.2	3.2–13.1
Any depressive disorder	1.4	0–3.0
Major depressive disorder	0.9	0–2.3
Dysthymic disorder	0.5	0–1.4
Oppositional or conduct disorder	30.0	14.9–45.0
Oppositional defiant disorder	28.1	13.9–42.2
Conduct disorder	3.2	0–7.1
Attention-deficit/hyperactivity disorder	28.2	13.3–43.0
Other disorders[d]	24.7	14.1–35.3
Enuresis	11.0	4.1–17.7
Encopresis	6.6	1.8–11.4
Tourette syndrome	4.8	0.1–9.5
Chronic tic disorder	9.0	3.3–14.6
Trichotillomania	3.9	0–10.3

Note: CIs = confidence intervals.

[a]Includes attention-deficit/hyperactivity disorder, oppositional and conduct disorders, and any emotional disorder.

[b]Includes all anxiety disorders, phobias, and mood disorders.

[c]Includes anxiety disorders, panic disorder, phobias, and obsessive-compulsive disorder.

[d]Includes Tourette syndrome, chronic tics, trichotillomania, enuresis, and encopresis.

Figure 1. 1. Weighted 3-month prevalence rates for other DSM-IV diagnoses in comorbidity with ASD in a British cohort of 112 ASD patients (Simonoff et al., 2008).

1.2. Heterogeneity of ASD etiology: genetic, epigenetic, and environmental factors

The exact etiology of ASD still remains unknown. Strong evidence suggests that ASD may arise from genetic, epigenetic, and environmental factors (Vorstman et al., 2017; Nardone and Elliott, 2016; Sun et al., 2016; Abdolmaleky et al., 2015).

ASD is genetically highly heterogeneous. Both inherited and de novo ASD-associated variants have been characterized in hundreds of genes (Figure 1.2). Separate transcriptome studies, aiming to identify points of convergence among these heterogeneous ASD-associated loci, show that common biological processes (discussed in Sections 1.3-4) play an essential role in this disorder. Much about ASD genetic origin and modes of inheritance has been understood through the investigation of rare medical genetic syndromes with high penetrance for ASD (Figure 1.2) (de la Torre-Ubieta et al., 2016).

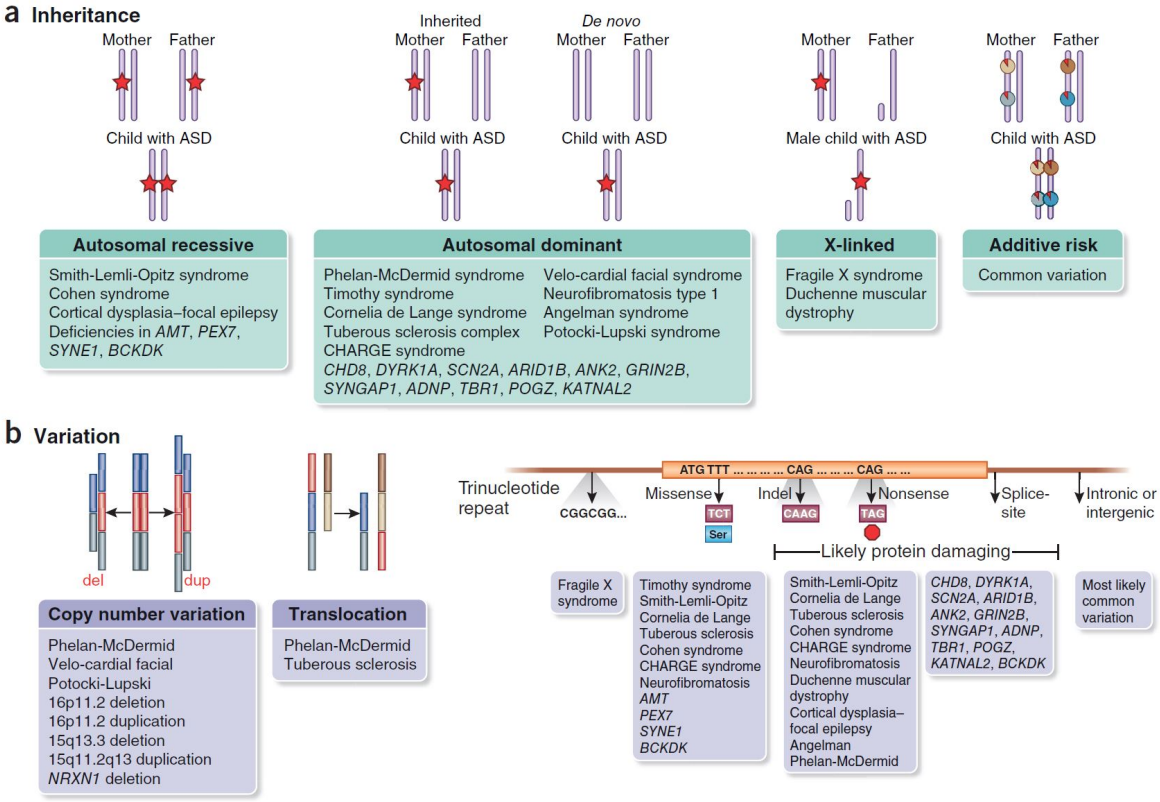

Figure 1. 2. Insight into the complex genetic architecture of ASD: lessons from rare syndromes with known genetic etiology and high incidence of autism and from genes recently identified to be associated with autism (de la Torre-Ubieta et al., 2016). *Panel (A) shows inheritance patterns for syndromes and genes, whereas panel (B) reports all the different types of genetic variation observed for those.*

Both inherited and de novo rare genetic variants (Figure 1.2A, left, middle-left, and middle-right panels) can be detected in 10-30% of ASD cases (Vorstman et al., 2017). Single common inherited variants (Figure 1.2A, right panel) can be found in approximately 1.1-1.2% of ASD cases; when considered cumulatively, these can explain 15-50% ASD cases (Vorstman et al., 2017). Therefore, at the two extremes on the allelic spectrum (Geschwind, 2011), syndromic forms of ASD represent rare exceptional cases associated to variants with large effect sizes, whereas common variants with small to moderate effect sizes increase susceptibility to ASD, without being individually sufficient to be causal (Figure 1.3). However, no common risk loci for ASD, that would be appropriate for its molecular diagnosis, have been identified to date (Figure 1.3) (Vorstman et al., 2017).

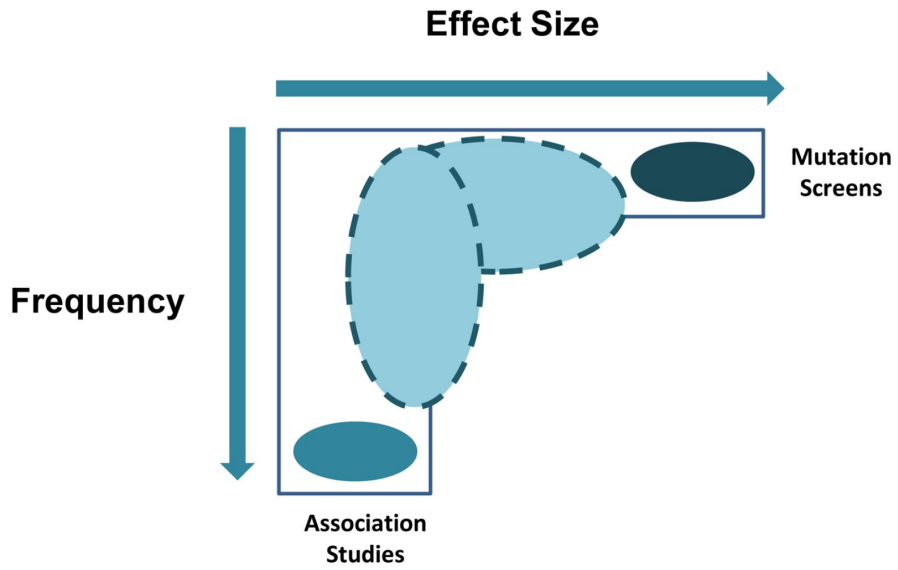

Figure 1. 3. Effect sizes of rare and common variants associated with ASD (Geschwind, 2011). *Association studies have helped the identification of SNPs associated with ASD with small to modest effect sizes; mutation screens and CNV studies, as well as the investigation of syndromic forms of ASD, have aided the discovery of rare variants with large effect sizes. Lower frequency intermediate effect alleles (depicted as ovals with dotted lines) still remain unexplored, and at the moment, there is no evidence supporting the existence of common alleles of large effect for ASD, those that could be efficiently used for its molecular diagnosis.*

Several analyses performed in post-mortem brain and blood samples demonstrate the involvement of DNA methylation alterations in the etiology of ASD (Abdolmaleky et al., 2015). Recent histone acetylome analysis has identified widespread and stable histone acetylation changes in syndromic and idiopathic ASD prefrontal and temporal cortical regions, that are both involved in social cognition, proving that this disorder may also arise from histone modifications: it is worth noting that those histone acetylation changes are over-represented near ASD gene candidates (Sun et al., 2016).

Moreover, consistent evidences indicate that ASD-linked epigenetic and immune dysregulation are causally dependent. In fact, both MIA (maternal immune activation) and maternal autoimmune diseases are associated with ASD and can be considered as *in utero* environmental insults, for the developing fetus, that, similarly to other known determinants like maternal age, diet, stress, depression, smoking, and serum folate levels (Abdolmaleky et al., 2015), have a strong impact on epigenetic mechanisms such as DNA methylation and histone acetylation (Nardone and Elliott, 2016).

Finally, many prenatal and perinatal factors, immune factors, maternal dietary and lifestyle factors, and environmental chemicals have been proposed with some level of converging evidence as candidate risk factors for ASD over the past decade (Lyall et al., 2016).

1.3. Multiple levels of ASD alterations

Neurotypical behavioral and cognitive functioning is the result of normal brain development, a complex phenomenon harmonized and finely regulated at multiple levels, requiring the generation, migration, and positioning of the correct number and type of cells, the growth and targeting of neuronal processes, and the formation of the precise number and type of synapses (de la Torre-Ubieta et al., 2016). Several molecular, cellular, and circuital alterations of all of these mechanisms have been identified in ASD (Figure 1.4) (de la Torre-Ubieta et al., 2016).

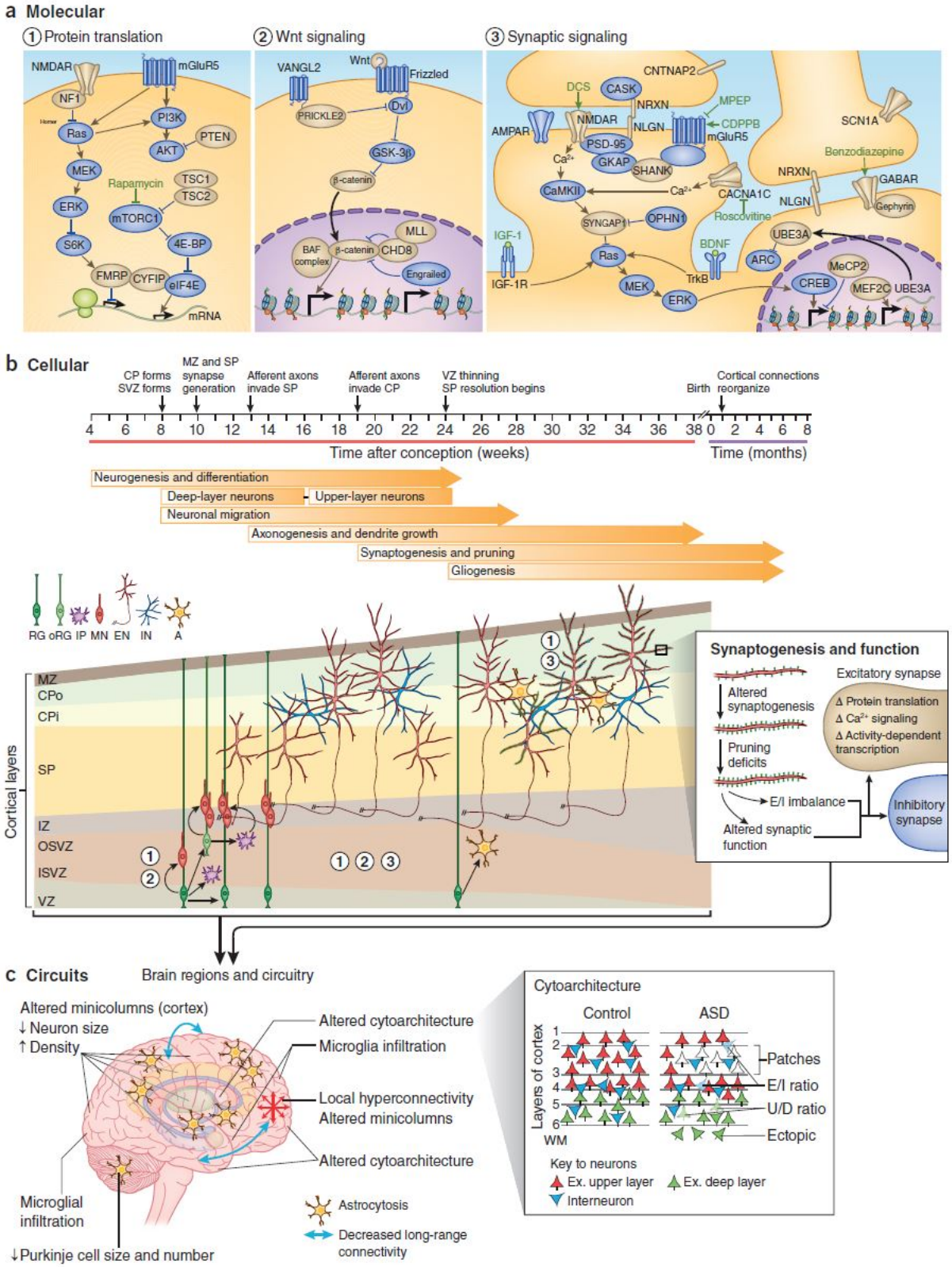

Figure 1. 4. Multiple levels of alteration in ASD (de la Torre-Ubieta et al., 2016). *A typical social and cognitive functioning is the result of normal brain development, a complex phenomenon that is finely regulated at the molecular (A), cellular (B), and circuital (C) levels. Several alterations of mechanisms at all of these levels have been identified in ASD. (A) Genes within these developmental pathways for which there is genetic evidence for a link to ASD are depicted in gold. (B) Cellular events (and*

corresponding pathways, see numbers) responsible for altered fetal cortical development and synaptic function observed in ASD. RG, radial glia; oRG, outer radial glia; IP, intermediate progenitor; MN, migrating neuron; EN, excitatory neuron; IN, interneuron; A, astrocyte; VZ, ventricular zone; ISVZ, inner subventricular zone; OSVZ, outer subventricular zone; IZ, intermediate zone; SP, subplate; CPi, inner cortical plate; Cpo, outer cortical plate; MZ, marginal zone. (C) Altered neuroanatomical phenotypes in ASD, regarding brain growth, cortical cytoarchitecture, and brain connectivity, emerge from defective neurogenesis, differentiation, migration, patterning, and synaptogenesis, in combination with reactive microglia infiltration and astrocytosis. E/I, excitatory or inhibitory neuron; U/D, upper-layer or deep-layer neuron; WM, white matter.

All the heterogeneous ASD susceptibility genes converge in a small number of commonly dysregulated biological processes and pathways, like synaptic function (including long-term potentiation and calcium signaling), immune and inflammatory responses, signaling by WNT, NOTCH, and SWI/SNF (switch/sucrose non-fermentable) and NCOR (nuclear receptor corepressor) complexes, and PI3K (phosphatidylinositol-4,5-bisphosphate 3-kinase)/mTOR (mammalian target of rapamycin) signaling (Figure 1.4A) (Levitt and Campbell, 2009; Chen et al., 2014; Voineagu and Eapen, 2013; Gokoolparsadh et al., 2016; Ansel et al., 2017). Resultant micro- and macro-structural and functional abnormalities, which emerge during brain development in ASD, create the dysfunction of neural networks involved in socio-emotional processing (Vissers et al., 2012; Maximo et al., 2014; Kern et al., 2015; Ecker, 2017).

Neuroanatomical studies prove that ASD is accompanied by differences in brain anatomy, functioning and connectivity (Figure 1.4C), highly variable depending on stage of development and biological sex. Between the age of 2–4 years, the brain of children with ASD is enlarged in total volume: this early brain overgrowth may slow down or arrest during early and late childhood, and then, turn into an accelerated decline in whole brain volume by late adolescence and early adulthood. Perturbations in the development of cortical white matter and corpus callosum may be already present in infants with ASD scanned at 6 months of age (Ecker, 2017). Histological studies show differences in neuronal density across cortical layers (Figure 1.4B-C), suggesting abnormalities in the cellular mechanisms of migration and apoptosis driving cortical development in ASD, which may contribute to the observed early brain overgrowth.

Evidence of ASD cortical underconnectivity (typically in adolescence and adulthood) and overconnectivity (in childhood) involving multiple brain networks have been reported (Figure 1.4C). Long-range underconnectivity is a consistent finding in ASD, while results on short-range disrupted connectivity are variable, depending on the areas of the brain examined (Vissers et al., 2012; Maximo et al., 2014). The severity of the disorder is correlated with both kind of disrupted functional brain connectivity, suggesting that overconnectivity, despite being hyperspecialized, is inefficient in any case. Long-range connectivity is responsible for conscious processing, central coherence, and information processing and integration: so, its impairment may contribute to all the cognitive and behavioral difficulties typical of ASD (Vissers et al., 2012; Maximo et al., 2014). This form of neuropathology

observed in ASD has also been found in ADHD and TS, which are known to share similar symptomatology with ASD (Kern et al., 2015). Atypical effective connectivity (Maximo et al., 2014) and impaired anatomical connectivity (Vissers et al., 2012; Maximo et al., 2014) in ASD have also been explored.

Many individual components of the nervous system have been independently associated to ASD: fronto-temporal and fronto-parietal regions, limbic brain regions, the fronto-striatal circuitry, and the cerebellum (Figure 1.4C). Atypical neural structures in ASD, such as the amygdala, overlap with regions that are integral parts of the so-called social and emotional brain, involved in social cognition and emotional processing (Ecker, 2017).

1.4. Converging molecular mechanisms in ASD

ASD is a highly hereditable condition characterized by marked genetic heterogeneity. Therefore, much effort has been put in large transcriptomic studies on post-mortem brain samples, aiming to discover, through the WGCNA (weighted gene co-expression network analysis) approach, if this myriad of genetic or environmental risk factors convergingly perturbed common underlying molecular pathways important for brain development (Voineagu et al., 2011; Parikshak et al., 2016; Wu et al., 2016).

These studies proved that regional patterns of gene expression that typically distinguish frontal and temporal cortex in normal brain are significantly attenuated in the ASD brain, suggesting alterations in cortical patterning (Voineagu et al., 2011; Parikshak et al., 2016). A genetically defined subtype of ASD, the chromosome 15q11.2-13.1 duplication syndrome (dup15q) endophenotype, shares the core transcriptomic signature observed in idiopathic ASD (Parikshak et al., 2016).

Through WGCNA approach, two main modules of co-expressed genes were found to be associated with ASD (Figure 1.5): (i) a downregulated neuronal module, enriched for known autism susceptibility genes and neuronal genes involved in synaptic function, and (ii) an upregulated module enriched for genes related to inflammatory and immune pathways and glial markers and function (Voineagu et al., 2011; Parikshak et al., 2016; Wu et al., 2016).

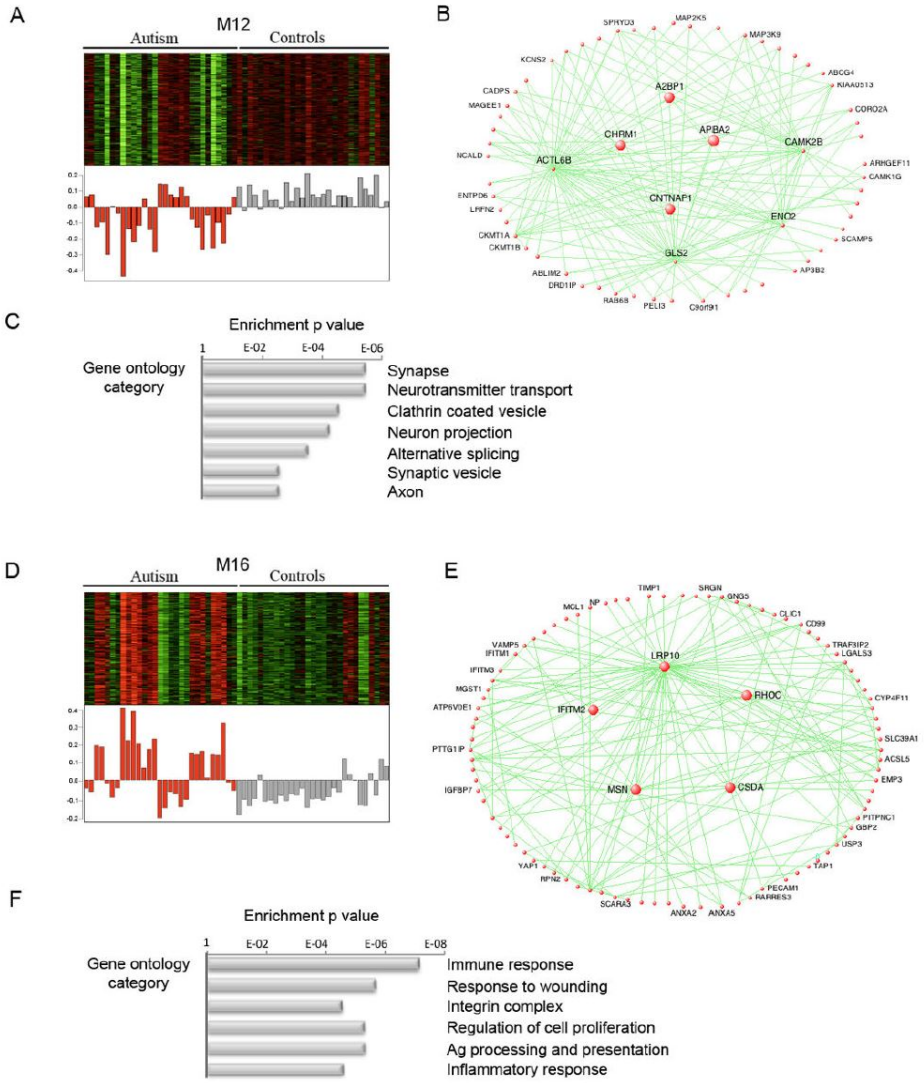

Figure 1. 5. Two main gene co-expression modules are associated with ASD (Voineagu et al., 2011). *Panels (A), (B), and (C) refer to the neuronal module, while panels (D), (E), and (F) represent the immune-glial one. For each ASD-associated module, heatmap of genes belonging to the module, corresponding module eigengene values across all samples, visualization of the module, and relevant gene ontology categories enriched in it are reported.*

Microglial and synaptic modules exhibit significant anticorrelation (Parikshak et al., 2016). The neuronal module is enriched for genetically associated variants, whereas the immune-glial module shows no enrichment for those, indicating a less pronounced genetic component for this immune upregulation, that is most likely either a secondary phenomenon or caused by environmental factors (Voineagu et al., 2011).

Collectively, these studies confirmed that transcriptional dysregulation is an important underlying mechanism of neuronal dysfunction in ASD and proved that diverse genetic perturbations can lead to phenotypic convergence at multiple biological levels in this complex neurodevelopmental disorder. These findings also provided a first molecular neuropathological basis for ASD. Since immune

molecules and cells such as microglia play a role in synaptic development and function, the observed immune up-modulation could be related to abnormal ongoing plasticity in ASD brain, a hypothesis supported by the striking attenuation of transcriptional differences observed between frontal and temporal cortex in ASD (Voineagu et al., 2011).

1.5. ASD behavior-based diagnosis

Since common risk loci for ASD have not been proposed yet (Vorstman et al., 2017), a molecular test for non-syndromic ASD is not available and diagnosis relies on clinical assessment and confirmation. Clinical diagnosis of ASD depends on behavioral observations, according to the Diagnostic and Statistical Manual of Mental Disorders (5th ed.; DSM–5; American Psychiatric Association, 2013) (Figure 1.6).

Panel 1: DSM-5 diagnostic criteria for autism spectrum disorder 299.00 (F84.0)

A) Persistent deficits in social communication and social interaction across multiple contexts, as manifested by the following, currently or by history (examples are illustrative, not exhaustive):

1 Deficits in social-emotional reciprocity, ranging, for example, from abnormal social approach and failure of normal back-and-forth conversation; to reduced sharing of interests, emotions, or affect; to failure to initiate or respond to social interactions.
2 Deficits in non-verbal communicative behaviours used for social interaction, ranging, for example, from poorly integrated verbal and non-verbal communication; to abnormalities in eye contact and body language or deficits in understanding and use of gestures; to a total lack of facial expressions and non-verbal communication.
3 Deficits in developing, maintaining, and understanding relationships, ranging, for example, from difficulties adjusting behaviour to suit various social contexts; to difficulties in sharing imaginative play or in making friends; to absence of interest in peers.

B) Restricted, repetitive patterns of behaviour, interests, or activities, as manifested by at least two of the following, currently or by history (examples are illustrative, not exhaustive):

1 Stereotyped or repetitive motor movements, use of objects, or speech (eg, simple motor stereotypies, lining up toys or flipping objects, echolalia, idiosyncratic phrases).
2 Insistence on sameness, inflexible adherence to routines, or ritualised patterns of verbal or non-verbal behaviour (eg, extreme distress at small changes, difficulties with transitions, rigid thinking patterns, greeting rituals, need to take same route or eat same food every day).
3 Highly restricted, fixated interests that are abnormal in intensity or focus (eg, strong attachment to or preoccupation with unusual objects, excessively circumscribed or perseverative interests).
4 Hyper- or hyporeactivity to sensory input or unusual interest in sensory aspects of the environment (eg, apparent indifference to pain/temperature, adverse response to specific sounds or textures, excessive smelling or touching of objects, visual fascination with lights or movement).

C) Symptoms must be present in the early developmental period (but may not become fully manifest until social demands exceed limited capacities, or may be masked by learned strategies in later life).

D) Symptoms cause clinically significant impairment in social, occupational, or other important areas of current functioning.

E) These disturbances are not better explained by intellectual disability (intellectual developmental disorder) or global developmental delay. Intellectual disability and autism spectrum disorder frequently co-occur; to make comorbid diagnoses of autism spectrum disorder and intellectual disability, social communication should be below that expected for general developmental level.

Note: Individuals with a well-established DSM-IV diagnosis of autistic disorder, Asperger's disorder, or pervasive developmental disorder not otherwise specified should be given the diagnosis of autism spectrum disorder. Individuals who have marked deficits in social communication, but whose symptoms do not otherwise meet criteria for autism spectrum disorder, should be evaluated for social (pragmatic) communication disorder.

Specify if:

- With or without accompanying intellectual impairment
- With or without accompanying language impairment
- Associated with a known medical or genetic condition or environmental factor
- Associated with another neurodevelopmental, mental, or behavioural disorder
- With catatonia (refer to the criteria for catatonia associated with another mental disorder)

Reproduced from the *Diagnostic and Statistical Manual of Mental Disorders*, fifth edition (DSM-5),[14] by permission of the American Psychiatric Association.

Figure 1. 6. Panel reporting DSM-5 diagnostic criteria for ASD (Constantino and Charman, 2016).

Accepted gold standard tools for diagnostic assessment of ASD are the Autism Diagnostic Observation Schedule (ADOS) and the Autism Diagnostic Interview-Revised (ADI-R) (Falkmer et al., 2013). Considering the clinical variation and etiological heterogeneity of ASD, a precise diagnosis can be very difficult. Behavior-based ASD gold standard diagnosis is a challenging process because: (i) it depends on the expertise of a multi-disciplinary team and on the quality of reports provided by caregivers and teachers; (ii) it is based on the direct observation of behavioral features and traits that are continuously, not categorically, distributed in the general population; (iii) it can be complicated by the wide range of ASD causes and presentations (Figure 1.7) and by its association with comorbid disorders (Figure 1.1) (Constantino and Charman, 2016); (iv) it depends on the use of different information gathering tools,

vulnerable to subjectivity and interpretive bias and often inappropriate to represent age, biological sex, and socio-cultural setting diversity of patients (Falkmer et al., 2013; Constantino and Charman, 2016; Varma and Iskandar, 2014).

	Social communication	Restricted, repetitive behaviours
Level 3 "Requiring very substantial support"	Severe deficits in verbal and non-verbal social communication skills cause severe impairments in functioning, very limited initiation of social interactions, and minimal response to social overtures from others. For example, a person with few words of intelligible speech who rarely initiates interaction and, when he or she does, makes unusual approaches to meet needs only and responds to only very direct social approaches.	Inflexibility of behaviour, extreme difficulty coping with change, or other restricted/repetitive behaviours markedly interfere with functioning in all spheres. Great distress/ difficulty changing focus or action.
Level 2 "Requiring substantial support"	Marked deficits in verbal and non-verbal social communication skills; social impairments apparent even with supports in place; limited initiation of social interactions; and reduced or abnormal responses to social overtures from others. For example, a person who speaks simple sentences, whose interaction is limited to narrow special interests, and who has markedly odd non-verbal communication.	Inflexibility of behaviour, difficulty coping with change or other restricted/repetitive behaviours appear frequently enough to be obvious to the casual observer and interfere with functioning in a variety of contexts. Distress and/or difficulty changing focus or action.
Level 1 "Requiring support"	Without supports in place, deficits in social communication cause noticeable impairments. Difficulty initiating social interactions, and clear examples of atypical or unsuccessful response to social overtures from others. May appear to have decreased interest in social interactions. For example, a person who is able to speak in full sentences and engages in communication but whose to-and-fro conversation with others fails, and whose attempts to make friends are odd and typically unsuccessful.	Inflexibility of behaviour causes significant interference with functioning in one or more contexts. Difficulty switching between activities. Problems of organisation and planning hamper independence.

Reproduced from the *Diagnostic and Statistical Manual of Mental Disorders*, fifth edition (DSM-5),[14] by permission of the American Psychiatric Association.

Table: **Severity specifiers for the characterisation of variation in adaptive functioning in autism spectrum disorder**

Figure 1. 7. Panel reporting severity specifiers for each DSM-5 diagnostic criterion for ASD (Constantino and Charman, 2016). *Severity specifiers translate the effect of symptoms in each criterion domain (social interaction and communication, fixed interests and repetitive behaviors) onto three broad categories of adaptive functioning, reflecting the level of support that an ASD patient would require.*

Therefore, there is an urgent need for potential ASD biomarkers that could support clinical discrimination of patients. The identification of ASD biomarkers could provide complementary and supportive means for a simpler, faster, and unbiased diagnosis and insight into ASD heterogeneous molecular basis.

1.6. References

Abdolmaleky HM, Zhou JR, Thiagalingam S. An update on the epigenetics of psychotic diseases and autism. Epigenomics 2015;7(3):427-49.

American Psychiatric Association. Diagnostic and statistical manual of mental disorders. 5th ed. Washington, DC: American Psychiatric Association; 2013.

Ansel A, Rosenzweig JP, Zisman PD, Melamed M, Gesundheit B. Variation in Gene Expression in Autism Spectrum Disorders: An Extensive Review of Transcriptomic Studies. Front Neurosci. 2017;10:601.

Chen J, Alberts I, Li X. Dysregulation of the IGF-I/PI3K/AKT/mTOR signaling pathway in autism spectrum disorders. Int J Dev Neurosci. 2014; 35:35-41. doi: 10.1016/j.ijdevneu.2014.03.006.

Christensen DL, Baio J, Van Naarden Braun K, Bilder D, Charles J, Constantino JN, Daniels J, Durkin MS, Fitzgerald RT, Kurzius-Spencer M, Lee LC, Pettygrove S, Robinson C, Schulz E, Wells C, Wingate MS, Zahorodny W, Yeargin-Allsopp M; Centers for Disease Control and Prevention (CDC). Prevalence and Characteristics of Autism Spectrum Disorder Among Children Aged 8 Years-Autism and Developmental Disabilities Monitoring Network, 11 Sites, United States, 2012. MMWR Surveill Summ. 2016;65(3):1-23. doi: 10.15585/mmwr.ss6503a1.

Constantino JN, Charman T. Diagnosis of autism spectrum disorder: reconciling the syndrome, its diverse origins, and variation in expression. Lancet Neurol. 2016;15(3):279-91.

de la Torre-Ubieta L, Won H, Stein JL, Geschwind DH. Advancing the understanding of autism disease mechanisms through genetics. Nat Med. 2016 Apr;22(4):345-61. doi: 10.1038/nm.4071.

Ecker C. The neuroanatomy of autism spectrum disorder: An overview of structural neuroimaging findings and their translatability to the clinical setting. Autism. 2017;21(1):18-28.

Falkmer T, Anderson K, Falkmer M, Horlin C. Diagnostic procedures in autism spectrum disorders: a systematic literature review. Eur Child Adolesc Psychiatry. 2013;22(6):329-40.

Geschwind DH. Genetics of autism spectrum disorders. Trends Cogn Sci. 2011 Sep;15(9):409-16. doi: 10.1016/j.tics.2011.07.003.

Gokoolparsadh A, Sutton GJ, Charamko A, Green NF, Pardy CJ, Voineagu I. Searching for convergent pathways in autism spectrum disorders: insights from human brain transcriptome studies. Cell Mol Life Sci. 2016;73(23):4517-4530.

Kern JK, Geier DA, King PG, Sykes LK, Mehta JA, Geier MR. Shared Brain Connectivity Issues, Symptoms, and Comorbidities in Autism Spectrum Disorder, Attention Deficit/Hyperactivity Disorder, and Tourette Syndrome. Brain Connect. 2015;5(6):321-35.

Levitt P, Campbell DB. The genetic and neurobiologic compass points toward common signaling dysfunctions in autism spectrum disorders. J Clin Invest. 2009; 119(4):747-54. doi: 10.1172/JCI37934.

Lyall K, Croen L, Daniels J, Fallin MD, Ladd-Acosta C, Lee BK, Park BY, Snyder NW, Schendel D, Volk H, Windham GC, Newschaffer C. The Changing Epidemiology of Autism Spectrum Disorders. Annu Rev Public Health 2016; 38:9.1-9.22.

Maximo JO, Cadena EJ, Kana RK. The implications of brain connectivity in the neuropsychology of autism. Neuropsychol Rev. 2014;24(1):16-31.

Nardone S, Elliott E. The Interaction between the Immune System and Epigenetics in the Etiology of Autism Spectrum Disorders. Front Neurosci 2016;10:329.

Parikshak NN, Swarup V, Belgard TG, Irimia M, Ramaswami G, Gandal MJ, Hartl C, Leppa V, de la Torre-Ubieta L, Huang J, Lowe JK, Blencowe BJ, Horvath S, Geschwind DH. Genome-wide changes in lncRNA, splicing, and regional gene expression patterns in autism. Nature. 2016;540(7633):423-427. doi: 10.1038/nature20612.

Simonoff E, Pickles A, Charman T, Chandler S, Loucas T, Baird G. Psychiatric disorders in children with autism spectrum disorders: prevalence, comorbidity, and associated factors in a population-derived sample. J Am Acad Child Adolesc Psychiatry 2008;47(8):921-9.

Sun W, Poschmann J, Cruz-Herrera Del Rosario R, Parikshak NN, Hajan HS, Kumar V, Ramasamy R, Belgard TG, Elanggovan B, Wong CCY, Mill J, Geschwind DH, Prabhakar S. Histone Acetylome-wide Association Study of Autism Spectrum Disorder. Cell. 2016;167(5):1385-1397.

Varma A, Iskandar J. Challenges in diagnosis of autism and the struggle of using western screening tools in different cultures. Psychiatrist's perspective. Indian Pediatr. 2014;51(5):356-7.

Vissers ME, Cohen MX, Geurts HM. Brain connectivity and high functioning autism: a promising path of research that needs refined models, methodological convergence, and stronger behavioral links. Neurosci Biobehav Rev. 2012;36(1):604-25.

Voineagu I, Eapen V. Converging Pathways in Autism Spectrum Disorders: Interplay between Synaptic Dysfunction and Immune Responses. Front Hum Neurosci. 2013;7:738.

Voineagu I, Wang X, Johnston P, Lowe JK, Tian Y, Horvath S, Mill J, Cantor RM, Blencowe BJ, Geschwind DH. Transcriptomic analysis of autistic brain reveals convergent molecular pathology. Nature. 2011;474(7351):380-4. doi: 10.1038/nature10110.

Vorstman JAS, Parr JR, Moreno-De-Luca D, Anney RJL, Nurnberger JI Jr, Hallmayer JF. Autism genetics: opportunities and challenges for clinical translation. Nat Rev Genet. 2017; 18(6):362-376. doi: 10.1038/nrg.2017.4.

Wu YE, Parikshak NN, Belgard TG, Geschwind DH. Genome-wide, integrative analysis implicates microRNA dysregulation in autism spectrum disorder. Nat Neurosci. 2016;19(11):1463-1476. doi: 10.1038/nn.4373.

Chapter 2. Circulating microRNAs as potential biomarkers for neurodevelopmental disorders

2.1. MicroRNAs (miRNAs): the best characterized class of non-coding RNAs

A genome is the complete set of DNA of an organism and each genome contains all of the information needed to build and maintain that organism, allowing it to grow and develop. Thanks to new NGS (next-generation sequencing) technologies it is now possible for scientists to easily retrieve these complete sets of genetic instructions, but still the biggest question about their interpretation remains open. How to decipher this unique genetic information, and finally, understand how each organism works?

The first successful attempts to interpret the genome were based on two general principles, stated by F. H. C. Crick in 1958, that have really shaped our proteome-based vision of the genome: the Sequence Hypothesis and the Central Dogma. The former assumes that the specificity of a nucleic acid is expressed solely by its base sequence, and that this sequence represents a simple code to produce a particular protein. The latter simply retraces the flow of sequence information and states that once information has passed into protein it cannot get out again (Figure 2.1) (Crick, 1958).

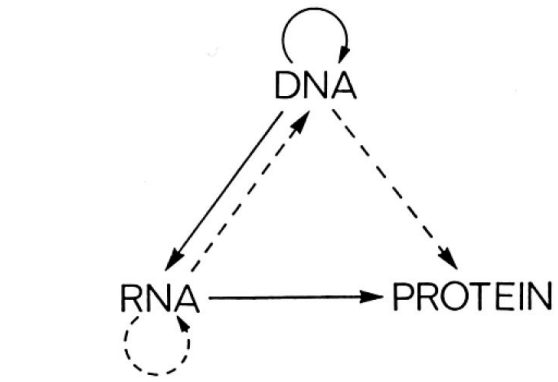

Fig. 3. A tentative classification for the present day. Solid arrows show general transfers; dotted arrows show special transfers. Again, the absent arrows are the undetected transfers specified by the central dogma.

Figure 2. 1. Visualization of the Central Dogma by F.H.C. Crick (Crick, 1970). *"In more detail, the transfer of information from nucleic acid to nucleic acid, or from nucleic acid to protein may be possible, but transfer from protein to protein, or from protein to nucleic acid is impossible" (Crick, 1958).*

As a consequence of the overestimation and misunderstanding of these two useful and inspiring principles, RNA was tacitly consigned to be the template (messenger RNA) and infrastructural platform (ribosomal and transfer RNAs) for protein synthesis.

However, sequencing studies on the whole genome of many organisms of increased developmental complexity (*Haemophilus influenzae* and *Mycoplasma genitalium* in 1995, *Saccharomyces cerevisiae* in 1996, *Caenorhabditis elegans* in 1998, *Drosophila melanogaster* in 2000, *Homo sapiens* in 2001) quickly taught scientists that the number of protein-coding genes does not reflect the complexity of organisms and that the extent of protein-coding sequences remains relatively static over a wide range of developmental complexity (an unexpected finding that formulated the G-value enigma) (Figure 2.2B). On the contrary, the non-coding genome size gets bigger as the structural complexity of organisms increases (Figure 2.2A) (Taft et al., 2007). Surprisingly, what made more sophisticated organisms different from less complex ones was the fact that their genome contained more DNA of unknown function, that was consequently referred to as "junk" DNA.

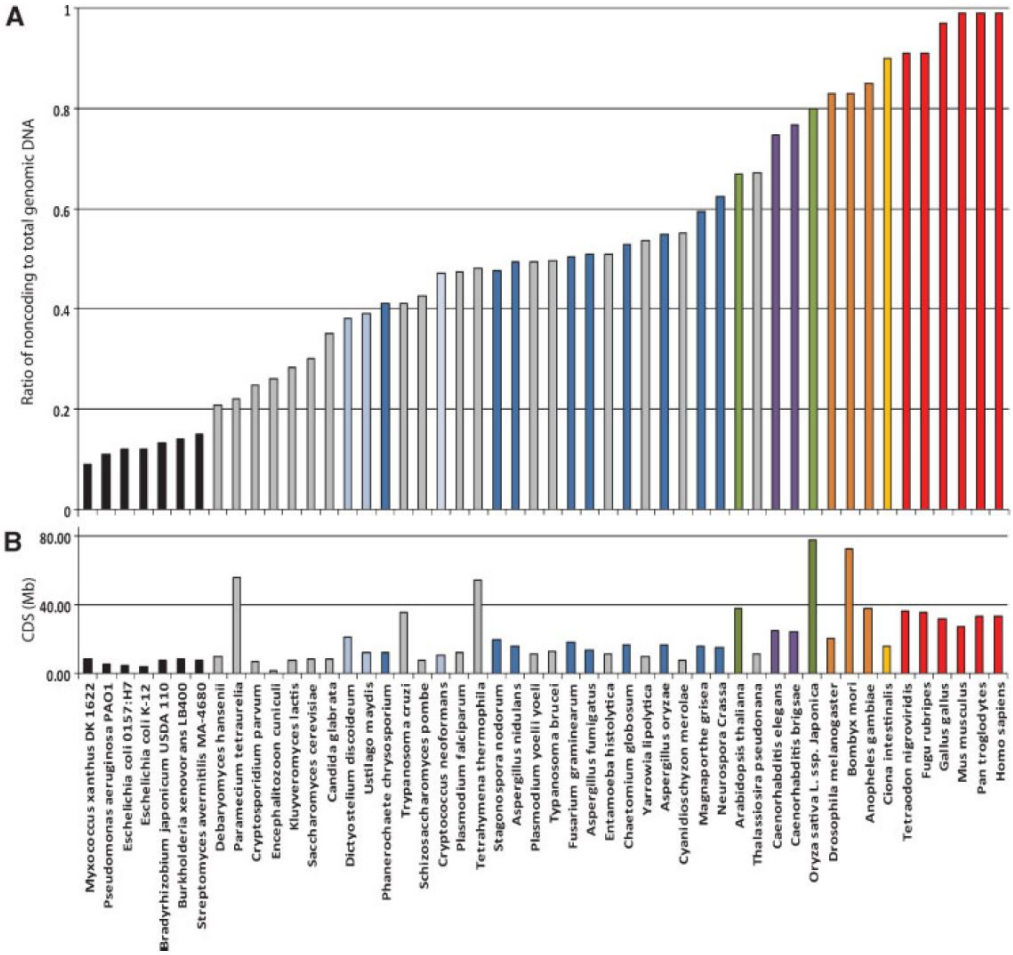

Figure 2. 2. Percentage of non-coding DNA (A) and amount of protein-coding sequences (B) per haploid genome across species (Taft et al., 2007).

The ENCODE Project (ENCODE Project Consortium, 2007; ENCODE Project Consortium, 2012), aiming to delineate all functional elements encoded in the human genome, marked the ending of the

"junk" DNA. The consortium confirmed that the human genome, of which less than 2% encodes for proteins, is pervasively transcribed and identified previously unrecognized transcription start sites responsible for the production of many novel non-coding transcripts. Also, it assigned to the vast majority (80.4%) of the human genome at least one biochemical RNA- and/or chromatin-associated event with a regulatory function.

Our DNA is no longer "junk" but still a "dark matter": however, regulatory non-coding RNAs may represent keys to the interpretation of our complexity in a new transcriptome-based vision of the genome. Our knowledge about the human non-coding transcriptome is continuously expanding. Figure 2.3 depicts the distribution of non-coding RNA types within the human genome (Malek et al., 2014).

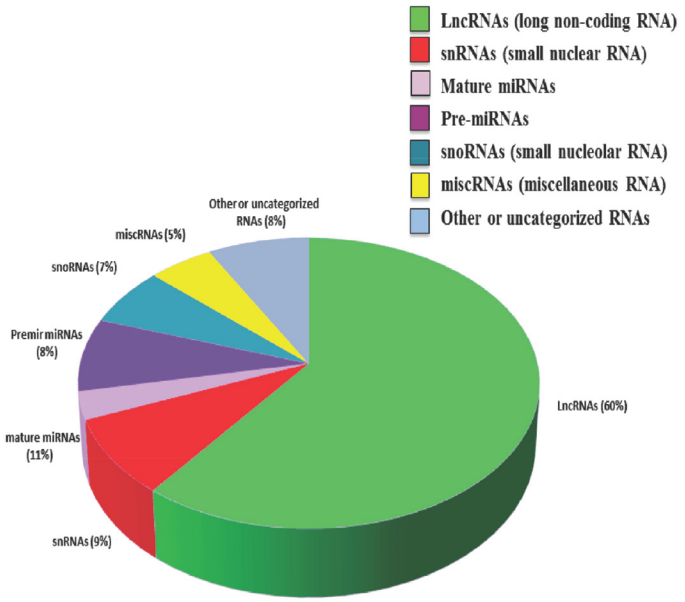

Figure 2. 3. Distribution of non-coding RNA types within the human genome (Malek et al., 2014).

MicroRNAs (miRNAs) represent the best characterized class of non-coding RNAs to date and they were the first one giving researchers some precious hints about the important regulatory role of non-coding RNA molecules and offering them just a glance at all the hidden layers of regulation of gene expression.

MiRNAs are 18-25 nucleotides long single-stranded RNAs that act as evolutionary conserved post-transcriptional regulators of gene expression, collectively increasing the precision and robustness of gene-regulatory networks and affecting all cellular pathways, from development to homeostasis, response to external factors, and metabolism (Berezikov, 2011). They negatively modulate the expression of their target mRNAs by binding to miRNA-binding sites present in the 3′-UTR of their

targets mRNAs through a specific sequence, named seed region, that is a string of at least 6 nucleotides starting at position two of the 5′ of the miRNA (Figure 2.4) (Filipowicz et al., 2008).

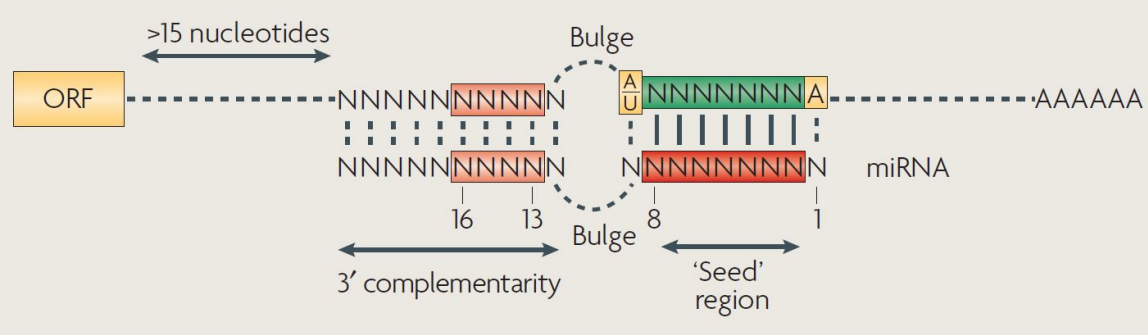

Figure 2. 4. Principles of microRNA–mRNA interactions in Metazoans (Filipowicz et al., 2008). *There must be a perfect and contiguous base pairing between the miRNA seed region and the specific target mRNA. Bulges or mismatches must be present in the central region of the miRNA–mRNA duplex. Finally, there must be reasonable complementarity of the target mRNA to the miRNA 3′ half to stabilize the interaction. Mismatches and bulges are generally tolerated in this region.*

Usually, miRNA-binding sites specific for the same or different miRNAs are present in multiple copies in the mRNA 3′ UTR. Therefore, a single miRNA can control the expression of several mRNAs, and a single mRNA may be targeted by more than one miRNA. Importantly, miRNA-binding sites are generally required in multiple copies for effective repression: when these are present close to each other, they tend to act cooperatively (Figure 2.5) (Filipowicz et al., 2008).

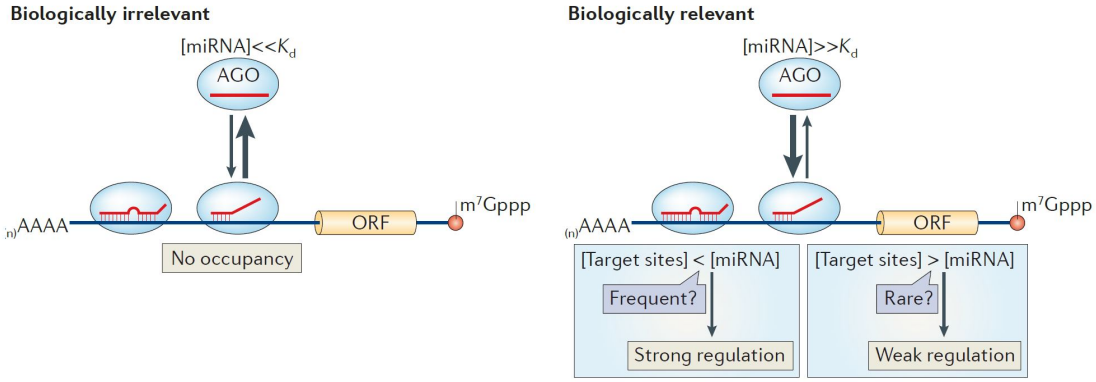

Figure 2. 5. A quantitative model of microRNA function (Ameres and Zamore, 2013). *The relative abundance of miRNAs and their targets inside the cell, together with the cumulative abundance of all target sites in the cell relative to the abundance of the miRNA, dictate the regulatory outcome.*

High complementarity of the target mRNA to the miRNA 3′ half leads to the direct cleavage of the mRNA, whereas low complementarity between these sequences causes mRNA translational repression or decay (Figure 2.6) (Ameres and Zamore, 2013). These molecular mechanisms are mediated by the

RISC (RNA-induced silencing complex) complex that includes proteins belonging to the AGO (Argonaute) family; specifically, RISC endonuclease activity depends exclusively on AGO2 protein (Figure 2.7) (Filipowicz et al., 2008).

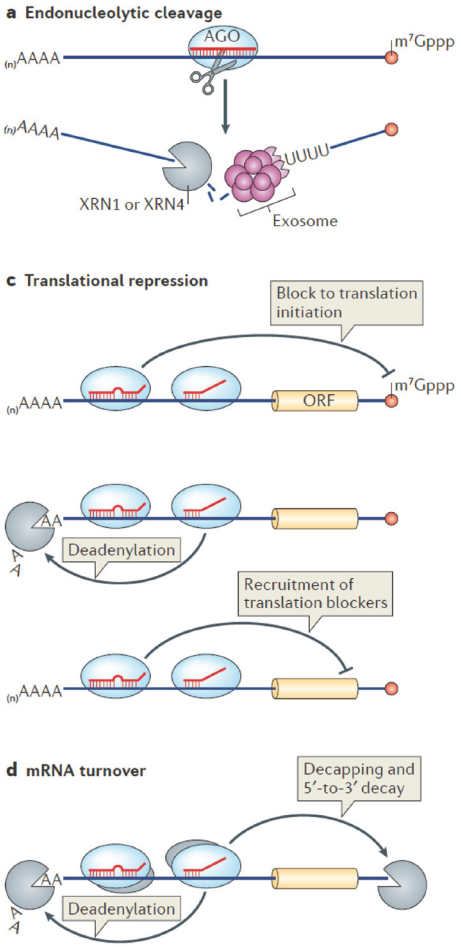

Figure 2. 6. MiRNA function in animals (Ameres and Zamore, 2013). *(A) The vast majority of plant miRNAs and just few animal miRNAs direct endonucleolytic cleavage of their mRNA targets. (C) In animals, miRNAs can mediate translational repression through the block of translational initiation, the mRNA poly(A) tail shortening or the recruitment of protein cofactors that can interfere with translation. (D) In many cells and tissues, miRNA-directed translational repression can be indistinguishable from mRNA turnover induction via decapping and 5′-to-3′ decay.*

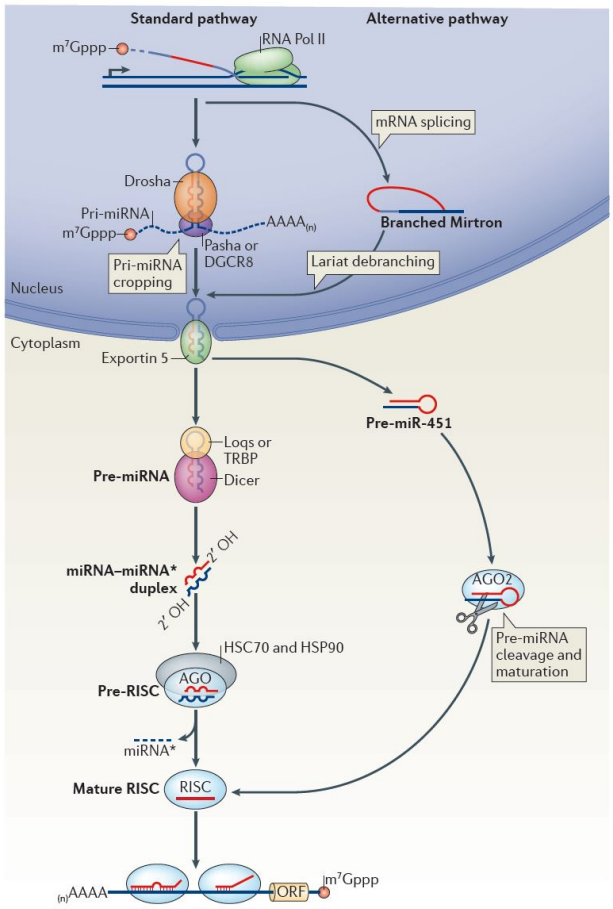

Figure 2. 7. MiRNA biogenesis (Ameres and Zamore, 2013). *A primary miRNA (pri-miRNA) can be transcribed by RNA polymerase II from independent genomic transcription units or from the introns of protein-coding genes. It has a stem-loop structure with a m7Gppp (7-methylguanosine) cap and a 3' poly(A) tail. The nuclear RNase III Drosha, along with the dsRNA-binding protein DGCR8, generates a precursor miRNA (pre-miRNA) with a ~60 nucleotide stem-loop structure. In the cytoplasm, the cytoplasmic RNase III Dicer, together with the dsRBP TRBP, cleaves the loop of the pre-miRNA producing a miRNA-miRNA* duplex, containing sequences that were at the 5' and 3' arms of the pre-miRNA, that will be loaded into an AGO protein as a dsRNA. However, the mature RISC will only load the more thermodynamically stable miRNA strand of the duplex, while the other one will be degraded. Cytoplasmic destinations of miRNAs include both P bodies and polysomes.*

Extensive studies have shown that miRNAs control cellular processes, such as cell proliferation, differentiation, migration, cell death, and angiogenesis, which are crucial in the pathogenesis of cancer. Many miRNAs have been mainly identified as potential oncogenes or tumor suppressors in cancer development and progression and have been reported to be causally related to the neoplastic features of the cells (Ragusa et al., 2017).

2.2. Role of miRNAs inside the nervous system cells

Other than in neoplastic and degenerative diseases, miRNA dysregulation has also been observed in several neurodevelopmental and neuropsychiatric disorders, such as schizophrenia, major depressive disorder, anxiety, BD (bipolar disorder), and ASD (Geaghan and Cairns, 2015; Omran et al., 2012; Scott et al., 2015). Some miRNAs show differential spatio-temporal and sex-biased expression patterns in the developing human brain and regulate targets that are highly enriched for genes related to transcriptional regulation, neurodevelopmental processes, and common neurodevelopmental disorders, such as ASD, schizophrenia, and BD (Ziats and Rennert, 2014). MiRNAs are main players in the brain, where they control many developmental processes, including patterning, cell specification, local translational control of neuronal plasticity (Figure 2.8), neurogenesis, and neuronal apoptosis (Kosik, 2006).

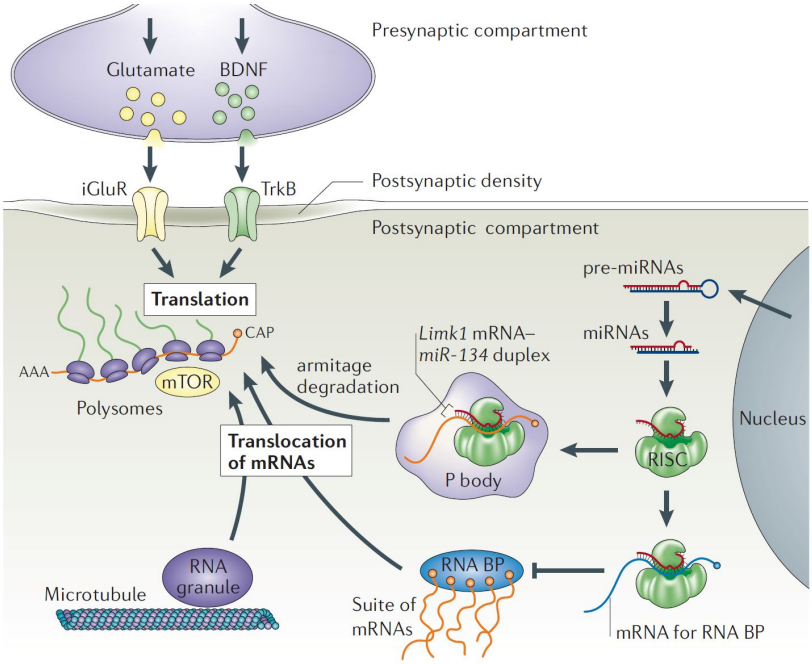

Figure 2. 8. MicroRNA local translational control of neuronal plasticity (Kosik, 2006). *Stimulation by neurotransmitters or neurotrophic factors can regulate the local translation of mRNAs in polysomes found at the base of dendritic spines, a process that can be further controlled by miRNAs. Silenced mRNAs can be also translocated to dendrites through other silencing structures such as RNA granules and RBP (RNA binding protein) platforms. The image shows a peculiar rat example: Limk1(LIM-domain kinase 1) mRNA controlled by miR-134. miR-134 is expressed in the rat hippocampus, and its expression increases as the brain matures. Limk1 is a kinase that can affect spine structure by regulating actin filament dynamics. When Limk1 mRNA is translationally inhibited by miR-134 the size of spines is negatively regulated. Intriguingly, it has been shown that the miRNA maintains the translational silencing of its target until a synaptic input overrides the silencing.*

2.2. Intracellular dysregulation of miRNAs in ASD

Altered expression patterns of miRNAs have been found in many tissues and cells from ASD patients, such as brain cortex regions and cerebellum (Ander et al., 2015; Mor et al., 2015; Wu et al, 2016; Schumann et al., 2017), olfactory mucosal stem cells (Nguyen et al., 2016), peripheral whole blood (Huang, Long et al., 2015; Huang, Zhou et al., 2015), and lymphoblastoid cell lines (Sarachana et al., 2010; Ghahramani Seno et al., 2011).

A large genome-wide miRNA expression profiling study on post-mortem human brain samples, using the WGCNA approach (see Chapter 1, Section 1.4), identified (i) miR-21-3p as upregulated in ASD and targeting neuronal genes downregulated in ASD, and (ii) hsa_can_1002-m, a previously unknown, primate-specific miRNA, as downregulated in ASD and regulating the epidermal growth factor receptor and fibroblast growth factor receptor signaling pathways involved in neural development and immune function (Wu et al, 2016).

2.3. Extracellular miRNAs as non-invasive biomedical tools: the alternative use of liquid biopsies in neurodevelopmental and psychiatric disorders

Since their identification and characterization in serum and plasma of humans and other animals (Chen et al., 2008; Chim et al., 2008), extracellular miRNAs have attracted researchers for their potential as new non-invasive tools for diagnosis, prognosis, and treatment evaluation of many human diseases and disorders. Extracellular miRNAs can be detected, associated with extracellular vesicles, like exosomes and macrovesicles, or conjugated to RNA-binding proteins and lipoproteins, in all mammalian body fluids: saliva, tears, urine, amniotic fluid, colostrum, breast milk, bronchial lavage, cerebrospinal fluid, vitreous humor of the eye, peritoneal fluid, pleural fluid, seminal fluid, and also feces, aside from serum and plasma (Figure 2.9) (Larrea et al., 2016).

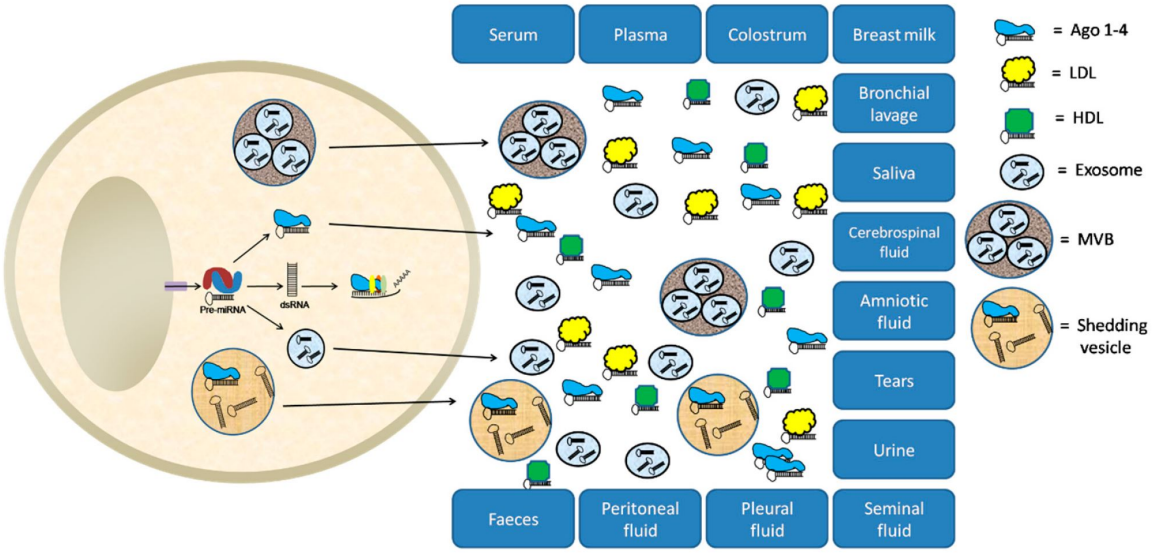

Figure 2. 9. Biological fluids as sources of potential miRNA-based biomarkers (Larrea et al., 2016). *LDL: Low-density lipoprotein; HDL: High-density lipoprotein; MVB: Multivesicular body.*

Stability and general consistency of levels among individuals, along with the existence of specific expression signatures in association with both physiological and pathological conditions, make circulating miRNAs appropriate biomarkers; these also suggest the prospective alternative use of liquid biopsies as sources of biomarkers in the clinic (Weiland et al., 2012; Larrea et al., 2016).

Numerous studies have identified either serum or plasma circulating miRNAs as promising biomarkers for neurodevelopmental and neuropsychiatric disorders, as ADHD (Wu et al., 2015), ASD (Mundalil Vasu et al., 2014; Chapters 3 and 4 of this doctoral thesis), TS (Rizzo et al., 2015), depression/anxiety disorder (Wang, Sundquist et al., 2015), posttraumatic stress disorder (Balakathiresan et al., 2014), BD (Rong et al., 2011), schizophrenia (Wei et al., 2015), and epilepsy (Wang, Tan et al., 2015; Wang, Yu et al., 2015; An et al., 2016), and other brain pathological conditions, like traumatic brain injury (Di Pietro et al., 2017) and vascular dementia (Ragusa et al., 2016).

However, when studying circulating miRNAs in pathologies, the biggest challenges are (i) to elucidate the relationship between the diseased tissue and the corresponding expression levels of these molecules observed in liquid biopsies and (ii) to verify if and how accurately these extracellular RNAs would reflect the transcriptomic snapshot of the physiological and pathological status of original cells (Ragusa et al., 2017). MiRNAs in circulation could either be passively released non-specific by-products of cellular activity and cell death or actively secreted cell-cell signaling messengers (Figure 2.10) (Larrea et al., 2016).

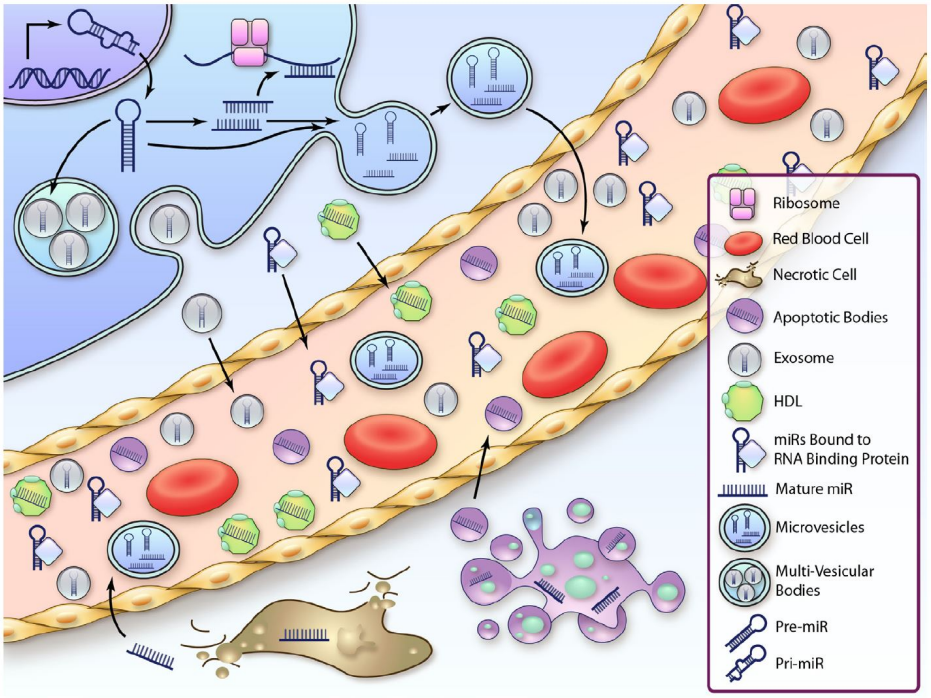

Figure 2. 10. The two hypotheses on the origin and biogenesis of circulating miRNAs (Kumarswamy and Thum, 2013).

In many neurodevelopmental and psychiatric disorders, as it is for ASD (see Chapter 1, Section 1.3), these challenges are further complicated by the fact that a specific and unique diseased tissue has not been identified yet. Focusing on the contribution of extracellular vesicles, such as exosomes, to the expression of circulating miRNAs might help clarify potential tissue-body fluid links (Witwer, 2015).

2.4. Project hypotheses and aims: an easy and innovative approach to address important biomedical questions and needs

My PhD research project consists of two studies, profiling circulating miRNAs in serum and saliva from ASD patients, respectively. To date, these two series of experiments specifically represent the third and fourth high-throughput studies profiling miRNAs in a body fluid from ASD patients, confirming that this research field is still mostly unexplored.

We hypothesized that the expression analysis of circulating miRNAs in serum and saliva could represent an easy and innovative approach to address and solve important biomedical issues related to ASD, such as the need for molecular biomarkers and the necessity to further investigate this disorder through more accessible patient biopsies.

In fact, while there are many studies proposing circulating miRNAs as appropriate biomarkers for human pathology, only a few of them exploit this easy liquid biopsy-based investigation approach in order to propose to the scientific community new potentially intriguing pathological mechanisms and central effectors in them. Even though retracing the role of dysregulated circulating miRNAs in a disorder is challenging (see Section 2.3) and making hypotheses about it can be very risky and misleading, using computational analyses to reconstruct their possible intracellular regulatory networks and functions can still be useful to gain further insight into the molecular basis of the disorder.

This is a particularly valuable option when investigating neurodevelopmental disorders, for which preferable tissue biopsies (post-mortem brain samples) are not readily and easily accessible to researchers. Overall, our computational analysis findings confirmed the validity of this alternative research use of liquid biopsies, since we were able to identify, at the same time, already known and completely new processes and molecules with a (potential) role in ASD.

2.5. References

Ameres SL, Zamore PD. Diversifying microRNA sequence and function. Nat Rev Mol Cell Biol. 2013;14(8):475-88. doi: 10.1038/nrm3611.

An N, Zhao W, Liu Y, Yang X, Chen P. Elevated serum miR-106b and miR-146a in patients with focal and generalized epilepsy. Epilepsy Res. 2016;127:311-316.

Ander BP, Barger N, Stamova B, Sharp FR, Schumann CM. Atypical miRNA expression in temporal cortex associated with dysregulation of immune, cell cycle, and other pathways in autism spectrum disorders. Mol Autism. 2015 Jun 19;6:37.

Balakathiresan NS, Chandran R, Bhomia M, Jia M, Li H, Maheshwari RK. Serum and amygdala microRNA signatures of posttraumatic stress: fear correlation and biomarker potential. J Psychiatr Res. 2014;57:65-73.

Berezikov E. Evolution of microRNA diversity and regulation in animals. Nat Rev Genet. 2011;12(12):846-60.

Chen X, Ba Y, Ma L, Cai X, Yin Y, Wang K, Guo J, Zhang Y, Chen J, Guo X, Li Q, Li X, Wang W, Zhang Y, Wang J, Jiang X, Xiang Y, Xu C, Zheng P, Zhang J, Li R, Zhang H, Shang X, Gong T, Ning G, Wang J, Zen K, Zhang J, Zhang CY. Characterization of microRNAs in serum: a novel class of biomarkers for diagnosis of cancer and other diseases. Cell Res. 2008;18(10):997-1006.

Chim SS, Shing TK, Hung EC, Leung TY, Lau TK, Chiu RW, Lo YM. Detection and characterization of placental microRNAs in maternal plasma. Clin Chem. 2008;54(3):482-90.

Crick F. Central dogma of molecular biology. Nature. 1970;227(5258):561-3.

Crick FH. On protein synthesis. Symp Soc Exp Biol. 1958;12:138-63.

Di Pietro V, Ragusa M, Davies D, Su Z, Hazeldine J, Lazzarino G, Hill LJ, Crombie N, Foster M, Purrello M, Logan A, Belli A. MicroRNAs as Novel Biomarkers for the Diagnosis and Prognosis of Mild and Severe Traumatic Brain Injury. J Neurotrauma. 2017;34(11):1948-1956. doi: 10.1089/neu.2016.4857.

ENCODE Project Consortium. An integrated encyclopedia of DNA elements in the human genome. Nature. 2012;489(7414):57-74. doi: 10.1038/nature11247.

ENCODE Project Consortium. Identification and analysis of functional elements in 1% of the human genome by the ENCODE pilot project. Nature. 2007;447(7146):799-816.

Filipowicz W, Bhattacharyya SN, Sonenberg N. Mechanisms of post-transcriptional regulation by microRNAs: are the answers in sight? Nat Rev Genet. 2008;9(2):102-14. doi: 10.1038/nrg2290.

Geaghan M, Cairns MJ. MicroRNA and Posttranscriptional Dysregulation in Psychiatry. Biol Psychiatry. 2015;78(4):231-9.

Ghahramani Seno MM, Hu P, Gwadry FG, Pinto D, Marshall CR, Casallo G, Scherer SW. Gene and miRNA expression profiles in autism spectrum disorders. Brain Res. 2011 Mar 22;1380:85-97.

Huang F, Long Z, Chen Z, Li J, Hu Z, Qiu R, Zhuang W, Tang B, Xia K, Jiang H. Investigation of Gene Regulatory Networks Associated with Autism Spectrum Disorder Based on MiRNA Expression in China. PLoS One. 2015 Jun 10;10(6):e0129052.

Huang F, Zhou T, Yao X, Yi J, Zhou F, Long Z, Hou X, Wang C, Chen Z, Jiang H. miRNA profiling in autism spectrum disorder in China. Genom Data. 2015 Aug 12;6:108-9.

Kosik KS. The neuronal microRNA system. Nat Rev Neurosci. 2006 Dec;7(12):911-20.

Kumarswamy R, Thum T. Non-coding RNAs in cardiac remodeling and heart failure. Circ Res. 2013;113(6):676-89. doi: 10.1161/CIRCRESAHA.113.300226.

Larrea E, Sole C, Manterola L, Goicoechea I, Armesto M, Arestin M, Caffarel MM, Araujo AM, Araiz M, Fernandez-Mercado M, Lawrie CH. New Concepts in Cancer Biomarkers: Circulating miRNAs in Liquid Biopsies. Int J Mol Sci. 2016;17(5).

Malek E, Jagannathan S, Driscoll JJ. Correlation of long non-coding RNA expression with metastasis, drug resistance and clinical outcome in cancer. Oncotarget. 2014;5(18):8027-38.

Mor M, Nardone S, Sams DS, Elliott E. Hypomethylation of miR-142 promoter and upregulation of microRNAs that target the oxytocin receptor gene in the autism prefrontal cortex. Mol Autism. 2015 Aug 14;6:46.

Mundalil Vasu M, Anitha A, Thanseem I, Suzuki K, Yamada K, Takahashi T, Wakuda T, Iwata K, Tsujii M, Sugiyama T, Mori N. Serum microRNA profiles in children with autism. Mol Autism. 2014;5:40. doi: 10.1186/2040-2392-5-40.

Nguyen LS, Lepleux M, Makhlouf M, Martin C, Fregeac J, Siquier-Pernet K, Philippe A, Feron F, Gepner B, Rougeulle C, Humeau Y, Colleaux L. Profiling olfactory stem cells from living patients identifies miRNAs relevant for autism pathophysiology. Mol Autism. 2016 Jan 8;7:1.

Omran A, Elimam D, Shalaby S, Peng J, Yin F. MicroRNAs: a light into the "black box" of neuropediatric diseases? Neuromolecular Med. 2012 Dec;14(4):244-61.

Ragusa M, Barbagallo C, Brex D, Caponnetto A, Cirnigliaro M, Battaglia R, Barbagallo D, Di Pietro C, Purrello M. Molecular Crosstalking among Noncoding RNAs: A New Network Layer of Genome Regulation in Cancer. Int J Genomics. 2017;2017:4723193. doi: 10.1155/2017/4723193.

Ragusa M, Barbagallo C, Cirnigliaro M, Battaglia R, Brex D, Caponnetto A, Barbagallo D, Di Pietro C, Purrello M. Asymmetric RNA Distribution among Cells and Their Secreted Exosomes: Biomedical Meaning and Considerations on Diagnostic Applications. Front Mol Biosci. 2017;4:66. doi: 10.3389/fmolb.2017.00066.

Ragusa M, Bosco P, Tamburello L, Barbagallo C, Condorelli AG, Tornitore M, Spada RS, Barbagallo D, Scalia M, Elia M, Di Pietro C, Purrello M. miRNAs Plasma Profiles in Vascular Dementia: Biomolecular Data and Biomedical Implications. Front Cell Neurosci. 2016;10:51. doi: 10.3389/fncel.2016.00051.

Rizzo R, Ragusa M, Barbagallo C, Sammito M, Gulisano M, Calì PV, Pappalardo C, Barchitta M, Granata M, Condorelli AG, Barbagallo D, Scalia M, Agodi A, Di Pietro C, Purrello M. Circulating miRNAs profiles in Tourette syndrome: molecular data and clinical implications. Mol Brain. 2015;8:44.

Rong H, Liu TB, Yang KJ, Yang HC, Wu DH, Liao CP, Hong F, Yang HZ, Wan F, Ye XY, Xu D, Zhang X, Chao CA, Shen QJ. MicroRNA-134 plasma levels before and after treatment for bipolar mania. J Psychiatr Res. 2011;45(1):92-5.

Sarachana T, Zhou R, Chen G, Manji HK, Hu VW. Investigation of post-transcriptional gene regulatory networks associated with autism spectrum disorders by microRNA expression profiling of lymphoblastoid cell lines. Genome Med. 2010 Apr 7;2(4):23.

Schumann CM, Sharp FR, Ander BP, Stamova B. Possible sexually dimorphic role of miRNA and other sncRNA in ASD brain. Mol Autism. 2017 Feb 7;8:4.

Scott KA, Hoban AE, Clarke G, Moloney GM, Dinan TG, Cryan JF. Thinking small: towards microRNA-based therapeutics for anxiety disorders. Expert Opin Investig Drugs. 2015 Apr;24(4):529-42.

Taft RJ, Pheasant M, Mattick JS. The relationship between non-protein-coding DNA and eukaryotic complexity. Bioessays. 2007;29(3):288-99.

Wang J, Tan L, Tan L, Tian Y, Ma J, Tan CC, Wang HF, Liu Y, Tan MS, Jiang T, Yu JT. Circulating microRNAs are promising novel biomarkers for drug-resistant epilepsy. Sci Rep. 2015;5:10201.

Wang J, Yu JT, Tan L, Tian Y, Ma J, Tan CC, Wang HF, Liu Y, Tan MS, Jiang T, Tan L. Genome-wide circulating microRNA expression profiling indicates biomarkers for epilepsy. Sci Rep. 2015;5:9522.

Wang X, Sundquist K, Hedelius A, Palmér K, Memon AA, Sundquist J. Circulating microRNA-144-5p is associated with depressive disorders. Clin Epigenetics. 2015;7:69.

Wei H, Yuan Y, Liu S, Wang C, Yang F, Lu Z, Wang C, Deng H, Zhao J, Shen Y, Zhang C, Yu X, Xu Q. Detection of circulating miRNA levels in schizophrenia. Am J Psychiatry. 2015;172(11):1141-7.

Weiland M, Gao XH, Zhou L, Mi QS. Small RNAs have a large impact: circulating microRNAs as biomarkers for human diseases. RNA Biol. 2012;9(6):850-9.

Witwer KW. Circulating microRNA biomarker studies: pitfalls and potential solutions. Clin Chem. 2015;61(1):56-63. doi: 10.1373/clinchem.2014.221341.

Wu LH, Peng M, Yu M, Zhao QL, Li C, Jin YT, Jiang Y, Chen ZY, Deng NH, Sun H, Wu XZ. Circulating MicroRNA Let-7d in Attention-Deficit/Hyperactivity Disorder. Neuromolecular Med. 2015;17(2):137-46.

Wu YE, Parikshak NN, Belgard TG, Geschwind DH. Genome-wide, integrative analysis implicates microRNA dysregulation in autism spectrum disorder. Nat Neurosci. 2016 Nov;19(11):1463-1476.

Ziats MN, Rennert OM. Identification of differentially expressed microRNAs across the developing human brain. Mol Psychiatry. 2014 Jul;19(7):848-52.

Summary of research

In my PhD research project, I profiled circulating miRNAs in serum and saliva from ASD patients to gain further insight into ASD heterogeneous etiology and pathological mechanisms and to identify potential biomarkers to support its behavior-based diagnosis, using an easy liquid biopsy-based investigation approach.

Chapter 3 describes the serum study and was adapted from the manuscript titled with "Expression and Regulatory Network Analysis of miR-140-3p, a New Potential Serum Biomarker for Autism Spectrum Disorder" published in August 2017 on the scientific journal "Frontiers in Molecular Neuroscience" and co-authored by Cirnigliaro M, Barbagallo C, Gulisano M, Domini CN, Barone R, Barbagallo D, Ragusa M, Di Pietro C, Rizzo R, and Purrello M. Our serum circulating miRNA profiling through TLDA (TaqMan Low Density Array) technology led us to the identification of miR-140-3p as a possible biomarker performing at a high level in the discrimination among ASD and TS+ASD patients and as a potential player in the regulation of altered circadian rhythms in ASD.

Chapter 4 reports the more recent saliva study and represents the first draft of a new manuscript that is about to be submitted. Through a supernatant saliva circulating miRNA profiling by using NanoString nCounter technology, we found miR-29a-3p and miR-141-3p as possible supportive means for the recognition of ASD verbal and social defects that can be efficiently used in combination and we proposed them as intriguing targets for future investigation given their potential central role in neurodevelopment.

Both of these successful initiatives were possible thanks to the inspiring and fertile collaboration between the research group coordinated by Professor Michele Purrello, that I have joined for my PhD program, and the research team from the Section of Child and Adolescent Psychiatry at University of Catania led by Professor Renata Rizzo. Both Professors conceived the two projects with contributions by their group members. Our research group was in charge of designing and performing all the experiments and subsequent analyses. Professor Renata Rizzo and her collaborators were in charge of the recruitment and clinical assessment of study participants, of the sampling process, and of a critical revision of our combined results. I am extremely grateful to my Supervisor for the amazing opportunity that he has been giving me for these three years of playing a central role in both of these scientific adventures.

Chapter 3. Expression and Regulatory Network Analysis of miR-140-3p, a New Potential Serum Biomarker for Autism Spectrum Disorder

3.1. Abstract

Given its prevalence and social impact, ASD is drawing much interest. Molecular basis of ASD is heterogeneous and only partially known. Many factors, including disorders comorbid with ASD, like TS (Tourette syndrome), complicate ASD behavior-based diagnosis and make it vulnerable to bias. To further investigate ASD etiology and to identify potential biomarkers to support its precise diagnosis, we used TLDA (TaqMan Low Density Array) technology to profile serum miRNAs from ASD, TS, and TS+ASD patients and NCs (unaffected controls). Through validation assays in 30 ASD, 24 TS, and 25 TS+ASD patients and 25 NCs, we demonstrated that miR-140-3p is upregulated in ASD vs: NC, TS, and TS+ASD (Tukey's test, p-values = 0.03, = 0.01, < 0.0001, respectively). ΔCt values for miR-140-3p and YGTSS (Yale Global Tic Severity Scale) scores are positively correlated (Spearman r = 0.33; BH (Benjamini-Hochberg) FDR (False Discovery Rate) adjusted p-value = 0.008) and show a linear relationship (p-value = 0.002). Network functional analysis showed that nodes controlled by miR-140-3p, especially CD38 (CD38 molecule) and NRIP1 (nuclear receptor interacting protein 1) that are its validated targets, are involved in processes convergingly dysregulated in ASD, such as synaptic plasticity, immune response, and chromatin binding. Biomarker analysis proved that serum miR-140-3p can discriminate among: (1) ASD and NC (AUC, Area under the ROC curve: 0.70; sensitivity: 63.33%; specificity: 68%); (2) ASD and TS (AUC: 0.72; sensitivity: 66.66%; specificity: 70.83%); (3) ASD and TS+ASD (AUC: 0.78; sensitivity: 73.33%; specificity: 76%). Characterization of miR-140-3p network would contribute to further clarify ASD etiology. Serum miR-140-3p could represent a potential non-invasive biomarker for ASD, easy to test through liquid biopsy.

3.2. Specific background and aims

One of the biggest revisions about ASD that have been introduced in DMS-5 is the possibility and appropriateness to simultaneously diagnose ASD with other disorders when there is ample evidence for comorbidity (American Psychiatric Association, 2013). In fact, many different comorbid neuropsychiatric and neurodevelopmental disorders contribute to ASD impairment, being common

(70.8%) and frequently multiple (57%) in ASD children (Simonoff et al., 2008). Such conditions include social anxiety disorder, ADHD, ODD, chronic tic disorder, and OCD.

Tourette syndrome is a neurodevelopmental disorder characterized by considerable motor as well as behavioral impairment: it affects approximately 1% of the population with a male:female ratio of 3:1. It is clinically defined by childhood onset of multiple motor tics and at least one phonic tic, which collectively must persist for at least 12 months (American Psychiatric Association, 2013). 88% of TS patients also show comorbidity and psychopathology. Comorbidity with ADHD and OCD is very common. Co-existent psychopathologies include depression, anxiety, learning difficulties, personality disorder, ODD, and conduct disorder (Robertson, 2012). TS can cause severe difficulties in social functioning and a reduced quality of life in patients suffering from it. Characteristic, but not essential for diagnosis, symptoms include complex tics, such as echolalia and echopraxia (copying others' vocalizations and actions, respectively), palilalia and palipraxia (repeating own words/phrases and actions, respectively), coprolalia (inappropriate involuntary swearing) as well as repeating of complex words (Robertson 2015).

It has been observed that 4.8% of ASD children also suffer from TS (Simonoff et al., 2008) and that 6-11% of TS cases show comorbidity with ASD (Robertson, 2012). TS and ASD share clinical symptomatology and many behavioral features. Genetic studies also support the existence of common susceptibility genes in both disorders (Clarke et al., 2012). The exact etiology of both disorders is still elusive.

Since common risk loci for ASD have not been proposed yet (Vorstman et al., 2017), a molecular test for non-syndromic ASD is not available and diagnosis relies on clinical assessment and confirmation. Considering the clinical variation and etiological heterogeneity of ASD, a precise diagnosis can be very difficult. ASD association with comorbid disorders (Constantino and Charman, 2016) further complicates it. Therefore, there is an urgent need for potential ASD biomarkers that could support clinical discrimination of patients. Although ASD research is progressively and actively growing, only two papers have characterized miRNAs in liquid biopsies from ASD patients with a high-throughput approach (Mundalil Vasu et al., 2014; Hicks et al., 2016); none of these studies has also focused on patients affected by other neurodevelopmental disorders comorbid with autism.

We hypothesized that the serum profile of circulating miRNAs may contain some specific fingerprints for ASD that could also be supportive in the discrimination among it and comorbid neurodevelopmental disorders. Aiming to gain more knowledge about ASD biomolecular basis and identify new potential biomarkers for this disorder, we exploited a high-throughput approach to analyze the expression of circulating miRNAs in serum from ASD, TS, and TS+ASD patients.

Following profiling of serum miRNAs through our previously published protocol (Rizzo et al., 2015; Ragusa et al., 2016), we validated serum miR-140-3p as significantly upregulated in ASD patients compared to unaffected controls, TS patients, and TS+ASD patients. In addition, we demonstrated that its serum expression levels are correlated with scores from the tic scale YGTSS. Then, we observed that miR-140-3p network node genes are involved in biological processes convergingly dysregulated in ASD (i.e., synaptic plasticity, immune response, and chromatin binding). Finally, through biomarker analysis, we proved that serum miR-140-3p could discriminate ASD from NC, TS, and TS+ASD.

3.3. Results

3.3.1. High-throughput expression analysis of circulating miRNAs in ASD, TS, and TS+ASD patients

By using TLDA technology, we investigated the expression levels of 754 miRNAs in sera from four ASD patients, five TS patients, four TS+ASD patients, and three unaffected NCs. We identified miR-146a and miR-223* as the best endogenous controls for panels A and B, respectively.

We found that four miRNAs from panel A (miR-140-3p, miR-222, miR-454, and miR-483-5p), and five miRNAs from panel B (miR-30d, miR-30e-3p, miR-148a*, miR-1274B, and miR-1290) were significantly DE (differentially expressed) in at least one of the comparisons made (FDR < 0.15 in each pairwise comparison).

3.3.2. Dysregulated expression levels of miR-140-3p in serum from ASD patients

We selected miR-30d, miR-140-3p, miR-148a*, and miR-222 for further validation through single TaqMan assays. MiR-146a was used as endogenous control in all the analyses carried out.

We found only miR-140-3p as significantly dysregulated in serum from ASD patients (ordinary one-way ANOVA, p-value = 0.0001). In particular, serum levels of miR-140-3p were higher in thirty ASD patients compared to twenty-five NCs (Tukey's multiple comparisons test, multiplicity adjusted p-value = 0.03), twenty-four TS patients (Tukey's multiple comparisons test, multiplicity adjusted p-value = 0.01), and twenty-five TS+ASD patients (Tukey's multiple comparisons test, multiplicity adjusted p-value < 0.0001) (Figure 3.1). We did not observe any expression differences for miR-140-3p when comparing TS patients to NCs (Tukey's multiple comparisons test, multiplicity adjusted p-value = 0.98), TS+ASD patients to NCs (Tukey's multiple comparisons test, multiplicity adjusted p-value = 0.29), and TS+ASD patients to TS patients (Tukey's multiple comparisons test, multiplicity adjusted p-value = 0.53).

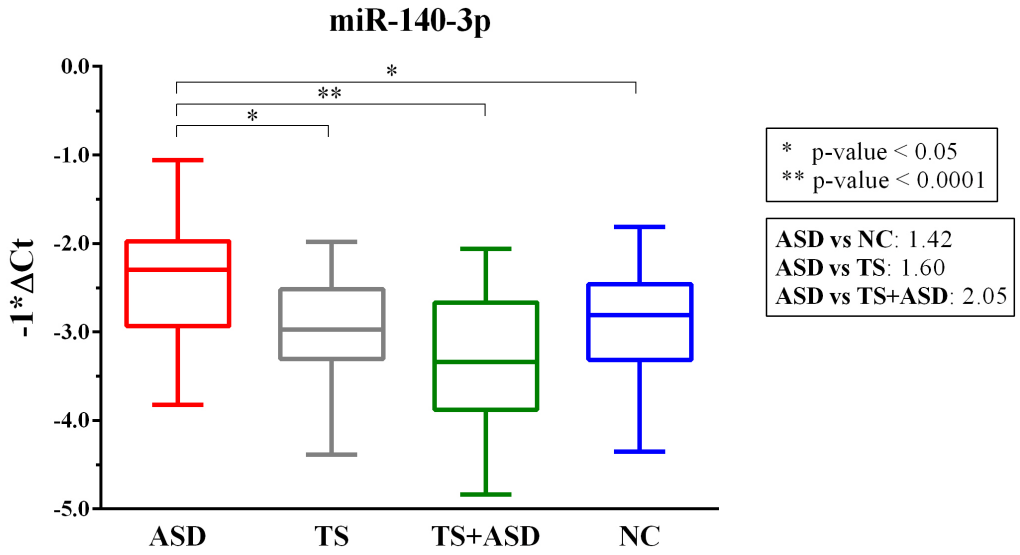

Figure 3. 1. MiR-140-3p is significantly dysregulated in serum of ASD patients. *Single TaqMan assays for miR-140-3p. Box and whiskers plot depicting serum levels of miR-140-3p in ASD, TS, and TS+ASD patients, and NCs. Y-axis represents the distribution of -1*ΔCt values for miR-140-3p. Multiplicity adjusted p-values from Tukey's multiple comparisons test and expression FC (Fold Change) values are shown in the boxes next to the plot.*

3.3.3. Correlation between miR-140-3p expression and neuropsychiatric parameters

In order to test if any link existed between serum expression of miR-140-3p and commonly used ASD and TS neuropsychiatric parameters, we computed the correlation between ΔCt values for miR-140-3p and various neuropsychiatric scores of study participants (Table 3.1).

Table 3. 1. Correlation between miR-140-3p expression and neuropsychiatric parameters. *We performed the analyses in both a general (Section 1) and a class-specific (Sections 2-4) manner. Either Pearson or Spearman r values from every analysis are reported. Bonferroni corrected α = 0.05/16 = 0.003. ASD: Autism Spectrum Disorder; TS: Tourette syndrome; NC: Unaffected Control; IQ: Intelligence Quotient; ADOS: Autism Diagnostic Observation Schedule; YGTSS: Yale Global Tic Severity Scale; 95% CI: 95% Confidence Interval; NT: Not Tested; FDR: False Discovery Rate.*

1. All patients and NCs						
	ΔCt vs. IQ	**ΔCt vs. YGTSS**	**ΔCt vs. ADOS Commu-nication**	**ΔCt vs. ADOS Social interaction**	**ΔCt vs. ADOS Imagination**	**ΔCt vs. ADOS Repetitive and restricted behaviors**
Spearman r	0.02	0.33	-0.13	-0.07	-0.17	NT
Pearson r	NT	NT	NT	NT	NT	-0.17
95% CI	-0.18 - 0.21	0.15 - 0.50	-0.32 - 0.07	-0.27 - 0.12	-0.36 - 0.03	-0.35 - 0.02
two-sided p-value	0.86	0.0005	0.18	0.45	0.09	0.08
Is p < Bonferroni	N	Y	N	N	N	N

corrected α?						
Bonferroni-Holm adjusted p-value	1.00	0.008	1.00	1.00	1.00	1.00
Benjamini-Hochberg p-value (FDR 1%)	0.86	0.008	0.29	0.51	0.23	0.23
Number of XY Pairs	104	104	104	104	104	104
2. ASD patients and NCs						
	ΔCt vs. ADOS Commu-nication	**ΔCt vs. ADOS Social interaction**	**ΔCt vs. ADOS Imagination**	**ΔCt vs. ADOS Repetitive and restricted behaviors**		
Spearman r	-0.27	-0.20	-0.31	NT		
Pearson r	NT	NT	NT	-0.29		
95% CI	-0.51 - 0.003	-0.45 - 0.08	-0.53- -0.04	-0.51- -0.02		
two-sided p-value	0.05	0.15	0.02	0.03		
Is p < Bonferroni corrected α?	N	N	N	N		
Bonferroni-Holm adjusted p-value	0.60	1.00	0.34	0.47		
Benjamini-Hochberg p-value (FDR 1%)	0.18	0.29	0.18	0.18		
Number of XY Pairs	55	55	55	55		
3. TS patients and NCs						
	ΔCt vs. YGTSS					
Spearman r	-0.03					
95% CI	-0.31 - 0.26					
two-sided p-value	0.84					
Is p < Bonferroni corrected α?	N					
Bonferroni-Holm adjusted p-value	1.00					
Benjamini-Hochberg p-value (FDR 1%)	0.86					
Number of XY Pairs	49					
4. TS+ASD patients and NCs						
	ΔCt vs. YGTSS	**ΔCt vs. ADOS Commu-nication**	**ΔCt vs. ADOS Social interaction**	**ΔCt vs. ADOS Imagination**	**ΔCt vs. ADOS Repetitive and restricted behaviors**	
Spearman r	0.21	0.17	0.15	0.17	0.20	
95% CI	-0.08 - 0.47	-0.12 - 0.43	-0.14 - 0.42	-0.12 - 0.44	-0.09 - 0.46	
two-sided p-value	0.14	0.24	0.28	0.23	0.17	
Is p < Bonferroni corrected α?	N	N	N	N	N	

Bonferroni-Holm adjusted p-value	1.00	1.00	1.00	1.00	1.00
Benjamini-Hochberg p-value (FDR 1%)	0.29	0.33	0.35	0.33	0.29
Number of XY Pairs	50	50	50	50	50

When we included all patients and controls in our analysis, we found a positive correlation (Spearman r = 0.33; two-sided p-value = 0.0005, significant according to Bonferroni correction; Holm-Bonferroni corrected p-value = 0.008; BH FDR adjusted p-value = 0.008) and a linear relationship (y = 4.537x - 3.269, y: YGTSS score, x: ΔCt value for miR-140-3p, two-sided p-value = 0.002) between miR-140-3p expression levels and YGTSS scores (Figure 3.2). We could assume that lower serum levels of miR-140-3p, which have been observed in TS+ASD patients, are potentially associated with both occurrence and worsening of motor and phonic tics and that higher serum levels of miR-140-3p, which we found in ASD patients, could be linked to the absence of tics.

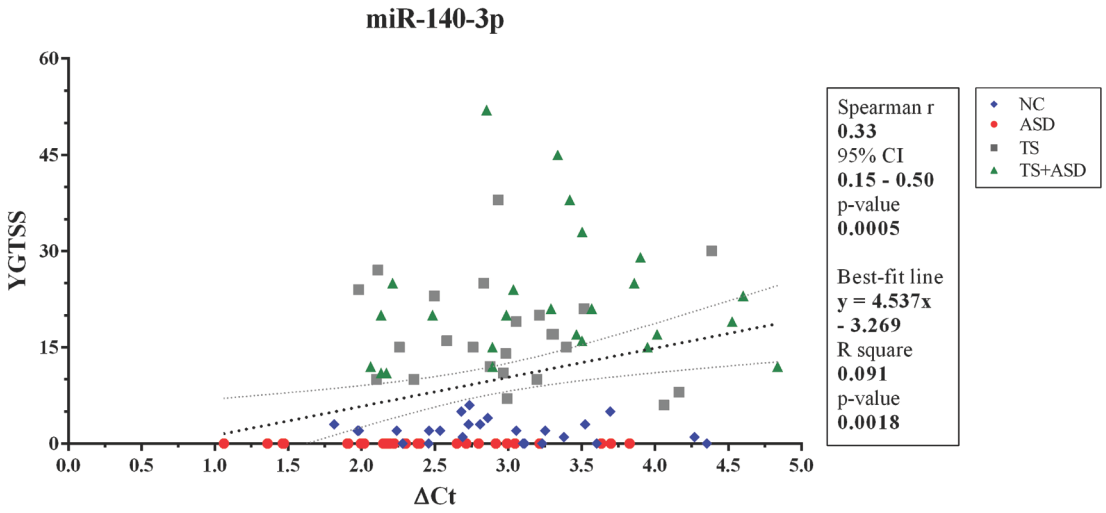

Figure 3. 2. Correlation between serum levels of miR-140-3p and scores from YGTSS scale. *The scatterplot refers to all the 104 analyzed samples and it also reports the best-fit line obtained from linear regression analysis. YGTSS: Yale Global Tic Severity Scale; 95% CI: 95% Confidence Interval.*

This analysis confirmed that serum expression of miR-140-3p correlated with a crucial neuropsychiatric scale for the clinical diagnosis of TS. We infer that miR-140-3p could prove to be useful to strengthen the behavior-based diagnosis of either ASD or TS+ASD, which can be particularly challenging in some clinical cases.

3.3.4. Reconstruction of miR-140-3p-mediated regulatory network: functional and expression analyses of network node genes

By searching on online databases of miRNA-mRNA interactions for validated targets of miR-140-3p, we retrieved CD38 and NRIP1 as its only targets whose validation was based on strong evidence. Through network analysis, we reconstructed the regulatory network composed of MIR140 (microRNA 140, the gene encoding miR-140-3p), CD38, NRIP1, and their first neighbors. This network had 111 nodes and 821 edges. NRIP1, POLR2A (RNA polymerase II subunit A), EP300 (E1A binding protein p300), E2F1 (E2F transcription factor 1), ESR1 (estrogen receptor 1), PHF8 (PHD finger protein 8), and TAF1 (TATA-box binding protein associated factor 1) were the nodes with the highest degree within it (Figure S3.1).

In order to investigate the potential etiological role of this miRNA-mediated network in ASD, we performed functional enrichment analysis of network node genes using GO (Gene Ontology), DO (Disease Ontology), KEGG (Kyoto Encyclopedia of Genes and Genomes), and Reactome gene annotation databases (Figure S3.2-4).

Genes from miR-140-3p-mediated regulatory network played a role in various mechanisms within the nervous system (i.e., neurogenesis, regulation of synaptic plasticity, long-term synaptic depression, cellular response to nerve growth factor, neuron differentiation, dendrite development, and neuronal death). In addition to their role in nervous system development, they were also involved in growth regulation, endocrine system development, heart development, respiratory system development, and tongue development (Table 3.2, Figure S3.5).

Table 3. 2. Over-represented GO Biological Process terms regarding nervous system and development in miR-140-3p-mediated regulatory network. *Term database ID, term description, corresponding BH adjusted p-value generated by the hypergeometric test, Gene Ratio, and Background Ratio values are reported for all the GO Biological Process terms regarding nervous system and development. Gene Ratio: the ratio of number of genes of interest that are annotated with a certain term from the database used to perform the analysis to number of genes of interest that are annotated with terms from the same database. Background Ratio: the ratio of number of genes in the genome that are annotated with a certain term from the database used to perform the analysis to number of genome genes that are annotated with terms from the same database. GO: Gene Ontology; BP: Biological Process; BH: Benjamini-Hochberg.*

GO BP term ID	GO BP term description	BH adjusted p-value	Gene Ratio	Background Ratio
GO:0061029	eyelid development in camera-type eye	2.31E-05	0.0482	0.0008
GO:1990090	cellular response to nerve growth factor stimulus	3.64E-05	0.0602	0.0021
GO:1990089	response to nerve growth factor	4.88E-05	0.0602	0.0023
GO:0048608	reproductive structure development	0.00015	0.1325	0.0244

GO:0061458	reproductive system development	0.00016	0.1325	0.0246
GO:0016049	cell growth	0.00048	0.1325	0.0289
GO:0048732	gland development	0.00061	0.1205	0.0244
GO:0001654	eye development	0.00066	0.1084	0.0197
GO:0051961	negative regulation of nervous system development	0.00068	0.0964	0.0152
GO:0048714	positive regulation of oligodendrocyte differentiation	0.00089	0.0361	0.0009
GO:0008584	male gonad development	0.00089	0.0723	0.0080
GO:0046546	development of primary male sexual characteristics	0.00089	0.0723	0.0080
GO:0008406	gonad development	0.0012	0.0843	0.0125
GO:0030850	prostate gland development	0.0012	0.0482	0.0028
GO:0070997	neuron death	0.0012	0.0964	0.0169
GO:0043010	camera-type eye development	0.0013	0.0964	0.0171
GO:0045137	development of primary sexual characteristics	0.0013	0.0843	0.0128
GO:0001558	regulation of cell growth	0.0016	0.1084	0.0229
GO:0061448	connective tissue development	0.0020	0.0843	0.0139
GO:0030308	negative regulation of cell growth	0.0020	0.0723	0.0098
GO:0007507	heart development	0.0021	0.1205	0.0296
GO:0050768	negative regulation of neurogenesis	0.0021	0.0843	0.0141
GO:1901215	negative regulation of neuron death	0.0024	0.0723	0.0102
GO:2000171	negative regulation of dendrite development	0.0028	0.0361	0.0015
GO:0045665	negative regulation of neuron differentiation	0.0033	0.0723	0.0111
GO:0061196	fungiform papilla development	0.0035	0.0241	0.0004
GO:0001893	maternal placenta development	0.0037	0.0361	0.0017
GO:0048713	regulation of oligodendrocyte differentiation	0.0037	0.0361	0.0017
GO:0010721	negative regulation of cell development	0.0037	0.0843	0.0163
GO:0060541	respiratory system development	0.0041	0.0723	0.0118
GO:0048709	oligodendrocyte differentiation	0.0053	0.0482	0.0047
GO:0035265	organ growth	0.0054	0.0602	0.0084
GO:0060534	trachea cartilage development	0.0054	0.0241	0.0005
GO:0007423	sensory organ development	0.0063	0.1084	0.0298
GO:0045926	negative regulation of growth	0.0069	0.0723	0.0136
GO:0060433	bronchus development	0.0088	0.0241	0.0007
GO:0060525	prostate glandular acinus development	0.0088	0.0241	0.0007
GO:1901214	regulation of neuron death	0.0098	0.0723	0.0150
GO:0060736	prostate gland growth	0.0098	0.0241	0.0007
GO:0060742	epithelial cell differentiation involved in prostate gland development	0.0098	0.0241	0.0007
GO:0030323	respiratory tube development	0.011	0.0602	0.0104
GO:0060348	bone development	0.011	0.0602	0.0105
GO:0051216	cartilage development	0.012	0.0602	0.0108
GO:0003417	growth plate cartilage development	0.012	0.0241	0.0008
GO:0001501	skeletal system development	0.015	0.0964	0.0290
GO:0035855	megakaryocyte development	0.015	0.0241	0.0010
GO:0071696	ectodermal placode development	0.015	0.0241	0.0010

GO:0048638	regulation of developmental growth	0.016	0.0723	0.0173
GO:0010977	negative regulation of neuron projection development	0.016	0.0482	0.0073
GO:0060749	mammary gland alveolus development	0.017	0.0241	0.0011
GO:0061377	mammary gland lobule development	0.017	0.0241	0.0011
GO:0071560	cellular response to transforming growth factor beta stimulus	0.018	0.0602	0.0124
GO:0035270	endocrine system development	0.018	0.0482	0.0077
GO:0071559	response to transforming growth factor beta	0.018	0.0602	0.0125
GO:0060438	trachea development	0.018	0.0241	0.0011
GO:0061180	mammary gland epithelium development	0.018	0.0361	0.0038
GO:0003416	endochondral bone growth	0.020	0.0241	0.0012
GO:0043586	tongue development	0.020	0.0241	0.0012
GO:0048167	regulation of synaptic plasticity	0.021	0.0482	0.0081
GO:0030325	adrenal gland development	0.021	0.0241	0.0013
GO:0001890	placenta development	0.022	0.0482	0.0083
GO:0035264	multicellular organism growth	0.022	0.0482	0.0083
GO:0060351	cartilage development involved in endochondral bone morphogenesis	0.023	0.0241	0.0013
GO:0098868	bone growth	0.023	0.0241	0.0013
GO:0060292	long term synaptic depression	0.024	0.0241	0.0014
GO:0010720	positive regulation of cell development	0.025	0.0843	0.0262
GO:0007176	regulation of epidermal growth factor-activated receptor activity	0.027	0.0241	0.0015
GO:0030878	thyroid gland development	0.027	0.0241	0.0015
GO:0060537	muscle tissue development	0.029	0.0723	0.0206
GO:0030900	forebrain development	0.030	0.0723	0.0209
GO:0048736	appendage development	0.036	0.0482	0.0101
GO:0060173	limb development	0.036	0.0482	0.0101
GO:0030324	lung development	0.037	0.0482	0.0102
GO:0008585	female gonad development	0.037	0.0361	0.0055
GO:0050769	positive regulation of neurogenesis	0.038	0.0723	0.0225
GO:0045684	positive regulation of epidermis development	0.038	0.0241	0.0019
GO:0060612	adipose tissue development	0.038	0.0241	0.0019
GO:0098751	bone cell development	0.038	0.0241	0.0019
GO:0046545	development of primary female sexual characteristics	0.040	0.0361	0.0057
GO:0048738	cardiac muscle tissue development	0.042	0.0482	0.0108
GO:0021761	limbic system development	0.042	0.0361	0.0058
GO:0031076	embryonic camera-type eye development	0.043	0.0241	0.0021
GO:0016358	dendrite development	0.047	0.0482	0.0113

MIR140 gene was annotated with the over-represented DO term physical disorder, that refers to diseases determined by a genetic abnormality, error with embryonic development, infection or compromised intrauterine environment (DOID:0080015; BH adjusted p-value = 0.027; Gene Ratio = 0.070;

Background Ratio = 0.017). Among the most interesting terms whose enrichment was determined by CD38, we found those regarding response to estradiol, retinoic acid, drugs, hypoxia, ketone, and oxidative stress, activation and proliferation of immune cells, regulation of protein localization, cellular calcium ion homeostasis, and blood circulation. We found bacterial infectious disease as the only DO term. Finally, CD38 was directly involved in the regulation of synaptic plasticity and long-term synaptic depression (Table 3.3, Figure S3.6).

Table 3. 3. Over-represented GO, DO, and KEGG terms associated with CD38 in miR-140-3p-mediated regulatory network. *Term database ID, term description, corresponding BH adjusted p-value generated by the hypergeometric test, Gene Ratio, and Background Ratio values are reported for all the over-represented terms with which CD38 is annotated. For in-depth description of the column names see Table 3.2 legend. GO: Gene Ontology; BP: Biological Process; DO: Disease Ontology; KEGG: Kyoto Encyclopedia of Genes and Genomes; BH: Benjamini-Hochberg.*

Annotation Database	Term ID	Term description	BH adjusted p-value	Gene Ratio	Background Ratio
GO BP	GO:0048545	response to steroid hormone	2.94E-35	0.4337	0.0221
GO BP	GO:0032355	response to estradiol	5.13E-08	0.1205	0.0070
GO BP	GO:0070482	response to oxygen levels	4.53E-07	0.1566	0.0181
KEGG	hsa05169	Epstein-Barr virus infection	3.36E-06	0.1884	0.0283
GO BP	GO:0001101	response to acid chemical	7.61E-06	0.1325	0.0158
GO BP	GO:0042493	response to drug	7.61E-06	0.1566	0.0238
GO BP	GO:0002764	immune response-regulating signaling pathway	3.86E-05	0.1566	0.0294
GO BP	GO:0051251	positive regulation of lymphocyte activation	4.72E-05	0.1205	0.0166
GO BP	GO:0036293	response to decreased oxygen levels	5.76E-05	0.1205	0.0171
GO BP	GO:0002768	immune response-regulating cell surface receptor signaling pathway	6.41E-05	0.1325	0.0217
GO BP	GO:0002694	regulation of leukocyte activation	7.86E-05	0.1446	0.0269
GO BP	GO:0002696	positive regulation of leukocyte activation	8.41E-05	0.1205	0.0180
GO BP	GO:0002757	immune response-activating signal transduction	8.67E-05	0.1446	0.0274
GO BP	GO:0050867	positive regulation of cell activation	9.75E-05	0.1205	0.0185
GO BP	GO:0051249	regulation of lymphocyte activation	0.00012	0.1325	0.0238
GO BP	GO:0050865	regulation of cell activation	0.00013	0.1446	0.0289
GO BP	GO:0002429	immune response-activating cell surface receptor signaling pathway	0.00015	0.1205	0.0197
GO BP	GO:0001666	response to hypoxia	0.00025	0.1084	0.0166
GO BP	GO:0032526	response to retinoic acid	0.00028	0.0723	0.0061
GO BP	GO:0016049	cell growth	0.00048	0.1325	0.0289
GO BP	GO:0007565	female pregnancy	0.00055	0.0843	0.0107
GO BP	GO:0044706	multi-multicellular organism process	0.0010	0.0843	0.0121
GO BP	GO:0050708	regulation of protein secretion	0.0015	0.1084	0.0226
GO BP	GO:0001558	regulation of cell growth	0.0016	0.1084	0.0229

GO BP	GO:0050851	antigen receptor-mediated signaling pathway	0.0017	0.0843	0.0134
GO BP	GO:0032844	regulation of homeostatic process	0.0032	0.1084	0.0260
GO BP	GO:0050670	regulation of lymphocyte proliferation	0.0033	0.0723	0.0111
GO BP	GO:0032944	regulation of mononuclear cell proliferation	0.0034	0.0723	0.0112
GO BP	GO:0070663	regulation of leukocyte proliferation	0.0039	0.0723	0.0117
GO BP	GO:0009306	protein secretion	0.0042	0.1084	0.0276
GO BP	GO:1904951	positive regulation of establishment of protein localization	0.0063	0.1084	0.0299
GO BP	GO:0046651	lymphocyte proliferation	0.0094	0.0723	0.0148
GO BP	GO:0032943	mononuclear cell proliferation	0.0097	0.0723	0.0149
GO BP	GO:0050796	regulation of insulin secretion	0.0098	0.0602	0.0101
GO BP	GO:0070661	leukocyte proliferation	0.012	0.0723	0.0158
GO BP	GO:0010817	regulation of hormone levels	0.012	0.0964	0.0276
GO BP	GO:0006979	response to oxidative stress	0.014	0.0843	0.0226
GO BP	GO:0090276	regulation of peptide hormone secretion	0.015	0.0602	0.0116
GO BP	GO:0030073	insulin secretion	0.015	0.0602	0.0118
GO BP	GO:0044057	regulation of system process	0.016	0.0964	0.0295
GO BP	GO:0002791	regulation of peptide secretion	0.016	0.0602	0.0119
GO BP	GO:0090087	regulation of peptide transport	0.016	0.0602	0.0121
GO BP	GO:0050671	positive regulation of lymphocyte proliferation	0.017	0.0482	0.0074
GO BP	GO:0032946	positive regulation of mononuclear cell proliferation	0.017	0.0482	0.0075
GO BP	GO:0050853	B cell receptor signaling pathway	0.018	0.0361	0.0038
GO BP	GO:0070665	positive regulation of leukocyte proliferation	0.019	0.0482	0.0079
GO BP	GO:0048167	regulation of synaptic plasticity	0.021	0.0482	0.0081
DO	DOID:104	bacterial infectious disease	0.022	0.1047	0.0338
GO BP	GO:0060292	long term synaptic depression	0.024	0.0241	0.0014
GO BP	GO:0030072	peptide hormone secretion	0.026	0.0602	0.0140
GO BP	GO:0042113	B cell activation	0.027	0.0602	0.0142
DO	DOID:0050338	primary bacterial infectious disease	0.027	0.0930	0.0297
GO BP	GO:0002790	peptide secretion	0.028	0.0602	0.0145
GO BP	GO:0046883	regulation of hormone secretion	0.030	0.0602	0.0148
GO BP	GO:1901654	response to ketone	0.032	0.0482	0.0097
GO BP	GO:0015833	peptide transport	0.033	0.0602	0.0154
GO BP	GO:0006874	cellular calcium ion homeostasis	0.037	0.0723	0.0222
GO BP	GO:0008015	blood circulation	0.037	0.0843	0.0290
GO BP	GO:0003013	circulatory system process	0.038	0.0843	0.0293
GO BP	GO:0055074	calcium ion homeostasis	0.041	0.0723	0.0230
GO BP	GO:0042886	amide transport	0.041	0.0602	0.0166
GO BP	GO:0072503	cellular divalent inorganic cation homeostasis	0.046	0.0723	0.0237
GO BP	GO:0046879	hormone secretion	0.047	0.0602	0.0173

Among the most interesting terms whose enrichment was determined by NRIP1, there were those related to response to estradiol and steroid hormones, reproductive system development, and development of primary sexual characteristics. NRIP1 was annotated with many molecular functions (i.e., histone deacetylase binding, nuclear hormone receptor binding, core promoter sequence-specific DNA binding, retinoic acid receptor binding, and retinoid X receptor binding). Finally, NRIP1 regulated the transcription of genes involved in circadian rhythm by interacting with RORA (RAR related orphan receptor A) (Table 3.4, Figure S3.7).

Table 3. 4. Over-represented GO, DO, and Reactome terms associated with NRIP1 in miR-140-3p-mediated regulatory network. *Term database ID, term description, corresponding BH adjusted p-value generated by the hypergeometric test, Gene Ratio, and Background Ratio values are reported for all the over-represented terms with which NRIP1 is annotated. For in-depth description of the column names see Table 3.2 legend. GO: Gene Ontology; BP: Biological Process; MF: Molecular Function; CC: Cellular Component; DO: Disease Ontology; BH: Benjamini-Hochberg.*

Annotation Database	Term ID	Term description	BH adjusted p-value	Gene Ratio	Background Ratio
GO BP	GO:0043401	steroid hormone mediated signaling pathway	8.14E-41	0.398	0.011
GO BP	GO:0071383	cellular response to steroid hormone stimulus	1.44E-40	0.422	0.014
GO BP	GO:0030522	intracellular receptor signaling pathway	1.44E-40	0.434	0.016
GO BP	GO:0009755	hormone-mediated signaling pathway	1.45E-38	0.398	0.013
GO BP	GO:0048545	response to steroid hormone	2.94E-35	0.434	0.022
GO BP	GO:0071396	cellular response to lipid	9.41E-34	0.458	0.029
GO BP	GO:0071407	cellular response to organic cyclic compound	1.55E-33	0.458	0.030
GO MF	GO:0008134	transcription factor binding	4.77E-24	0.373	0.031
GO MF	GO:0003713	transcription coactivator activity	1.56E-14	0.229	0.018
GO MF	GO:0035257	nuclear hormone receptor binding	3.23E-12	0.157	0.008
GO BP	GO:0030518	intracellular steroid hormone receptor signaling pathway	9.27E-12	0.157	0.007
GO MF	GO:0051427	hormone receptor binding	2.09E-11	0.157	0.009
GO CC	GO:0000790	nuclear chromatin	1.09E-10	0.190	0.017
GO CC	GO:0044454	nuclear chromosome part	1.16E-10	0.226	0.028
GO CC	GO:0000785	chromatin	1.61E-10	0.214	0.025
GO MF	GO:0001047	core promoter binding	6.28E-10	0.145	0.010
GO MF	GO:0035258	steroid hormone receptor binding	4.19E-09	0.108	0.005
GO BP	GO:0048511	rhythmic process	6.87E-09	0.181	0.019
GO BP	GO:0007623	circadian rhythm	3.12E-08	0.145	0.011
GO BP	GO:0032355	response to estradiol	5.13E-08	0.120	0.007
GO MF	GO:0042826	histone deacetylase binding	5.96E-08	0.108	0.006
GO MF	GO:0001046	core promoter sequence-specific DNA binding	7.31E-07	0.096	0.006

GO MF	GO:0042974	retinoic acid receptor binding	1.63E-06	0.060	0.001
GO MF	GO:0003714	transcription corepressor activity	2.20E-06	0.120	0.013
GO MF	GO:0046965	retinoid X receptor binding	8.63E-06	0.048	0.001
GO BP	GO:0032922	circadian regulation of gene expression	2.31E-05	0.072	0.003
GO BP	GO:0030521	androgen receptor signaling pathway	3.24E-05	0.072	0.004
GO BP	GO:0048608	reproductive structure development	0.00015	0.133	0.024
GO MF	GO:0035259	glucocorticoid receptor binding	0.00016	0.036	0.001
GO BP	GO:0061458	reproductive system development	0.00016	0.133	0.025
GO CC	GO:0000118	histone deacetylase complex	0.00019	0.060	0.003
GO MF	GO:0030331	estrogen receptor binding	0.00024	0.048	0.002
GO MF	GO:0050681	androgen receptor binding	0.00033	0.048	0.002
GO BP	GO:0019915	lipid storage	0.00035	0.060	0.004
GO BP	GO:0051235	maintenance of location	0.00035	0.108	0.018
GO BP	GO:0007548	sex differentiation	0.00084	0.096	0.016
Reactome	400253	Circadian Clock	0.00091	0.069	0.005
GO BP	GO:0008406	gonad development	0.0012	0.084	0.012
GO BP	GO:0045137	development of primary sexual characteristics	0.0013	0.084	0.013
Reactome	1368082	RORA activates gene expression	0.0018	0.042	0.001
DO	DOID:3308	embryonal carcinoma	0.0028	0.047	0.003
GO BP	GO:0071392	cellular response to estradiol stimulus	0.0040	0.036	0.002
GO BP	GO:0010876	lipid localization	0.011	0.084	0.021
DO	DOID:11612	polycystic ovary syndrome	0.020	0.081	0.021
DO	DOID:688	embryonal cancer	0.020	0.128	0.047
DO	DOID:2994	germ cell cancer	0.029	0.128	0.051
GO BP	GO:0022602	ovulation cycle process	0.030	0.036	0.005
GO BP	GO:0008585	female gonad development	0.037	0.036	0.005
GO BP	GO:0046545	development of primary female sexual characteristics	0.040	0.036	0.006
GO BP	GO:0042698	ovulation cycle	0.048	0.036	0.006

To verify if dysregulation of network node genes was implicated in ASD, we used publicly available raw high-throughput gene expression datasets produced from the analysis of ASD samples. Ten genes were found to be downregulated in whole blood of ASD patients compared to NCs (log_2FC, Fold Change < -1): CCDC85B (coiled-coil domain containing 85B), CD3E (CD3e molecule), CIB1 (calcium and integrin binding 1), CTBP1 (C-terminal binding protein 1), LCK (LCK proto-oncogene, Src family tyrosine kinase), MAP3K7 (mitogen-activated protein kinase kinase kinase 7), NR1H2 (nuclear receptor subfamily 1 group H member 2), RARA (retinoic acid receptor alpha), STAT3 (signal transducer and activator of transcription 3), and ZAP70 (zeta chain of T cell receptor associated protein kinase 70); two were found to be overexpressed ($log_2FC > 1$): PHF8 and TAF1 (Figure 3.3).

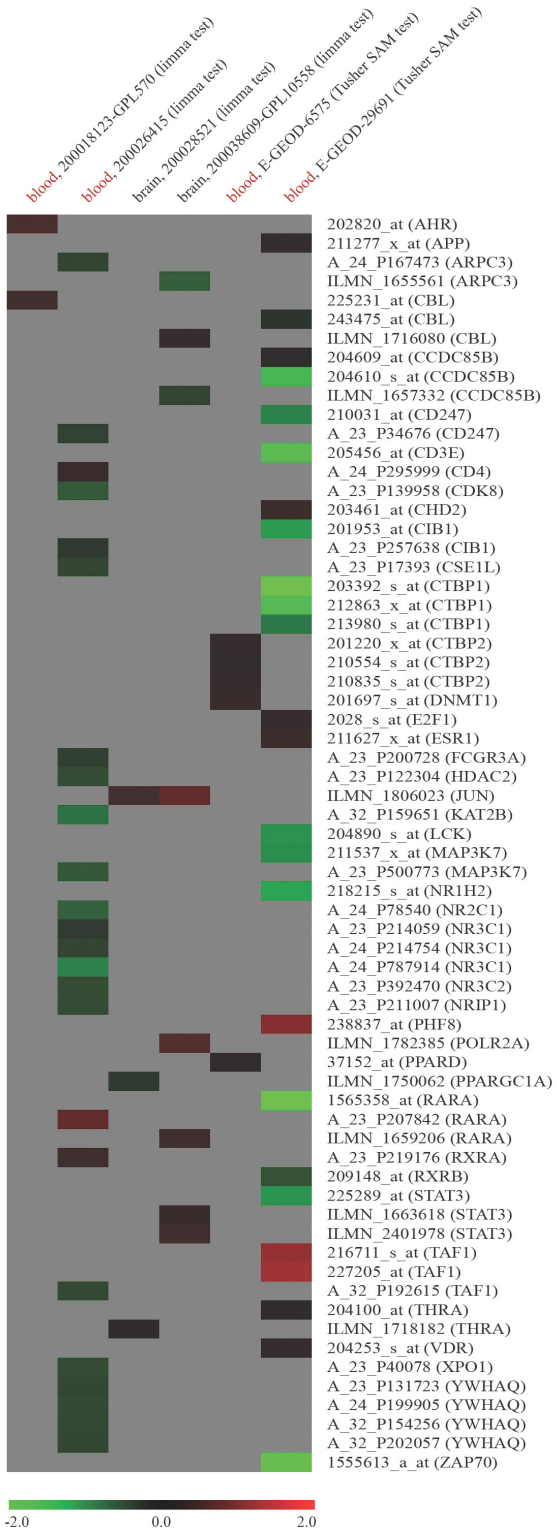

Figure 3. 3. Expression analysis of node genes within miR-140-3p-mediated regulatory network in human ASD high-throughput gene expression datasets retrieved from GEO DataSets and ArrayExpress. *Datasets used for the expression analysis (human ASD source tissue, dataset ID, platform type, statistical test performed) and microarray probe IDs along with their corresponding gene symbols are reported in columns and rows of this gene expression heatmap, respectively. Colored heatmap cells represent genes that are DE in a certain dataset. Data are shown as log_2FC expression values. For more information about gene expression trend, see figure legend.*

3.3.5. Serum levels of miR-140-3p in the discrimination of ASD patients

We used ΔCt values for miR-140-3p to perform a classical univariate ROC (Receiver Operator Characteristic) curve analysis for each of the comparisons where we found this miRNA to be dysregulated. The univariate ROC plots revealed an AUC of 0.71 for the comparison ASD vs NC (p-value = 0.006), 0.73 for ASD vs TS (p-value = 0.002), and 0.78 for ASD vs TS+ASD (p-value = 0.00007) (Figure 3.4).

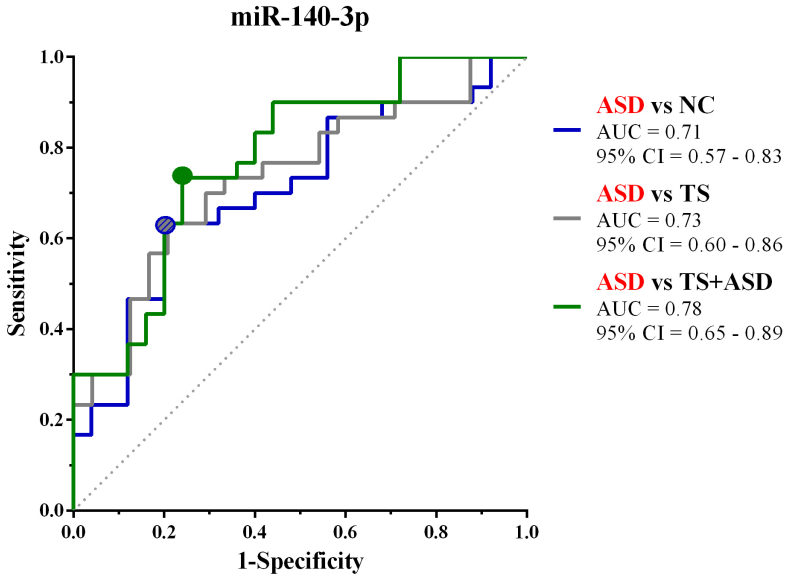

Figure 3. 4. Classical univariate ROC curve analyses for the comparisons in which miR-140-3p is dysregulated. *This graph compares three ROC curves, one for each comparison where we found miR-140-3p to be dysregulated. Each point on the ROC curves represents a sensitivity/specificity pair corresponding to a particular decision threshold (ΔCt value cut-off). Circles on the curves refer to the sensitivity/specificity pairs with the highest Youden index J. AUC: Area under the ROC curve; 95% CI: 95% Confidence Interval.*

We used ΔCt value cut-offs corresponding to the sensitivity/specificity pair with the highest Youden index J for every computed ROC curve to perform a blind diagnosis on all the 104 analyzed samples (Figure 3.5).

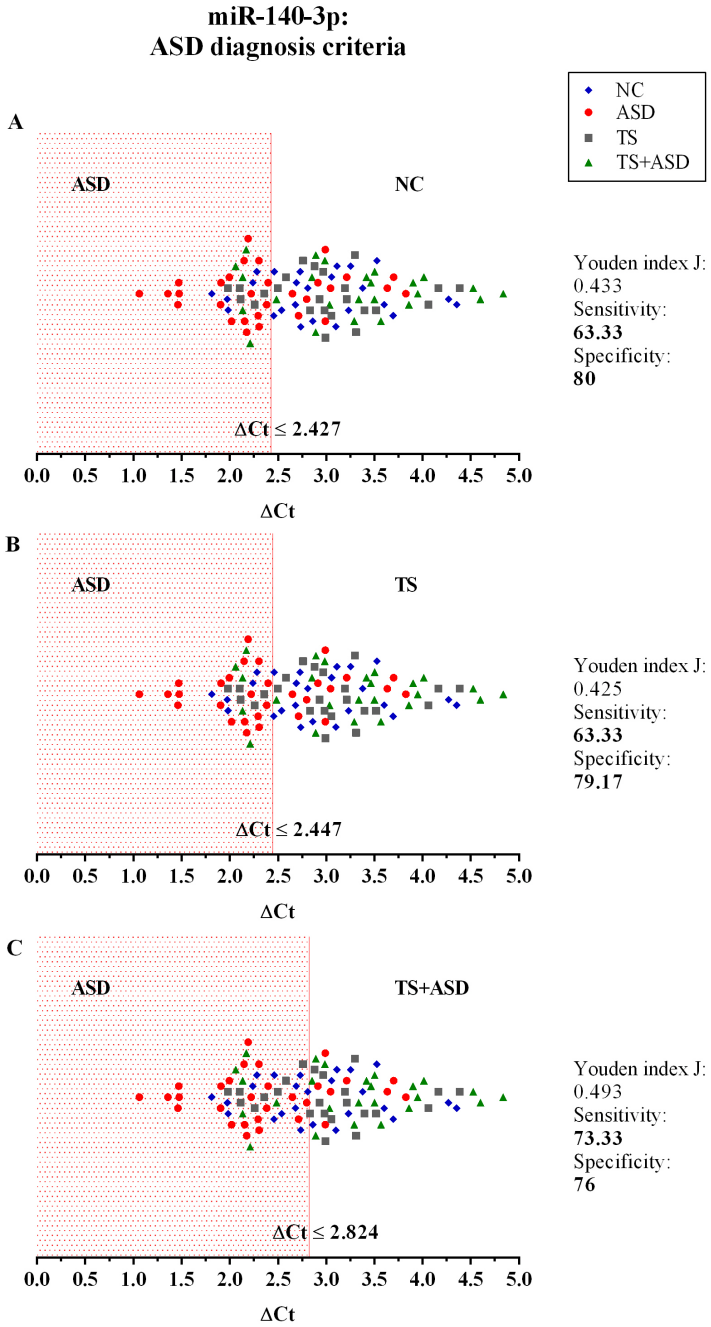

Figure 3. 5. The potential use of serum miR-140-3p as a biomarker: criteria for ASD diagnosis. *The graphs show the distribution of ΔCt values of all the 104 analyzed samples, for which we already had a clinical diagnosis. We used data from classical univariate ROC curve analyses to perform a blind diagnosis of all study participants. In panel (A), the ΔCt ≤ 2.427 criterion divides ASD patients from NCs and determines the correct discrimination of 19/32 ASD patients and 20/25 NCs. In panel (B), the ΔCt ≤ 2.447 criterion divides ASD patients from TS patients and determines the correct discrimination of 19/32 ASD patients and 19/24 TS patients. In panel (C), the ΔCt ≤ 2.824 criterion separates ASD patients from TS+ASD patients and determines the correct discrimination of 22/32 ASD patients and 19/25 TS+ASD patients.*

Then, we built a logistic regression model for miR-140-3p expression in each comparison and we tested those predictive models through CV (cross-validation) and permutation testing. 100-time repeated random sub-sampling CV was used to test the performance of the logistic regression models. MiR-140-3p continued to perform at a good level for the comparison ASD vs NC, with an average AUC of 0.70, a sensitivity of 63.33%, and a specificity of 68% (Figure 3.6.1C-D). MiR-140-3p continued to perform at a good level also for the comparison ASD vs TS, with an average AUC of 0.72, a sensitivity of 66.66%, and a specificity of 70.83% (Figure 3.6.2C-D). MiR-140-3p continued to perform at a very high level for the comparison ASD vs TS+ASD, with an average AUC of 0.78, a sensitivity of 73.33%, and a specificity of 76% (Figure 3.6.3C-D). CV results demonstrated the general applicability of these predictive models. 100-time repeated permutation tests on the performance measure AUC were carried out to validate the structure of these models. Permutation testing results were significant and quite stable in different runs for all the models tested (Figure 3.6.1E, .2E, and .3E).

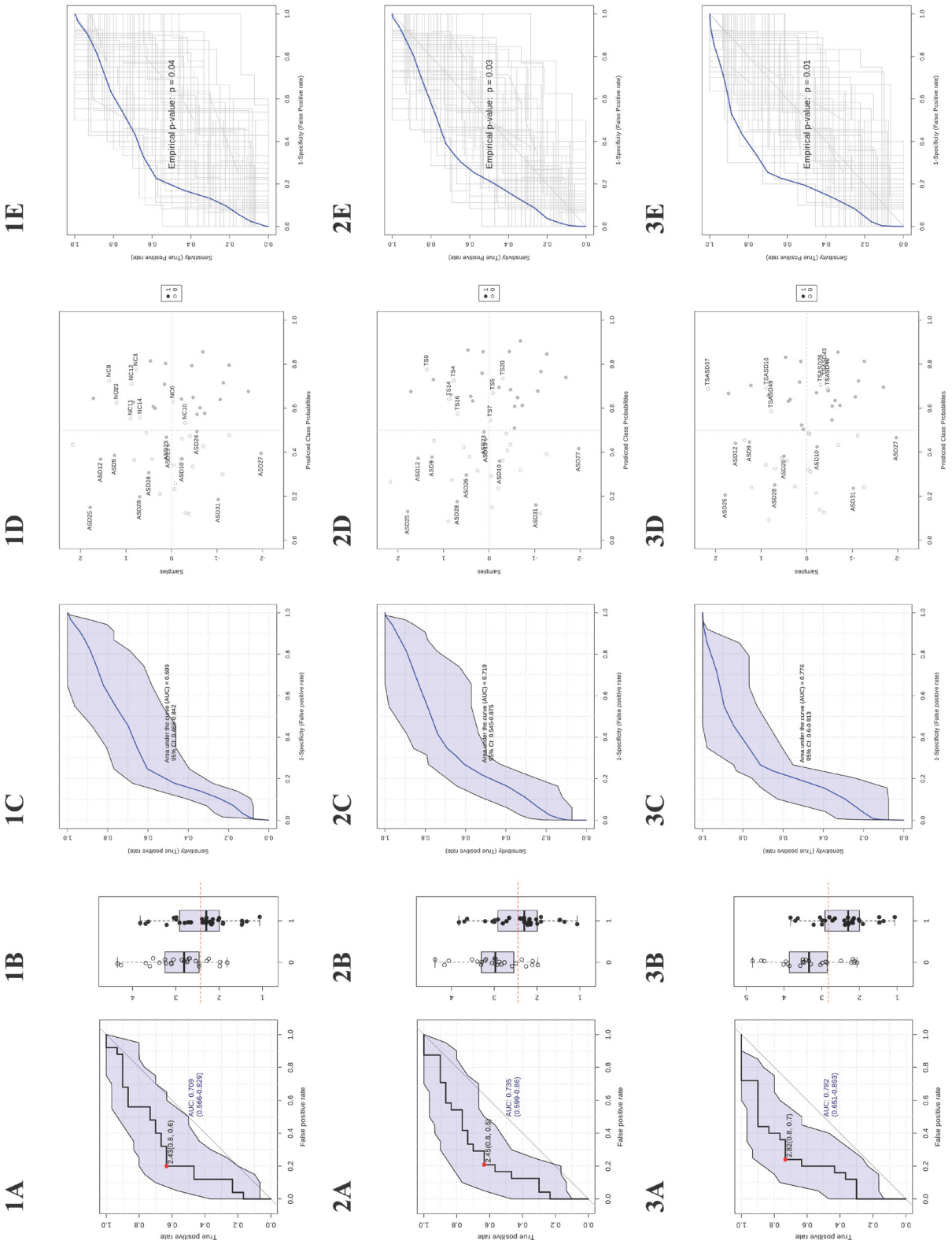

Figure 3. 6. Serum miR-140-3p could be used to discriminate ASD patients. *(1) The graphs refer to the comparison ASD vs NC. (2) The graphs refer to the comparison ASD vs TS. (3) The graphs refer to the comparison ASD vs TS+ASD. (A) Classical univariate ROC curve analysis. The red dot represents the sensitivity/specificity pair with the highest Youden index J. (B) Boxplot depicting the distribution of ΔCt values in the two groups. The red line represents the ΔCt value cut-off corresponding to the red dot on the curve in (A). The label 1 refers to the ASD group, 0 to the other group. (C) Average ROC curve*

from 100-time repeated random sub-sampling CV of the built logistic regression model. (D) Average predicted class probabilities (x-axis) of each sample (y-axis) from the 100 CV iterations. Probability scores more than 0.5 belong to the ASD group, those less than 0.5 belong to the other group. Incorrectly classified subjects are identified by their ID number. (E) Results from the permutation tests on the model performance measure AUC. Average ROC curve and corresponding p-value are reported. AUC: Area under the ROC curve; 95% CI: 95% Confidence Interval.

These data proved that serum miR-140-3p could be used in the discrimination of ASD patients. In particular, it could potentially support the differential behavior-based diagnostic process of two classes of neurodevelopmental disorders, ASD and TS+ASD.

3.4. Discussion

Many factors, including disorders that are comorbid with ASD, like TS, complicate ASD behavior-based diagnosis and make it vulnerable to bias. Stability, general consistency of expression among individuals, and condition-specific expression profile make circulating miRNAs appropriate non-invasive diagnostic biomarkers (Weiland et al., 2012; Larrea et al., 2016). We hypothesized that serum profile of circulating miRNAs may contain specific fingerprints for ASD: these could provide some hints to the molecular basis of ASD and be used as supportive means to the clinical diagnostic process, especially in the discrimination among neurodevelopmental disorders.

Using TLDA technology, we profiled serum expression of 754 human miRNAs in a discovery set of samples, including four ASD, five TS, and four TS+ASD patients and three NCs. The undeniable limit of this profiling approach is that, despite analyzing a total number of 16 samples in this exploratory step, we could have missed some significantly dysregulated circulating miRNAs because of the small number of samples in each compared group. However, we also applied very strict selection criteria for the identification of those 9 miRNAs (miR-30d, miR-30e-3p, miR-140-3p, miR-148a*, miR-222, miR-454, miR-483-5p, miR-1274B, and miR-1290) as differentially expressed, in order to spot more robust findings, likely to be confirmed in the next validation step. Nevertheless, through single TaqMan assays we observed the dysregulation of just one (miR-140-3p) of the four miRNAs selected for validation (miR-30d, miR-140-3p, miR-148a*, and miR-222) even if, according to results from profiling, those showed the most interesting and marked expression trends. This could be explained by the fact that TLDA approach is still a high-throughput one: the preliminary step of preamplification suggested for TLDA analysis may have inserted an amplification bias, leading to not very accurate results. Knowing how crucial validation is, we have also performed this step by TaqMan assay, a probe-based system that is designed to specifically detect the expression of miRNAs of interests.

There is no consensus about optimal normalization strategies and accurate reference genes for both intracellular and extracellular miRNAs (Schwarzenbach et al., 2015). Suggested endogenous controls

for miRNAs differ depending on: (1) the species considered; (2) either the tissue or body fluid analyzed; (3) either the physiological or pathological condition investigated; (4) different sample preparation methods, especially for circulating miRNAs (Marabita et al., 2016). On one hand, researchers can select reference miRNA genes according to reports from similar studies in the literature, and then, validate them for the set of samples under analysis (Schwarzenbach et al., 2015). On the other, they can screen the specific samples for more suitable endogenous controls through the profiling of a large number of genes. In this case, it is suggested to use either the mean expression values of all the profiled miRNAs in each of the samples or genes with expression levels similar to these values as the screened endogenous controls (Schwarzenbach et al., 2015; Marabita et al., 2016). At the moment, accurately described normalization approaches and validated reference genes for serum miRNAs in ASD patients lack: this, together with different ethnicity of participants and other potential diverse analytic variables in studies similar to ours, led us to prefer our customized normalization approach over reference gene selection from literature. This approach, which is inspired to the recommended miRNA array normalization strategy reported above (Schwarzenbach et al., 2015; Marabita et al., 2016), has proved its value in other works on neurological disorders published by our group (Rizzo et al., 2015; Ragusa et al., 2016). Thanks to it, we have selected miR-146a and miR-223* as the most appropriate and accurate reference genes for our system. Some studies have identified miR-146a as either dysregulated in human ASD tissues (Mor et al., 2015; Nguyen et al., 2016) or associated to inflammation and immune response observed in neurodegenerative and neurological disorders (Iyer et al., 2012; Kiko et al., 2014; Müller et al., 2014; Wang et al., 2015; An et al., 2016; Romano et al., 2017): however, this neither discourages its use as reference miRNA in our dataset nor affects the applicability of our results from differential expression analysis.

Through our expression analysis, we have identified miR-140-3p as dysregulated in serum from ASD patients. It is upregulated in ASD patients compared to NCs, TS patients, and TS+ASD patients: its levels are the highest in the ASD group (Figure 3.1). We observed that miR-140-3p levels are the lowest in the TS+ASD group. It is interesting that the two groups ASD and TS+ASD showed such a different expression trend for this miRNA. It is likely that the lower miR-140-3p expression reflects the presence of phonic and motor tics due to the comorbidity of TS with ASD. It may also depend on other either physiological conditions or comorbidities: this needs to be further investigated. On the contrary, according to our previous study on TS (Rizzo et al., 2015), we expected not to find any difference in miR-140-3p expression between TS patients and NCs.

According to expression data from the Human miRNA Tissue Atlas (Ludwig et al., 2016), miR-140-3p is highly expressed in bone, nerves, arteries, meninges (arachnoid mater and dura mater), muscle, and adipose tissue. Published data also confirm that miR-140-3p is one of the top highly expressed miRNAs in the human brain cortex (Shao et al., 2010) and that it is not specific for any of the different human

blood cell compounds (Leidinger et al., 2014). The intracellular roles exerted by miR-140-3p have been mainly investigated in human pathologies, such as cancer (Lionetti et al., 2009; Tan et al., 2011; Miles et al., 2012; Piepoli et al., 2012; Sand, Skrygan, Georgas et al., 2012; Sand, Skrygan, Sand et al., 2012; Serrano et al., 2012; Bayrak et al., 2013; Yuan et al., 2014; Zou et al., 2014; Kong et al., 2015; Reddemann et al., 2015; Chang et al., 2016; Dong et al., 2016; Gulluoglu et al., 2016; Salem et al., 2016; Zhu et al., 2016), asthma (Jude et al., 2012; Dileepan et al., 2016), osteoarthritis (Rasheed et al., 2017), and rheumatoid arthritis (Peng, Chen, et al., 2016). Studies on mouse and rat models have also proved its involvement in spermatogenesis (Lou et al., 2015) and testis differentiation (Rakoczy et al., 2013), chondrogenesis and growth (Pando et al., 2012; Waki et al., 2016), and sensitivity of fetal neural development to ethanol and nicotine (Balaraman et al., 2012). Circulating miR-140-3p has been identified as dysregulated in either plasma or serum from patients with different pathological conditions and it has already been suggested as a potential biomarker for some of them, like myotonic dystrophy type 1 and type 2 (Perfetti et al., 2014; 2016), biliary atresia (Peng, Yang, et al., 2016), papillary thyroid carcinoma (Li et al., 2015), wet age-related macular degeneration (Ertekin et al., 2014), and myasthenia gravis (Nogales-Gadea et al., 2014). Its potential as non-invasive intracellular biomarker has also been demonstrated in blood samples from patients affected by coronary artery disease (Taurino et al., 2010; Karakas et al., 2017) and type 2 diabetes mellitus (Collares et al., 2013). Finally, it has already been associated with two psychiatric mood disorders: it is upregulated in whole blood of BD patients (Maffioletti et al., 2016) and major depression patients after 12 weeks of antidepressant treatment (Bocchio-Chiavetto et al., 2013).

We found a positive correlation and a linear relationship between ΔCt values for miR-140-3p and YGTSS scores of all study participants (Figure 3.2). Lower serum levels of miR-140-3p, which we observed in TS+ASD patients, could be potentially associated with both occurrence and worsening of motor and phonic tics, whereas higher serum levels of miR-140-3p, which we found in ASD patients, could be linked to the absence of tics. This finding indicates that expression analysis of serum miR-140-3p could strengthen the clinical diagnostic process of either ASD or TS+ASD. Moreover, this result gives strength to the hypothesis that the presence of phonic and motor tics, determining the comorbidity of TS with ASD, may be responsible for the different levels of serum miR-140-3p between ASD and TS+ASD patients.

Through network functional analysis, we observed that the regulatory network mediated by miR-140-3p is partly involved in managing structural and functional integrity of the nervous system and in the development of several human systems and organs (Table 3.2, Figure S3.5). In particular, our computational data showed that CD38 and NRIP1, validated targets of miR-140-3p, take part in a set of biological processes convergingly dysregulated in ASD, like synaptic plasticity, immune response, and

chromatin binding (Voineagu and Eapen, 2013; Gokoolparsadh et al., 2016; Ansel et al., 2017) (Tables 3.3-4, Figures S3.6-7).

CD38 was initially identified as an activation marker of immune cells, but it is now considered a virtually ubiquitous multifunctional molecule, involved in signaling and cell homeostasis. It is expressed in human lymphoid tissues as well as non-lymphoid ones, such as brain, eye, prostate, gut, pancreas, muscle, bone, and kidney. It is highly expressed in the brain, particularly in the hypothalamus (Quarona et al., 2013). It plays a dual role as both transmembrane receptor and enzyme since it catalyzes the formation of cyclic ADP ribose (cADPR), ADP ribose (ADPR), and nicotinic acid adenine dinucleotide phosphate (NAADP) from nicotinamide adenine dinucleotide (NAD+). Thanks to its ADP-ribosyl cyclase activity, CD38 regulates the mobilization of calcium ion from intracellular stores and therefore, it is mainly involved in proliferation, contraction, and secretion. Moreover, being a NAD glycohydrolase (NADase), it controls aging, cell protection, and energy metabolism (Quarona et al., 2013). It has also been found in a soluble form, maintaining this enzymatic activity, in body fluids and in exosomes (Quarona et al., 2013). CD38 has been linked to HIV infection, cancer, type 2 diabetes mellitus, and asthma (Quarona et al., 2013). Its enzymatic activity is responsible for the secretion of oxytocin (OT) and makes it one of the principal regulators of the social brain (Jin et al., 2007). In fact, it has been observed that adult CD38 knockout (CD38-/-) mice had marked defects in social behavior and strongly decreased plasma and CSF (cerebrospinal fluid) levels of OT. Social defects could be rescued with either subcutaneous OT injection or CD38 re-expression in the hypothalamus. Final in vitro experiments on oxytocinergic neurohypophysial axon terminals proved that ADP-ribosyl cyclase activity of CD38 was responsible for the secretion of OT (Jin et al., 2007). Other than in social behavior, CD38 plays a role also in hippocampus-dependent learning and memory (Kim et al., 2016) and in postnatal glial development (Hattori et al., 2017). It is not surprising that much evidence has linked CD38 to ASD. Two genetic variants of CD38, the intronic SNP rs3796863 and the common Japanese SNP rs1800561 (causing the R140W mutation), have been associated with high-functioning ASD in Caucasian patients and with ASD in Japanese patients, respectively (Munesue et al., 2010). In a study on two young sisters with ASD, a deletion of 4p15.32 resulting in a BST1 (bone marrow stromal cell antigen 1) - CD38 fusion transcript and in disruption of CD38 expression was identified only in the girl affected by more severe ASD and asthma (Ceroni et al., 2014). CD38 expression is markedly reduced in LBC (lymphoblastoid cell) lines derived from ASD patients compared to their unaffected parents (Lerer et al., 2010); ATRA (all-trans retinoic acid) can upmodulate CD38 expression in these cells (Riebold et al., 2011). Finally, in a study evaluating differences in number and phenotype of circulating blood cells in young ASD patients compared to healthy controls, it has been observed that ASD patients have a higher absolute number of B cells per volume of blood and number of B cells expressing the cellular activation marker CD38 (Ashwood et al., 2011).

NRIP1 (also known as RIP140, receptor-interacting protein 140) is a widely expressed, multifaceted transcription co-regulator. Its primary physiological action is to trigger hormone-controlled gene suppression. It can interact with most nuclear receptors (such as estrogen, retinoic acid, and glucocorticoid receptors) and bind many other transcription factors, co-regulators, and DNA and histone modifying enzymes (Nautiyal et al., 2013). NRIP1 mainly controls female fertility in the ovary, promoting ovulation, and energy homeostasis in metabolic tissues, acting either as a nuclear corepressor through its four autonomous repression domains or as a cytoplasmic protein. It exerts a co-activator function in the regulation of circadian rhythms, inflammatory cascade, and mammary gland development (Nautiyal et al., 2013). NRIP1, apart from being linked to metabolic disorders, through various oncogenic signaling pathways, also takes part in development and progression of solid tumors, such as ovarian cancer, breast cancer, colon cancer, and hepatocellular carcinoma (Lapierre et al., 2015). NRIP1 is also expressed in the cortical and hippocampal areas of the brain (Nautiyal et al., 2013). It plays a crucial role in brain development and functioning and in cognitive and emotional processes (Duclot et al., 2012; Flaisher-Grinberg et al., 2014; Feng et al., 2015). NRIP1 knockout (RIP140-/-) mice show learning and memory deficits and increased stress response (Duclot et al., 2012). Transgenic mice with macrophage-specific knockdown of NRIP1 (MΦRIPKD mice) show increased baseline and provoked anxiety-like behavior and higher depressive-like behavior, in association with a reduced NRIP1 expression within the macrophage/microglia population of the VMH (ventromedial hypothalamus). Intra-VMH NRIP1 re-expression rescues the depressive-like behavior, having just a minor effect on the anxiety-like one. Moreover, macrophage NRIP1 expression correlates with the astrocyte one of NPY (neuropeptide Y), a neuromodulator agent, controlling mood and stress (Flaisher-Grinberg et al., 2014). Behavioral stressful experiences, like FSS (forced swim stress) for mice, induce stress-like behavior, depending on decreased NRIP1 level in cortical astrocytes, hippocampus, and medial basal hypothalamus and a simultaneous brain cholesterol accumulation (Feng et al., 2015). Downregulation of NRIP1 nuclear form controls mice brain aging (Ghosh et al., 2009) whereas its cytosolic form acts as a neuroprotector in mice brain, preventing endoplasmic reticulum stress-induced neuronal apoptosis (Feng et al., 2014) and maintaining brain cholesterol homeostasis (Feng et al., 2015). In mice hippocampus, increased levels of NRIP1 expression are also associated with depression-like symptoms (Chunhua et al., 2016). NRIP1 protein levels are considerably increased in the hippocampus from Down syndrome patients (Gardiner, 2006). NRIP1 has been suggested as a potential candidate gene in autism, on the basis of in silico analysis of chromosomal regions involved in an unbalanced rearrangement del(21)(q11.2q21.2), identified in an ASD patient from a cohort of 126 ASD patients through high-resolution comparative genome hybridization (Iurov et al., 2010). Its potential etiological role in ASD has not been further investigated, but evidence suggests that NRIP1 and ASD could be indirectly linked. NRIP1 represents a molecular bridge between circadian rhythms and metabolism. It is part of a feedback mechanism regulating the circadian clock: it is under circadian regulation and it

can alter basal levels of other clock genes, by also acting as a co-activator for the nuclear receptor RORα, known to be a stimulator of clock genes' transcription (Poliandri et al., 2011). RORA has been identified as dysregulated in many tissues from ASD patients (Cook et al., 2015). Some major evidence: RORA expression is reduced in cerebellum and cortex of ASD patients; RORA is differentially methylated in LBC lines from ASD and non-ASD siblings; RORα-deficient mice show reduced number and size of Purkinje cells, as it has been observed in cerebellar specimens from ASD patients; RORα controls the expression of a number of ASD-associated genes in human neurons, including A2BP1 (ataxin binding protein), NLGN1 (neuroligin 1), and CYP19A1 (aromatase) (Cook et al., 2015). In general, mutations affecting the function of circadian-relevant genes are more frequent in ASD patients than in unaffected controls (Yang et al., 2016). All these findings give strength to other results that have previously linked ASD and circadian clock genes, leading to the interpretation of ASD as a neurodevelopmental disorder arising from atypical biological and behavioral rhythms (Yang et al., 2016): NRIP1 contribution to this association is worthy of further investigation.

When studying circulating miRNAs in pathologies, the biggest challenge is to elucidate the relationship between the diseased tissue and the corresponding expression levels of these molecules observed in liquid biopsies. In ASD, this challenge is further complicated by the fact that a specific and unique diseased tissue has not been identified yet. In a gene expression dataset obtained from the analysis of whole blood samples of ASD patients, we found a marked dysregulation of twelve node genes from miR-140-3p-mediated network (Figure 3.3). Even though we have detected the differential expression of some network node genes in all six ASD datasets reported, no one of those genes showed a marked and consistent expression trend in two or more datasets. Although it is not unexpected that independent microarray studies, using different technologies and platforms, give inconsistent results, we could not demonstrate a striking involvement of dysregulation of miR-140-3p-mediated network in ASD. Given the expression of miR-140-3p, CD38, and NRIP1 in the brain, it is also conceivable that brain tissues are responsible for serum dysregulation of miR-140-3p. Focusing on the contribution of serum extracellular vesicles to the expression of circulating miR-140-3p in ASD patients might help clarify potential tissue-serum links (Witwer, 2015). Nevertheless, our computational analysis of the potential functional role of intracellular miR-140-3p and of its possible involvement in ASD etiology suggests to the scientific community new processes, molecules, and mechanisms to further investigate in the context of ASD.

Through ROC curve analyses and performance evaluation of predictive models, we proved that serum levels of miR-140-3p could be used in the discrimination of ASD patients from NCs, TS patients, and TS+ASD patients (Figures 3.4-6). We obtained the highest performance of serum miR-140-3p as a biomarker for the discrimination among ASD and TS+ASD patients. It was crucial to evaluate the performance of the biomarker through CV and permutation testing, since these predictive models were

based on a miRNA already identified as DE between the compared groups. We suggest that serum miR-140-3p could serve as a potential non-invasive biomarker to complement and support the behavior-based diagnosis of ASD, especially the differential one between ASD and TS+ASD. The main limit of our biomarker analysis is that we had only one miRNA to test for its predictive accuracy. It is well known that a single biomarker can hardly be as performing as a combination of them. Further studies on larger cohorts and on participants of lower age would be necessary in order to get compelling evidence on miR-140-3p discriminatory power and prove its value in supporting early diagnosis of ASD. In this context, it would be interesting to identify which factors can be responsible for ASD patient misclassification (Figure 3.6.1-3D) by miR-140-3p, in order to optimize its predictive performance.

Our study, just like many others on circulating miRNAs to be used as biomarkers, has some limitations. The first one regards diagnostic specificity. As reported above, circulating miR-140-3p has already been associated with multiple pathological conditions and this denote that it could be simply indicative of a general disease state (i.e., inflammation and response to stress). The second one is reproducibility. There is little overlap between circulating miRNAs reported as biomarkers from independent investigators and this challenges their clinical utility. Just one of two other independent studies on miRNA expression in human ASD liquid biopsies (discussed below) is consistent with ours. That is why results should be validated in larger cohorts and experimental conditions should be carefully standardized (Witwer, 2015).

Our study is the third high-throughput one profiling miRNAs in a body fluid from ASD patients in order to discover some potential biomarkers.

The first study (Mundalil Vasu et al., 2014) was carried out on serum from a Japanese cohort of 55 ASD patients and 55 unaffected controls. The authors identified and validated 13 circulating miRNAs as dysregulated in serum from ASD patients and showed the accurate predictive power of 5 of them in discriminating ASD patients (Mundalil Vasu et al., 2014). None of circulating miRNAs from this study matches those from our profile. Our ASD and NC sample size is smaller than the one from this work, but we have used an array technology that allowed us to profile the expression of many more miRNAs than the 139 that the authors analyzed. We tested the expression of these 5 predictive miRNAs (miR-19b-3p, miR-130a-3p, miR-181b-5p, miR-320a, and miR-572) (Mundalil Vasu et al., 2014), together with miR-429 from our previous investigation on TS (Rizzo et al., 2015), in sera from 15 ASD patients, 15 TS patients, and 15 NCs. We did not observe any difference in miRNA expression among groups with the exception of miR-429, which we confirmed as DE between TS patients and NCs. Differences in sample size (55 samples per group vs 15 samples per group) did not alter the result on miR-429 expression (Rizzo et al., 2015). However, functional enrichment analyses from both studies (Mundalil Vasu et al., 2014; this chapter) demonstrated over-representation of the same neurological pathways, as TGF-β signaling, Hedgehog signaling, Wnt signaling, and regulation of synaptic plasticity. This observation suggests that discrepancies can be explained with differences in pre-analytic variables, such

as genetic structure of studied populations, cohort composition, sample processing, validation technique, and data normalization (Witwer, 2015). Ethnicity of participants, cohort size, and miRNA panel and intercalating dye-based system used may have determined the inconsistencies observed.

The second paper (Hicks et al., 2016) describes a pilot study on whole saliva from an US cohort of 24 ASD patients and 21 unaffected controls, whose results partly match with ours. By RNA-sequencing, the authors identified 14 miRNAs as dysregulated in saliva from ASD patients and showed the discriminative accuracy of this molecular signature (Hicks et al., 2016). MiR-140-3p is part of this ASD molecular fingerprint and is upregulated in ASD patients compared to unaffected controls, as in our study (Hicks et al., 2016; this chapter). Moreover, in agreement with our results, their functional enrichment analysis detected significant over-representation of target genes related to neuronal development and transcriptional activation (Hicks et al., 2016). Our ASD and NC sample size is slightly bigger than the one from this work. In addition, sequencing data from it have not been validated through miRNA-specific qPCR assays. Discrepancies between this work and our study can also be explained, other than with all the factors listed above (in particular, differences in pre-analytic variables: processed serum vs whole saliva), with the fact that they investigated two different human body fluids. It is interesting that miR-140-3p shows the same expression trend in both saliva and serum. This observation may suggest that shared mechanisms could determine the increased levels of miR-140-3p in both body fluids.

These two studies, differently from ours, have identified more than one biomarker for ASD. Furthermore, they have focused only on ASD patients and NCs, whereas our study is the first high-throughput one profiling circulating miRNAs also in patients suffering from another neurodevelopmental disorder comorbid with ASD, TS+ASD patients.

3.5. Summary and conclusions

Through the identification of a serum biomarker, this study provides insight into concealed molecular mechanisms determining ASD and a potential complementary and supportive mean for a simpler, faster, and unbiased ASD diagnosis. The network that miR-140-3p regulates is involved in a set of biological processes convergingly dysregulated in ASD. Molecular characterization of miR-140-3p network would contribute to further clarify the heterogeneous molecular basis of ASD. Moreover, serum miR-140-3p could potentially be used as a non-invasive biomarker for ASD, easy to test through liquid biopsies.

This study confirmed the appropriateness and applicability of our approach for the investigation of ASD and let us spot some interesting potential links and shared mechanisms of miRNA secretion between different human body fluids. These observations led us to a subsequent analysis of circulating miRNAs

in processed saliva samples from ASD patients. Importantly, among all body fluids, saliva represents the most accessible and complete source of different types of molecules that could reflect genetic, epigenetic, environmental, metabolic, emotional, and behavioral alterations in ASD.

3.6. Materials and methods

3.6.1. Patient selection

From a database of more than 2000 patients (from the Section of Child and Adolescent Psychiatry, Department of Clinical and Experimental Medicine, University of Catania), seventy-nine Caucasian patients, aged 3-13 years and from varying socio-economic contexts, were randomly recruited and studied from January to November 2016. Thirty patients affected by ASD [mean age: 6.5 (SD, standard deviation: 3.5); M:F 22:8], twenty-four patients affected by TS [mean age: 8.7 (SD: 5.2); M:F 21:3], and twenty-five patients affected by TS+ASD [mean age: 9.3 (SD: 6.7); M:F 25:0] were included in the study. They were compared to twenty-five randomly selected neurologically intact unaffected NCs [mean age: 9.5 (SD: 3.9); M:F 16:9], recruited from local schools, without any history of either ASD or TS and who suffered from neither chronic diseases nor psychiatric disorders (Table 3.5). Serum samples from these participants were part of the discovery set used for miRNA profiling data validation.

The discovery set of serum samples used for miRNA profiling was created by randomly selecting from the database four ASD (M:F 3:1), five TS (M:F 4:1), and four TS+ASD (M:F 4:0) patients with severe symptoms. In this set, an extra TS patient was preferred in place of a NC (M:F for NC group 3:0, three NCs) because of the strong interest in investigating the comparisons TS+ASD vs TS and ASD vs TS.

TS and ASD affect males more than females with M:F ratios of 3:1 (Robertson, 2012) and 4:1 (Christensen et al., 2016), respectively. For this reason, it was inevitable that the three clinical groups were mainly composed of males: females are not easy to recruit. We performed a gender control analysis to check if those different group compositions could have an effect on downstream results. Gender distribution is not different between ASD and NC (Fisher's exact test, two-sided p-value = 0.56), TS and NC (p-value = 0.10), TS+ASD and TS (p-value = 0.11), and ASD and TS (p-value = 0.31). However, it is different between TS+ASD and NC (p-value = 0.002) and TS+ASD and ASD (p-value = 0.006). This demonstrated that the TS+ASD group, the most intriguing to analyze, was particularly problematic: recruiting female patients suffering from TS+ASD was difficult, as it is possible to infer from the TS and ASD M:F ratios reported above. That is why we repeated a final gender control analysis (see Section 3.6.8) to validate and confirm the accuracy of results from the biomarker performance evaluation analysis in the comparison TS+ASD vs NC.

Table 3. 5. Clinical and neuropsychological features of study participants. *Data are shown as means and standard deviations between parentheses. ASD: Autism Spectrum Disorder; TS: Tourette syndrome; NC: Unaffected Control; M: male; F: female; IQ: Intelligence Quotient; YGTSS: Yale Global Tic Severity Scale; ADOS: Autism Diagnostic Observation Schedule.*

	Number of participants	Age	M:F ratio	IQ	YGTSS	ADOS			
						Communication	Social interaction	Imagination	Repetitive and restricted behaviors
ASD	30	6.5 (3.5)	22:8	59.4 (20.6)	0	7.3 (2.3)	7.6 (2.1)	3 (2.5)	3.5 (1.6)
TS	24	8.7 (5.2)	21:3	93.7 (19.1)	17.1 (7.9)	0	0	0	2.4 (1.6)
TS+ ASD	25	9.3 (6.7)	25:0	94.6 (8.9)	22.12 (10.5)	6.4 (3.2)	8.5 (3.9)	3.1 (4.3)	3.7 (1.9)
NC	25	9.5 (3.9)	16:9	80.9 (24.5)	1.9 (1.7)	0	0	0	0

The study was approved by the local Ethics Committee. All parents gave written informed consent.

Diagnoses of ASD, TS, and other clinical conditions were made according to both DSM-IV-TR (Diagnostic and Statistical Manual of Mental Disorders, IV edition – Text Revision) and DSM-5 criteria by a child neurologist (Professor Renata Rizzo). All the participants were evaluated at the University Hospital Policlinico-Vittorio Emanuele of Catania. The three clinical groups (ASD, TS, and TS+ASD) and the NCs were assessed using the following scales/schedules: ADOS and ADI-R to evaluate ASD symptoms; YGTSS to evaluate presence and severity of tics. Moreover, the three clinical groups (ASD, TS, and TS+ASD) and the NCs were also assessed by a psychologist through WISC-III (Wechsler Intelligence Scale for Children, III edition) as an evaluation of both IQ and cognitive functioning. Neuropsychological features of patients are summarized in Table 3.5.

In a previous study (Rizzo et al., 2015), we reported that only miR-429 was significantly DE in the serum of TS patients compared to NCs: TS patients were included in this experimental series only aiming to compare them with the other classes of neuropsychiatric patients.

3.6.2. Sample processing

Peripheral blood samples from all participants were taken in the morning using a butterfly device into serum separator collection tubes, provided with Clot activator and gel for serum separation as additives (BD Biosciences). Collection tubes were treated according to current procedures for clinical samples. In order to separate serum from blood cells, tubes were rotated end-over-end at 20°C for 30’ and then

centrifuged at 3500 rpm at 4°C for 15' in a Beckman J6-M Centrifuge. Supernatants were aliquoted into 1.5 ml RNase-free tubes and stored at −80°C. Prior to RNA extraction, stored supernatants were centrifuged again at 3500 rpm at 4 °C for 15' to remove circulating cells or debris. Serum samples were aliquoted into 1.5 ml RNase-free tubes and they were either immediately used for RNA extraction or stored at −80°C until analysis (Rizzo et al., 2015).

3.6.3. RNA extraction

RNA was extracted from 400 µl serum samples using Qiagen miRNeasy Mini Kit (Qiagen), according to Qiagen Supplementary Protocol for purification of total RNA, including small RNAs, from serum or plasma. RNA was eluted in a 40 µl total volume of RNase-free water with two consecutive steps of elution (30 µl followed by another 10 µl of RNase-free water) performed in the same collection tube.

3.6.4. MiRNA profiling

We used TLDA technology to profile the serum expression of 754 different human miRNAs of four ASD patients, five TS patients, four TS+ASD patients, and three NCs (discovery set). 3 µl of RNA were reverse transcribed and preamplified according to manufacturer's instructions. Preamplified products were loaded on TaqMan Human MicroRNA Array v3.0 A and B 384-well microfluidic cards (Applied Biosystems). PCR reactions on TLDAs were performed on a 7900HT Fast Real Time PCR System (Applied Biosystems) (Ragusa et al., 2016).

We individually carried out the analysis on microfluidic cards A and B. We used a customized normalization approach for the relative quantification analysis. For each comparison, a Ct value matrix (miRNAs in rows, samples in columns) was created. In a similar way to the GMN (global median normalization) method (Park et al., 2003), for each sample of the comparison, the median and mean Ct values within the array, reflecting the loaded mass of template cDNA, were calculated. However, all Ct values representing a specific miRNA were kept out of these calculations if even just one of them corresponded to a flagged well. Then, using the Pearson correlation, miRNAs, whose expression profile was closer (more positively correlated) to these values, were identified as the best endogenous controls within the arrays. We normalized miRNAs to the top three stable miRNAs within the arrays. miR-146a and miR-223* were the most frequently stable miRNAs for cards A and B, respectively, and the most abundant among those we could select.

Therefore, for each comparison, three ΔCt value matrices (miRNAs in rows, samples in columns) were produced according to the $2^{-\Delta\Delta Ct}$ method (Schmittgen and Livak, 2008). DE circulating miRNAs were obtained performing SAM (Significance of Microarrays Analysis) statistical analysis on these matrices with MeV (Multi experiment viewer v4.8.1) statistical analysis software (http://mev.tm4.org). For each pairwise comparison, we used a two-class unpaired test, based on at least 100 permutations per miRNA,

with a FDR cut-off of 0.15, in order to detect dysregulated miRNAs. This analysis identified many DE miRNAs for each comparison. However, we have used very strict criteria to select miRNAs for further validation (i.e., number of SAM tests in which they were identified as DE, number of comparisons in which they resulted as DE, their abundance, and the quality of their amplification curves during the profiling runs) in order to investigate only the most promising ones.

3.6.5. MiRNA profiling data validation

RNA from sera of thirty ASD, twenty-four TS, and twenty-five TS+ASD patients and twenty-five NCs (validation set) was used to perform miRNA-specific reverse transcription reactions producing miRNA-specific cDNAs for real-time PCRs. These RT-PCR analyses were performed using TaqMan MicroRNA Assays (Applied Biosystems) specific for the most interesting miRNAs identified as DE, miR-30d, miR-140-3p, miR-148a*, and miR-222, and for the selected endogenous control, miR-146a. At first, the ASD group was composed of thirty-two patients. We checked if some of those samples should be considered as outliers, within this original ASD group, for: (1) the serum expression of miR-140-3p; (2) the severity of ASD symptoms. We looked at their ΔCt values for miR-140-3p and at scores that they obtained for the four items of the ADOS scale (A: Communication; B: Social interaction; C: Imagination; D: Repetitive and restricted behaviors). For these expression values and ADOS scores, we defined the corresponding mean ± 2*(SD) ranges and we considered patients with a value and/or score outside of those ranges as outliers. Two ASD patients were excluded from the original ASD group since: (1) both were outliers for miR-140-3p expression; (2) one was an outlier for the Imagination item (1/4 ADOS items), whereas the other one was an outlier for the Imagination and Repetitive and restricted behaviors items (2/4 ADOS items). All the following analyses were performed with GraphPad Prism for Windows v6.01 (GraphPad Software) (www.graphpad.com). D'Agostino-Pearson omnibus K2 test and Shapiro-Wilk test were performed to check if data from every small group were normally distributed. Ordinary one-way ANOVA was used to test the differential expression of those miRNAs between the four groups. Statistical significance was established at a p-value ≤ 0.05. Tukey's multiple comparisons test was performed to identify which groups differed in the selected miRNAs' expression. Statistical significance was established at a multiplicity adjusted p-value ≤ 0.05. Expression FC values of miRNAs were calculated by applying the $2^{-\Delta\Delta Ct}$ method (Schmittgen and Livak, 2008).

3.6.6. Correlation between miR-140-3p expression and neuropsychiatric parameters

Correlation between ΔCt values for miR-140-3p, obtained from the normalization to miR-146a, and neuropsychiatric parameters was analyzed in both a general (all patients and controls) and a class-specific (just one class of patients and controls) way, since some of these parameters were only related to a certain class of neuropsychiatric disorders. IQ (Intelligence Quotient), ADOS items regarding communication, social interaction, imagination, and repetitive and restricted behaviors (ADOS items A-

D), and YGTSS were the neuropsychiatric parameters chosen for this analysis. Either Pearson or Spearman correlation was computed on GraphPad Prism software when analyzing normally and not normally distributed data, respectively. Two-sided p-values from this correlation analysis were corrected for multiple comparisons by using three different approaches: Bonferroni correction, Holm-Bonferroni correction, and BH FDR procedure. Statistical significance was established at a p-value ≤ Bonferroni corrected $\alpha = 0.05/16 = 0.003$, at a Holm-Bonferroni corrected p-value ≤ 0.05, and at a BH FDR adjusted p-value ≤ 0.01. Linear regression analysis was also carried out on GraphPad Prism software only for significant correlations. Statistical significance was established at a p-value ≤ 0.05.

3.6.7. Computational Analyses

3.6.7.1. Reconstruction of the miR-140-3p-mediated regulatory network

miR-140-3p targets whose validation was based on strong evidence were retrieved by DIANA-TarBase v7.0 (Vlachos et al., 2015) (http://diana.imis.athena-innovation.gr/DianaTools/index.php?r=tarbase/index) and miRTarBase (Chou et al., 2016) (http://mirtarbase.mbc.nctu.edu.tw/) databases. The biological network, composed of MIR140, these targets, and their first neighbors, was built retrieving interactome data through BisoGenet v3.0.0 Plug-in (Martin et al., 2010) in Cytoscape v3.4.0 (Shannon et al., 2003). Network centrality analysis, permitting the identification of the nodes that, more than others, were good candidates as regulators of the underlying biological processes in which the network is involved, was carried out through CentiScaPe v2.1 Plug-in (Scardoni et al., 2014).

3.6.7.2. Network functional analysis

clusterProfiler v3.2.11 R package (Yu et al., 2012) was used to perform functional enrichment analyses on miR-140-3p-mediated regulatory network node genes in R v3.3.2 (R Core Team, 2016) (https://www.R-project.org/). We searched for the gene annotation terms from the GO, DO, KEGG, and Reactome databases that were over-represented in the list of network node genes compared to the entire genome. Statistical significance for the hypergeometric test was established at a BH adjusted p-value ≤ 0.05. gofilter() and simplify() functions in clusterProfiler were employed in order to select level-specific GO terms and to remove the most redundant ones, respectively.

3.6.7.3. Network expression analysis

In order to investigate if deregulation of network node genes was implicated in ASD, we searched for raw high-throughput gene expression datasets (Gregg et al., 2008; Kuwano et al., 2011; Voineagu et al., 2011; Ginsberg et al., 2012; Kong et al., 2012) produced from the analysis of samples of ASD patients on two public repositories, GEO (Gene Expression Omnibus) DataSets (Edgar et al., 2002) and ArrayExpress (Kolesnikov et al., 2015). Datasets retrieved by GEO DataSets were analyzed performing

limma tests with the GEO2R tool (Barrett et al, 2013) (https://www.ncbi.nlm.nih.gov/geo/info/geo2r.html), whereas datasets retrieved by ArrayExpress were analyzed performing Tusher SAM tests with MeV software. We reported only network node genes whose log_2FC expression was significantly higher than 1 and lower than -1 as upregulated and downregulated, respectively, within ASD datasets. MeV software was also used to produce the curated ASD expression heatmap.

3.6.8. ROC curve analysis and biomarker performance evaluation

ΔCt values for miR-140-3p, obtained from the normalization to miR-146a, served as input data to perform a classical univariate ROC curve analysis for each of the comparisons where we found this miRNA to be dysregulated on the server Metaboanalyst 3.0 (Xia and Wishart, 2016) (http://www.metaboanalyst.ca/). An appropriate ΔCt cut-off point maximizing both sensitivity and specificity (that is, the threshold that maximizes the distance to the diagonal line) was found for each curve by calculating the maximum Youden index J (max [(sensitivity + specificity) – 1]). GraphPad Prism software was used to create Figure 3.4 and 3.5. The true positive rate (y-axis) was plotted in function of the false positive rate (x-axis), for different ΔCt cut-off points.

Since these ROC curves were based on a miRNA already identified as DE between the compared groups, through them we could only assess the idealized miR-140-3p discriminative power. It is possible that this miRNA only accurately predicts outcomes in the initial data set and that minor fluctuations in the training data could markedly lower its predictive performance.

Therefore, after these preliminary ROC curve analyses, we built corresponding logistic regression models for miR-140-3p expression and we tested them through CV and permutation testing, once again, by using the server Metaboanalyst 3.0. CV gives an indication of how accurate a given model might be in predicting new samples, validating its general applicability (Xia et al., 2013). 100-time repeated random sub-sampling CV was used to test the performance of the built logistic regression models. At each CV, 2/3 of samples are used for model training and the remaining 1/3 of samples is used for testing. Permutation testing indicates if a given model is significantly different from a random guessing model for the sample population, validating the proposed model structure (Xia et al., 2013). Permutation testing on the performance measure AUC was used to calculate the significance of the built logistic regression models. The permutation tests use this procedure: random label re-assignment to each sample; 3-time repeated random sub-sampling CV; comparison of the performance measures between the models obtained by using the original and the permuted sample labels. This procedure was repeated 100 times. If the performance measure of the original data lies outside the normal distribution of the one of the permuted data, then the tested model is significant. Statistical significance was established at a p-value ≤ 0.05. The ASD vs NC and ASD vs TS models incorrectly classified the same 11 ASD patients (M:F

ratio 8:3), whereas the ASD vs TS+ASD model incorrectly classified only 8 (of those previously mentioned 11 ones) ASD patients (M:F ratio 5:3). In light of what showed in Section 3.6.1, we tested if gender distribution was significantly different between ASD patients that were either correctly or incorrectly identified by the three models, to check if gender represented an attribute that could potentially lead to misclassification of ASD patients. Gender distribution was not different for neither the ASD vs NC and ASD vs TS models (Fisher's exact test, two-sided p-values = 1.00), nor for the ASD vs TS+ASD model (Fisher's exact test, two-sided p-values = 0.64).

3.7. Supplementary Figures

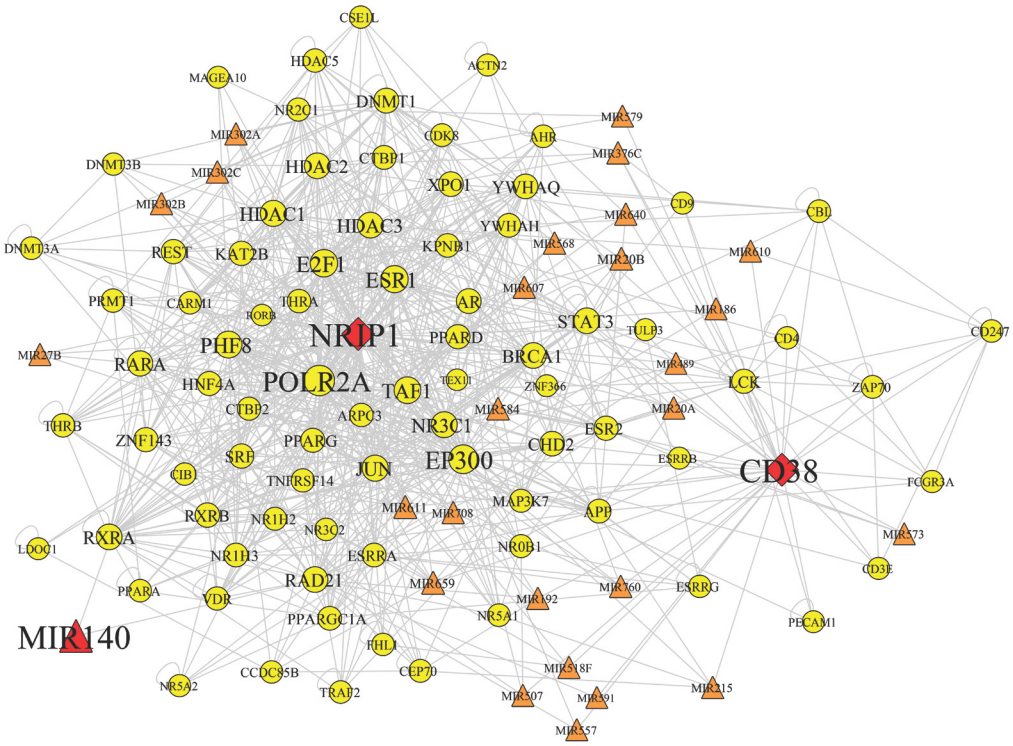

Figure S3. 1. MiR-140-3p-mediated regulatory network. *Nodes representing MIR140 gene and direct target genes of miR-140-3p are depicted as red triangle and red diamonds, respectively; those symbolizing protein-coding genes are drawn as yellow circles; those standing for miRNA-coding genes are illustrated as orange triangles. Size of both nodes and node labels, except for CD38, MIR140, and NRIP1, is directly proportional to node degree within the network.*

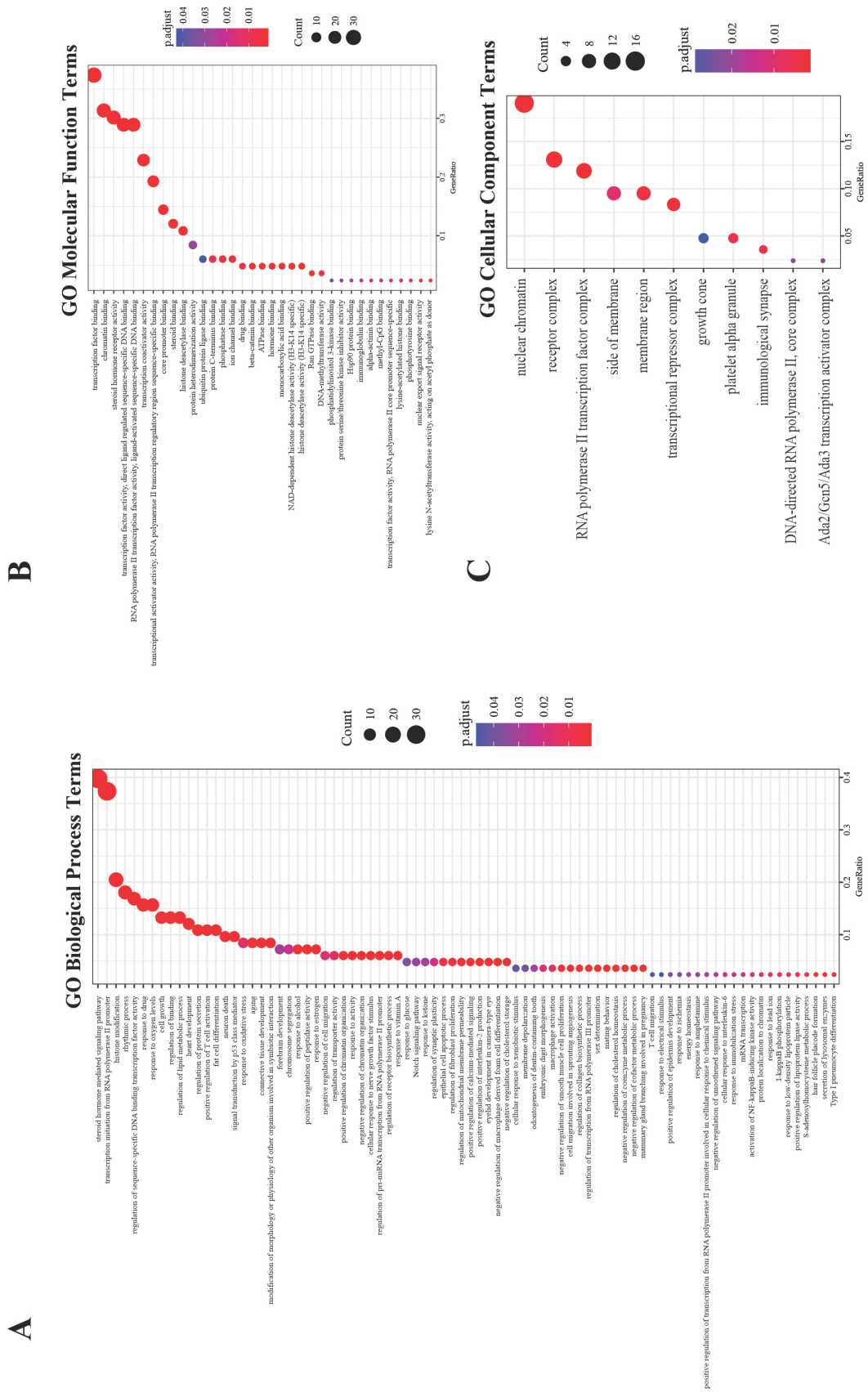

Figure S3. 2. Over-represented GO terms in miR-140-3p-mediated regulatory network compared to the entire genome. *(A) Dot plot for GO Biological Process terms. (B) Dot plot for GO Molecular*

Function terms. (C) Dot plot for GO Cellular Component terms. Each circle in the plots symbolizes an over-represented term: its x-axis coordinate reflects the Gene Ratio value; its size is directly proportional to the Count value; its color represents the Benjamini-Hochberg adjusted p-value generated by the hypergeometric test. Gene Ratio: the ratio of number of genes of interest that are annotated with a certain term from the database used to perform the analysis to number of genes of interest that are annotated with terms from the same database. Count: number of node genes within the network that are annotated with a certain term. GO: Gene Ontology.

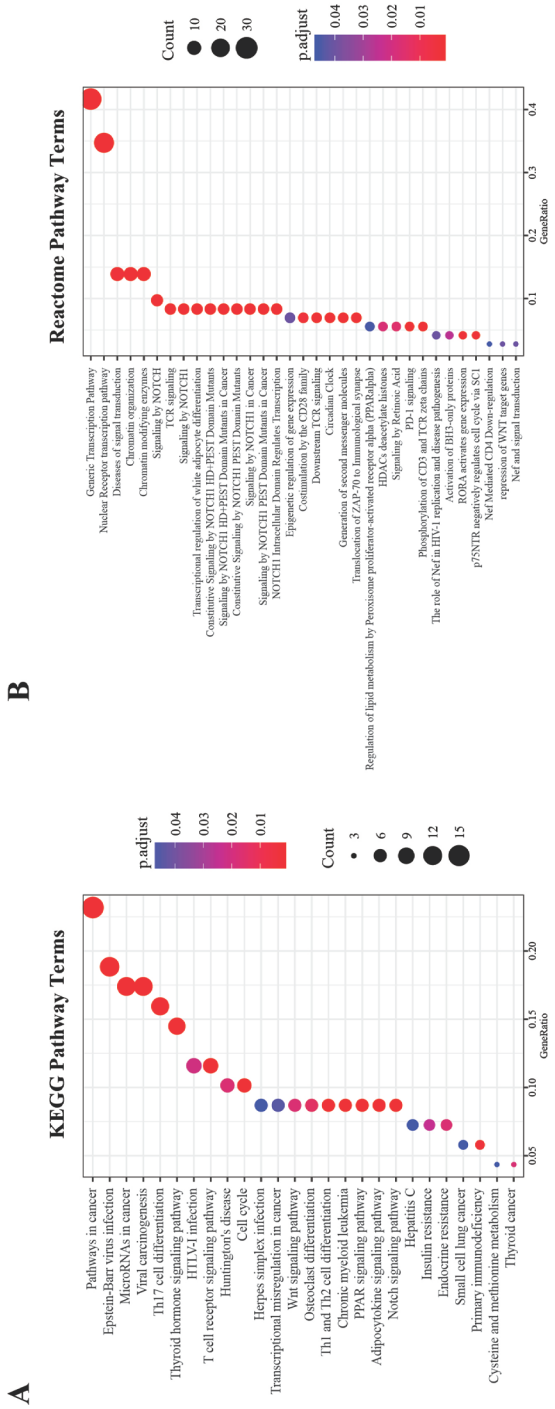

Figure S3. 3. Over-represented KEGG and Reactome terms in miR-140-3p-mediated regulatory network compared to the entire genome. *(A) Dot plot for KEGG Pathway terms. (B) Dot plot for*

Reactome Pathway terms. For in-depth description of the plots see Figure S3.2 legend. KEGG: Kyoto Encyclopedia of Genes and Genomes.

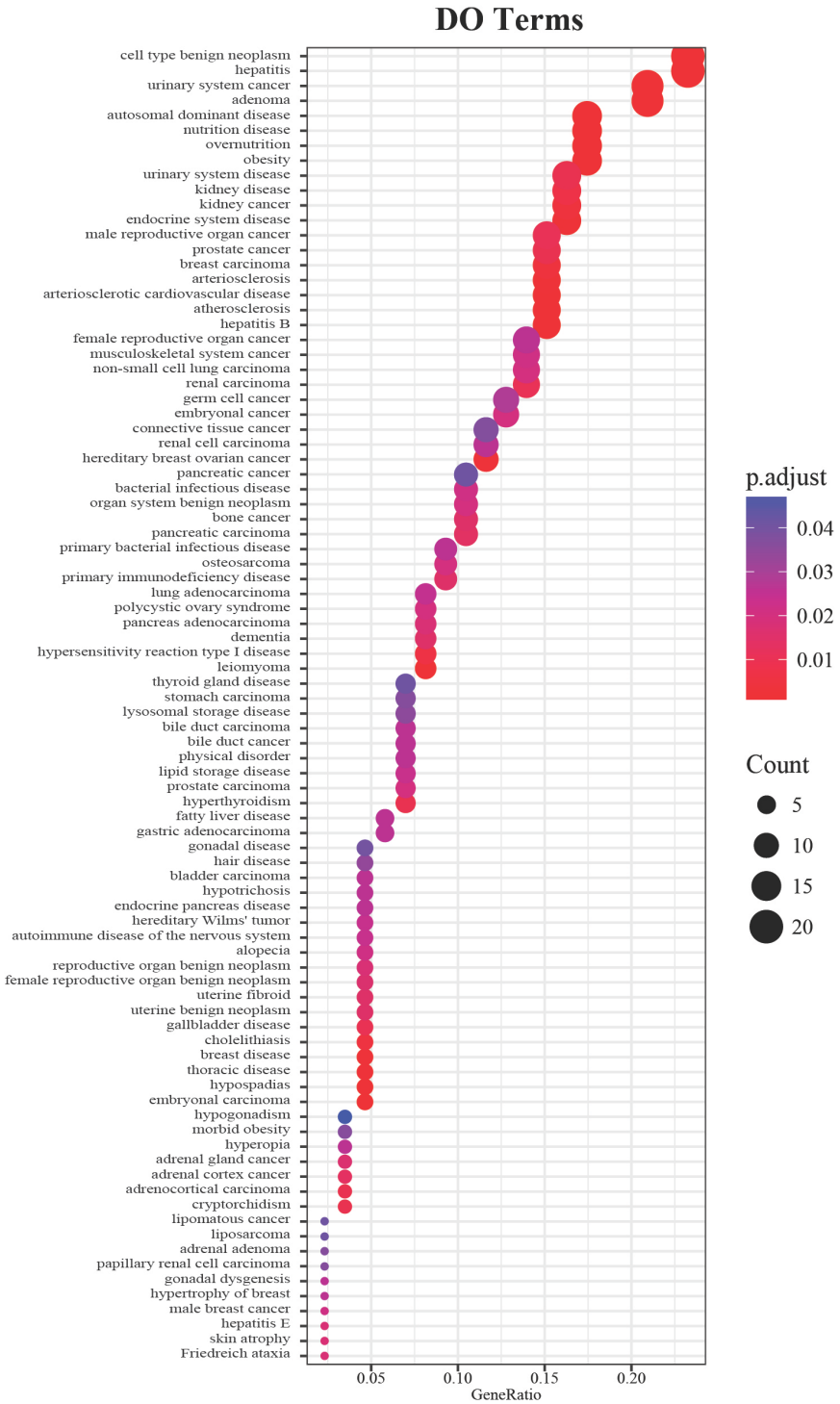

Figure S3. 4. Over-represented DO terms in miR-140-3p-mediated regulatory network compared to the entire genome. *Dot plot for DO terms. For in-depth description of the plot see Figure S3.2 legend. DO: Disease Ontology.*

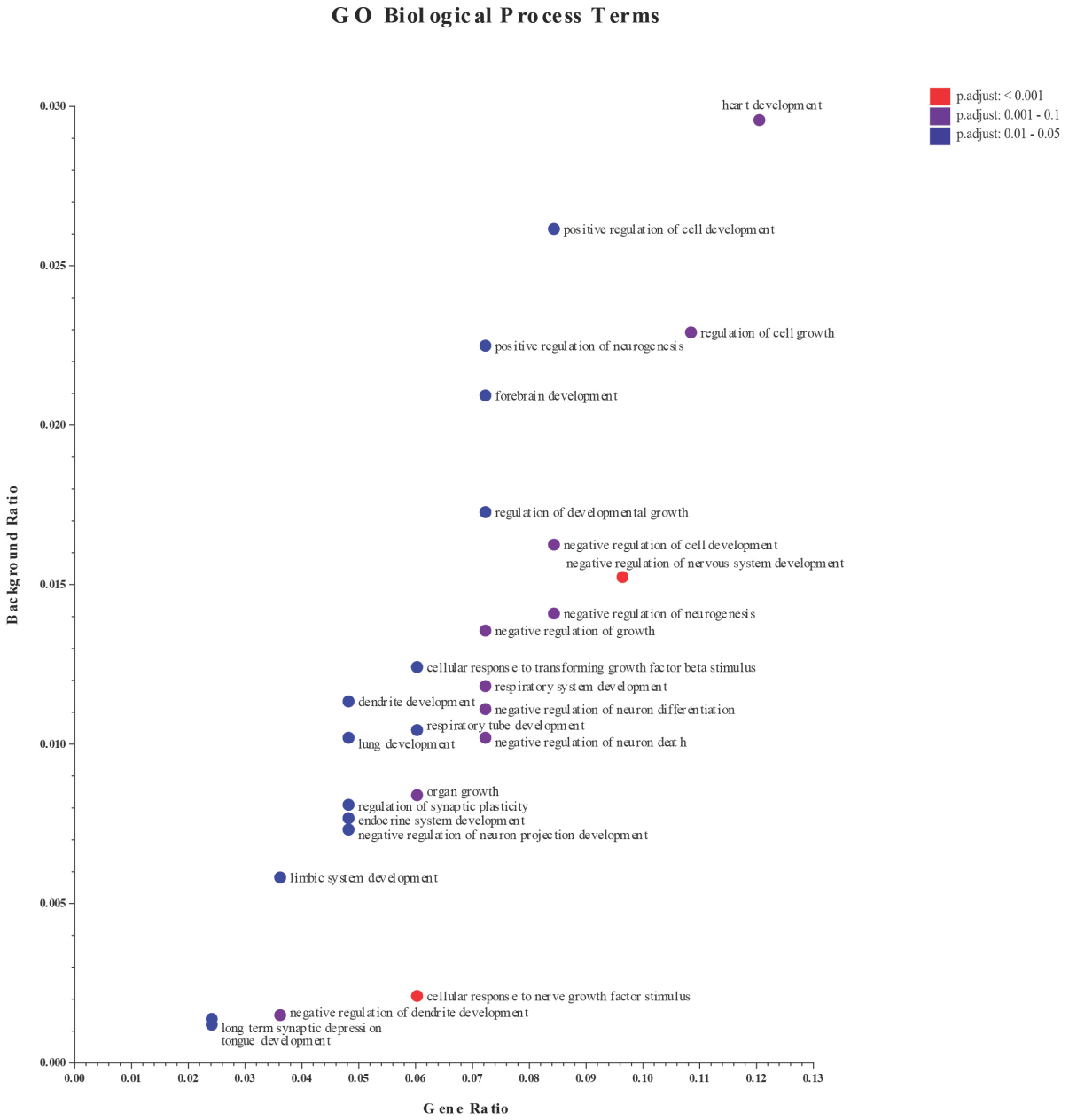

Figure S3. 5. Over-represented GO Biological Process terms regarding nervous system and development in miR-140-3p-mediated regulatory network. *Dot plot for all the most interesting GO Biological Process terms regarding nervous system and development. Each symbol in the plot symbolizes an over-represented term: its x-axis coordinate reflects the Gene Ratio value; its y-axis coordinate reflects the Background Ratio value; its color represents the Benjamini-Hochberg adjusted p-value generated by the hypergeometric test. Gene Ratio: the ratio of number of genes of interest that are annotated with a certain term from the database used to perform the analysis to number of genes of interest that are annotated with terms from the same database. Background Ratio: the ratio of number of genes in the genome that are annotated with a certain term from the database used to perform the analysis to number of genome genes that are annotated with terms from the same database. GO: Gene Ontology.*

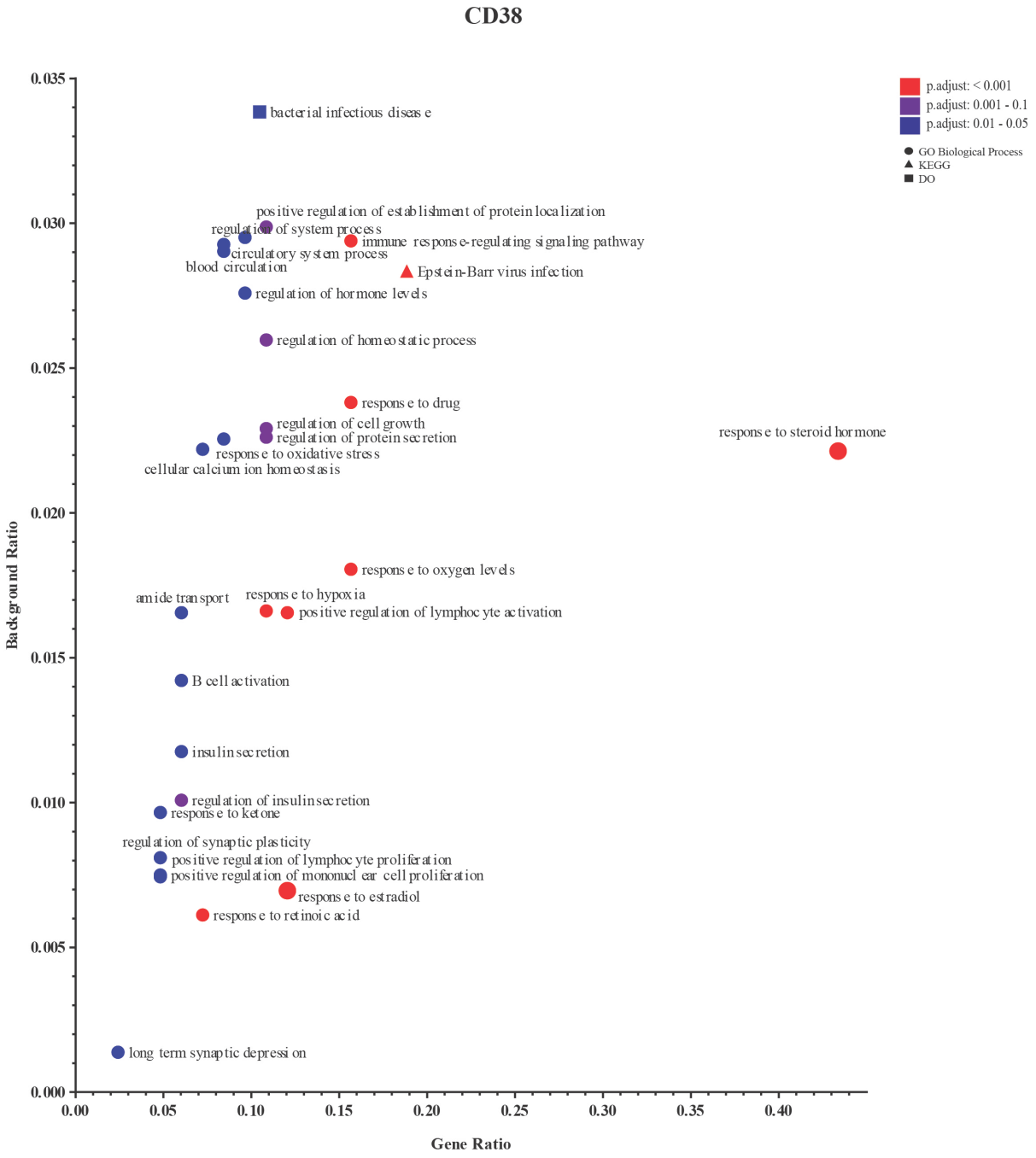

Figure S3. 6. Over-represented GO, DO, and KEGG terms associated with CD38 in miR-140-3p-mediated regulatory network. *Dot plot for all the most interesting GO, DO, and KEGG terms whose enrichment is determined by CD38. For in-depth description of the plot see Figure S3.5 legend. For more information about what symbol shapes stand for see figure legend. GO terms whose enrichment is determined by both CD38 and NRIP1 are represented by bigger symbols. GO: Gene Ontology; DO: Disease Ontology; KEGG: Kyoto Encyclopedia of Genes and Genomes.*

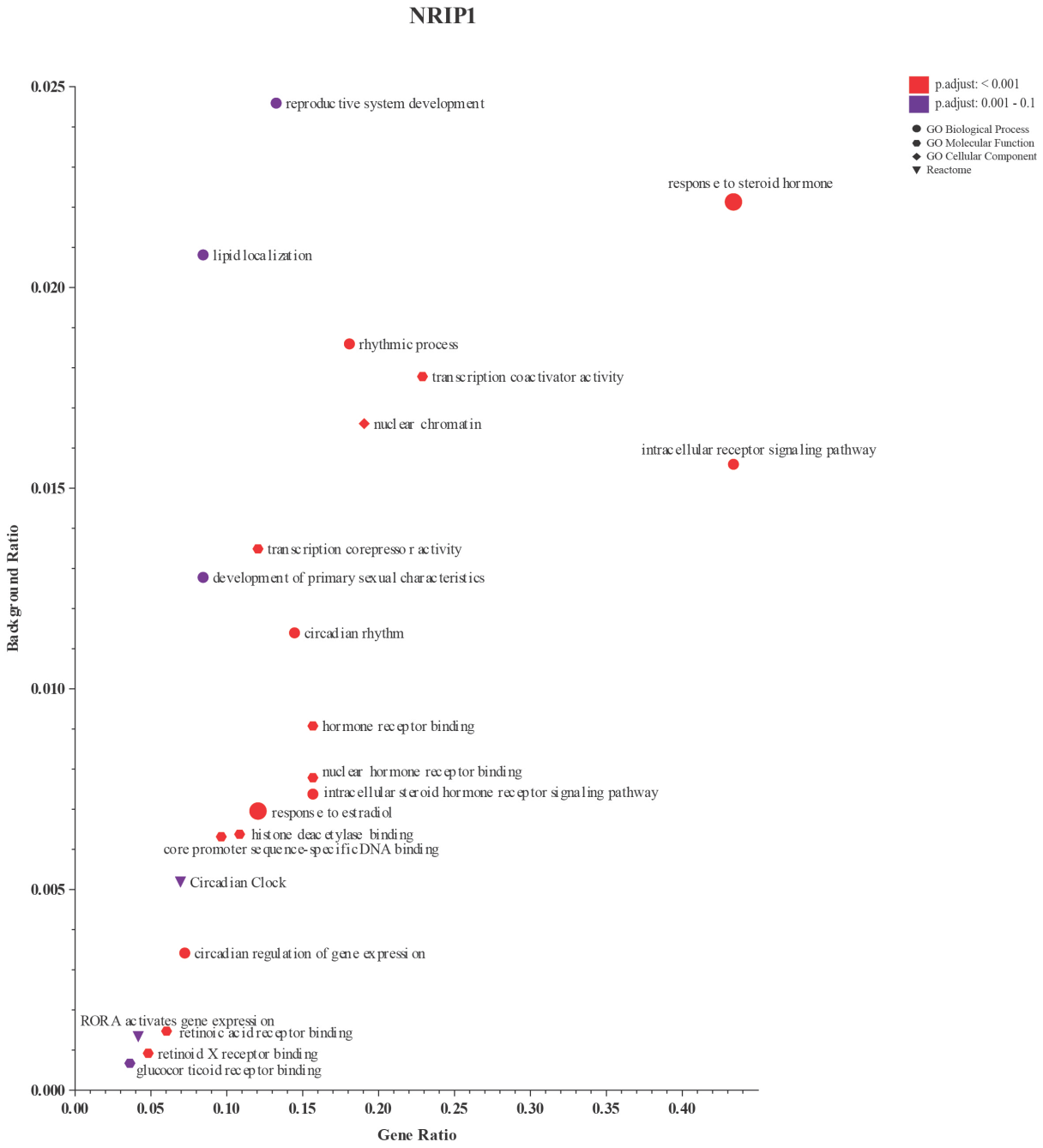

Figure S3. 7. Over-represented GO and Reactome terms associated with NRIP1 in miR-140-3p-mediated regulatory network. *Dot plot for all the most interesting GO and Reactome terms whose enrichment is determined by NRIP1. For in-depth description of the plot see Figure S3.5 legend. For more information about what symbol shape stands for see figure legend. GO terms whose enrichment is determined by both CD38 and NRIP1 are represented by bigger symbols. GO: Gene Ontology.*

Five more supplementary files can be found online (as part of the final paper published on Frontiers in Molecular Neuroscience in August 2017) at: http://journal.frontiersin.org/article/10.3389/fnmol.2017.00250/full#supplementary-material

3.8. References

American Psychiatric Association. Diagnostic and statistical manual of mental disorders. 5th ed. Washington, DC: Author; 2013.

An N, Zhao W, Liu Y, Yang X, Chen P. Elevated serum miR-106b and miR-146a in patients with focal and generalized epilepsy. Epilepsy Res. 2016;127:311-316. doi: 10.1016/j.eplepsyres.2016.09.019.

Ashwood P, Corbett BA, Kantor A, Schulman H, Van de Water J, Amaral DG. In search of cellular immunophenotypes in the blood of children with autism. PLoS One. 2011;6(5):e19299. doi: 10.1371/journal.pone.0019299.

Balaraman S, Winzer-Serhan UH, Miranda RC. Opposing actions of ethanol and nicotine on microRNAs are mediated by nicotinic acetylcholine receptors in fetal cerebral cortical-derived neural progenitor cells. Alcohol Clin Exp Res. 2012;36(10):1669-77. doi: 10.1111/j.1530-0277.2012.01793.x.

Barrett T, Wilhite SE, Ledoux P, Evangelista C, Kim IF, Tomashevsky M, Marshall KA, Phillippy KH, Sherman PM, Holko M, Yefanov A, Lee H, Zhang N, Robertson CL, Serova N, Davis S, Soboleva A. NCBI GEO: archive for functional genomics data sets--update. Nucleic Acids Res 2013;41(Database issue):D991-5. doi: 10.1093/nar/gks1193.

Bayrak OF, Gulluoglu S, Aydemir E, Ture U, Acar H, Atalay B, Demir Z, Sevli S, Creighton CJ, Ittmann M, Sahin F, Ozen M. MicroRNA expression profiling reveals the potential function of microRNA-31 in chordomas. J Neurooncol. 2013;115(2):143-51. doi: 10.1007/s11060-013-1211-6.

Bocchio-Chiavetto L, Maffioletti E, Bettinsoli P, Giovannini C, Bignotti S, Tardito D, Corrada D, Milanesi L, Gennarelli M. Blood microRNA changes in depressed patients during antidepressant treatment. Eur Neuropsychopharmacol. 2013;23(7):602-11. doi: 10.1016/j.euroneuro.2012.06.013.

Ceroni F, Sagar A, Simpson NH, Gawthrope AJ, Newbury DF, Pinto D, Francis SM, Tessman DC, Cook EH, Monaco AP, Maestrini E, Pagnamenta AT, Jacob S. A deletion involving CD38 and BST1 results in a fusion transcript in a patient with autism and asthma. Autism Res. 2014;7(2):254-63. doi: 10.1002/aur.1365.

Chang JT, Wang F, Chapin W, Huang RS. Identification of MicroRNAs as Breast Cancer Prognosis Markers through the Cancer Genome Atlas. PLoS One. 2016;11(12):e0168284. doi: 10.1371/journal.pone.0168284.

Chou CH, Chang NW, Shrestha S, Hsu SD, Lin YL, Lee WH, Yang CD, Hong HC, Wei TY, Tu SJ, Tsai TR, Ho SY, Jian TY, Wu HY, Chen PR, Lin NC, Huang HT, Yang TL, Pai CY, Tai CS, Chen WL, Huang CY, Liu CC, Weng SL, Liao KW, Hsu WL, Huang HD. miRTarBase 2016: updates to the

experimentally validated miRNA-target interactions database. Nucleic Acids Res 2016;44(D1):D239-47. doi: 10.1093/nar/gkv1258.

Christensen DL, Baio J, Van Naarden Braun K, Bilder D, Charles J, Constantino JN, Daniels J, Durkin MS, Fitzgerald RT, Kurzius-Spencer M, Lee LC, Pettygrove S, Robinson C, Schulz E, Wells C, Wingate MS, Zahorodny W, Yeargin-Allsopp M. Prevalence and Characteristics of Autism Spectrum Disorder Among Children Aged 8 Years-Autism and Developmental Disabilities Monitoring Network, 11 Sites, United States, 2012. MMWR Surveill Summ. 2016;65(3):1-23. doi: 10.15585/mmwr.ss6503a1.

Chunhua M, Lingdong K, Hongyan L, Zhangqiang M. Umbelliferone reverses depression-like behavior in chronic unpredictable mild stress-induced mice via RIP140/NF-κB pathway. IUBMB Life. 2016; doi: 10.1002/iub.1570.

Clarke RA, Lee S, Eapen V. Pathogenetic model for Tourette syndrome delineates overlap with related neurodevelopmental disorders including Autism. Transl Psychiatry. 2012; 2:e158. doi: 10.1038/tp.2012.75.

Collares CV, Evangelista AF, Xavier DJ, Rassi DM, Arns T, Foss-Freitas MC, Foss MC, Puthier D, Sakamoto-Hojo ET, Passos GA, Donadi EA. Identifying common and specific microRNAs expressed in peripheral blood mononuclear cell of type 1, type 2, and gestational diabetes mellitus patients. BMC Res Notes. 2013;6:491. doi: 10.1186/1756-0500-6-491.

Constantino JN, Charman T. Diagnosis of autism spectrum disorder: reconciling the syndrome, its diverse origins, and variation in expression. Lancet Neurol. 2016;15(3):279-91. doi: 10.1016/S1474-4422(15)00151-9.

Cook DN, Kang HS, Jetten AM. Retinoic Acid-Related Orphan Receptors (RORs): Regulatory Functions in Immunity, Development, Circadian Rhythm, and Metabolism. Nucl Receptor Res. 2015; doi: 10.11131/2015/101185.

Dileepan M, Sarver AE, Rao SP, Panettieri RA Jr, Subramanian S, Kannan MS. MicroRNA Mediated Chemokine Responses in Human Airway Smooth Muscle Cells. PLoS One. 2016;11(3):e0150842. doi: 10.1371/journal.pone.0150842.

Dong W, Yao C, Teng X, Chai J, Yang X, Li B. MiR-140-3p suppressed cell growth and invasion by downregulating the expression of ATP8A1 in non-small cell lung cancer. Tumour Biol. 2016;37(3):2973-85. doi: 10.1007/s13277-015-3452-9.

Duclot F, Lapierre M, Fritsch S, White R, Parker MG, Maurice T, Cavaillès V. Cognitive impairments in adult mice with constitutive inactivation of RIP140 gene expression. Genes Brain Behav. 2012;11(1):69-78. doi: 10.1111/j.1601-183X.2011.00731.x.

Edgar R, Domrachev M, Lash AE. Gene Expression Omnibus: NCBI gene expression and hybridization array data repository. Nucleic Acids Res 2002;30(1):207-10.

Ertekin S, Yıldırım O, Dinç E, Ayaz L, Fidancı SB, Tamer L. Evaluation of circulating miRNAs in wet age-related macular degeneration. Mol Vis. 2014;20:1057-66.

Feng X, Krogh KA, Wu CY, Lin YW, Tsai HC, Thayer SA, Wei LN. Receptor-interacting protein 140 attenuates endoplasmic reticulum stress in neurons and protects against cell death. Nat Commun. 2014;5:4487. doi: 10.1038/ncomms5487.

Feng X, Lin YL, Wei LN. Behavioral stress reduces RIP140 expression in astrocyte and increases brain lipid accumulation. Brain Behav Immun. 2015;46:270-9. doi: 10.1016/j.bbi.2015.02.008.

Flaisher-Grinberg S, Tsai HC, Feng X, Wei LN. Emotional regulatory function of receptor interacting protein 140 revealed in the ventromedial hypothalamus. Brain Behav Immun. 2014;40:226-34. doi: 10.1016/j.bbi.2014.03.019.

Gardiner K. Transcriptional dysregulation in Down syndrome: predictions for altered protein complex stoichiometries and post-translational modifications, and consequences for learning/behavior genes ELK, CREB, and the estrogen and glucocorticoid receptors. Behav Genet. 2006;36(3):439-53. doi: 10.1007/s10519-006-9051-1.

Ghosh S, Thakur MK. Interaction of estrogen receptor-alpha ligand binding domain with nuclear proteins of aging mouse brain. J Neurosci Res. 2009;87(11):2591-600. doi: 10.1002/jnr.22068.

Ginsberg MR, Rubin RA, Falcone T, Ting AH, Natowicz MR. Brain transcriptional and epigenetic associations with autism. PLoS One. 2012;7(9):e44736. doi: 10.1371/journal.pone.0044736.

Gokoolparsadh A, Sutton GJ, Charamko A, Green NF, Pardy CJ, Voineagu I. Searching for convergent pathways in autism spectrum disorders: insights from human brain transcriptome studies. Cell Mol Life Sci. 2016;73(23):4517-4530. doi: 10.1007/s00018-016-2304-0.

Gregg JP, Lit L, Baron CA, Hertz-Picciotto I, Walker W, Davis RA, Croen LA, Ozonoff S, Hansen R, Pessah IN, Sharp FR. Gene expression changes in children with autism. Genomics. 2008;91(1):22-9. doi: 10.1016/j.ygeno.2007.09.003.

Gulluoglu S, Tuysuz EC, Kuskucu A, Ture U, Atalay B, Sahin F, Bayrak OF. The potential function of microRNA in chordomas. Gene. 2016;585(1):76-83. doi: 10.1016/j.gene.2016.03.032.

Hattori T, Kaji M, Ishii H, Jureepon R, Takarada-Iemata M, Minh Ta H, Manh Le T, Konno A, Hirai H, Shiraishi Y, Ozaki N, Yamamoto Y, Okamoto H, Yokoyama S, Higashida H, Kitao Y, Hori O. CD38

positively regulates postnatal development of astrocytes cell-autonomously and oligodendrocytes non-cell-autonomously. Glia. 2017; doi: 10.1002/glia.23139.

Hicks SD, Ignacio C, Gentile K, Middleton FA. Salivary miRNA profiles identify children with autism spectrum disorder, correlate with adaptive behavior, and implicate ASD candidate genes involved in neurodevelopment. BMC Pediatr. 2016;16:52. doi: 10.1186/s12887-016-0586-x.

Iurov IIu, Vorsanova SG, Saprina EA, Iurov IuB. [Identification of candidate genes of autism on the basis of molecular cytogenetic and in silico studies of the genome organization of chromosomal regions involved in unbalanced rearrangements]. Genetika. 2010;46(10):1348-51.

Iyer A, Zurolo E, Prabowo A, Fluiter K, Spliet WG, van Rijen PC, Gorter JA, Aronica E. MicroRNA-146a: a key regulator of astrocyte-mediated inflammatory response. PLoS One. 2012;7(9):e44789. doi: 10.1371/journal.pone.0044789.

Jin D, Liu HX, Hirai H, Torashima T, Nagai T, Lopatina O, Shnayder NA, Yamada K, Noda M, Seike T, Fujita K, Takasawa S, Yokoyama S, Koizumi K, Shiraishi Y, Tanaka S, Hashii M, Yoshihara T, Higashida K, Islam MS, Yamada N, Hayashi K, Noguchi N, Kato I, Okamoto H, Matsushima A, Salmina A, Munesue T, Shimizu N, Mochida S, Asano M, Higashida H. CD38 is critical for social behaviour by regulating oxytocin secretion. Nature. 2007;446(7131):41-5. doi: 10.1038/nature05526.

Jude JA, Dileepan M, Subramanian S, Solway J, Panettieri RA Jr, Walseth TF, Kannan MS. miR-140-3p regulation of TNF-α-induced CD38 expression in human airway smooth muscle cells. Am J Physiol Lung Cell Mol Physiol. 2012;303(5):L460-8. doi: 10.1152/ajplung.00041.2012.

Karakas M, Schulte C, Appelbaum S, Ojeda F, Lackner KJ, Münzel T, Schnabel RB, Blankenberg S, Zeller T. Circulating microRNAs strongly predict cardiovascular death in patients with coronary artery disease-results from the large AtheroGene study. Eur Heart J. 2017; 38(7):516-523. doi: 10.1093/eurheartj/ehw250.

Kiko T, Nakagawa K, Tsuduki T, Furukawa K, Arai H, Miyazawa T. MicroRNAs in plasma and cerebrospinal fluid as potential markers for Alzheimer's disease. J Alzheimers Dis. 2014;39(2):253-9. doi: 10.3233/JAD-130932.

Kim S, Kim T, Lee HR, Jang EH, Ryu HH, Kang M, Rah SY, Yoo J, Lee B, Kim JI, Lim CS, Kim SJ, Kim UH, Lee YS, Kaang BK. Impaired learning and memory in CD38 null mutant mice. Mol Brain. 2016;9:16. doi: 10.1186/s13041-016-0195-5.

Kolesnikov N, Hastings E, Keays M, Melnichuk O, Tang YA, Williams E, Dylag M, Kurbatova N, Brandizi M, Burdett T, Megy K, Pilicheva E, Rustici G, Tikhonov A, Parkinson H, Petryszak R, Sarkans

U, Brazma A. ArrayExpress update--simplifying data submissions. Nucleic Acids Res 2015;43(Database issue):D1113-6. doi: 10.1093/nar/gku1057.

Kong SW, Collins CD, Shimizu-Motohashi Y, Holm IA, Campbell MG, Lee IH, Brewster SJ, Hanson E, Harris HK, Lowe KR, Saada A, Mora A, Madison K, Hundley R, Egan J, McCarthy J, Eran A, Galdzicki M, Rappaport L, Kunkel LM, Kohane IS. Characteristics and predictive value of blood transcriptome signature in males with autism spectrum disorders. PLoS One. 2012;7(12):e49475. doi: 10.1371/journal.pone.0049475.

Kong XM, Zhang GH, Huo YK, Zhao XH, Cao DW, Guo SF, Li AM, Zhang XR. MicroRNA-140-3p inhibits proliferation, migration and invasion of lung cancer cells by targeting ATP6AP2. Int J Clin Exp Pathol. 2015;8(10):12845-52.

Kuwano Y, Kamio Y, Kawai T, Katsuura S, Inada N, Takaki A, Rokutan K. Autism-associated gene expression in peripheral leucocytes commonly observed between subjects with autism and healthy women having autistic children. PLoS One. 2011;6(9):e24723. doi: 10.1371/journal.pone.0024723.

Lapierre M, Docquier A, Castet-Nicolas A, Gitenay D, Jalaguier S, Teyssier C, Cavaillès V. The emerging role of the transcriptional coregulator RIP140 in solid tumors. Biochim Biophys Acta. 2015;1856(1):144-50. doi: 10.1016/j.bbcan.2015.06.006.

Larrea E, Sole C, Manterola L, Goicoechea I, Armesto M, Arestin M, Caffarel MM, Araujo AM, Araiz M, Fernandez-Mercado M, Lawrie CH. New Concepts in Cancer Biomarkers: Circulating miRNAs in Liquid Biopsies. Int J Mol Sci. 2016;17(5). doi: 10.3390/ijms17050627.

Leidinger P, Backes C, Meder B, Meese E, Keller A. The human miRNA repertoire of different blood compounds. BMC Genomics. 2014;15:474. doi: 10.1186/1471-2164-15-474.

Lerer E, Levi S, Israel S, Yaari M, Nemanov L, Mankuta D, Nurit Y, Ebstein RP. Low CD38 expression in lymphoblastoid cells and haplotypes are both associated with autism in a family-based study. Autism Res. 2010;3(6):293-302. doi: 10.1002/aur.156.

Li M, Song Q, Li H, Lou Y, Wang L. Circulating miR-25-3p and miR-451a May Be Potential Biomarkers for the Diagnosis of Papillary Thyroid Carcinoma. PLoS One. 2015;10(7):e0132403. doi: 10.1371/journal.pone.0132403.

Lionetti M, Biasiolo M, Agnelli L, Todoerti K, Mosca L, Fabris S, Sales G, Deliliers GL, Bicciato S, Lombardi L, Bortoluzzi S, Neri A. Identification of microRNA expression patterns and definition of a microRNA/mRNA regulatory network in distinct molecular groups of multiple myeloma. Blood. 2009;114(25):e20-6. doi: 10.1182/blood-2009-08-237495.

Ludwig N, Leidinger P, Becker K, Backes C, Fehlmann T, Pallasch C, Rheinheimer S, Meder B, Stähler C, Meese E, Keller A. Distribution of miRNA expression across human tissues. Nucleic Acids Res. 2016;44(8):3865-77. doi: 10.1093/nar/gkw116.

Maffioletti E, Cattaneo A, Rosso G, Maina G, Maj C, Gennarelli M, Tardito D, Bocchio-Chiavetto L. Peripheral whole blood microRNA alterations in major depression and bipolar disorder. J Affect Disord. 2016;200:250-8. doi: 10.1016/j.jad.2016.04.021.

Marabita F, de Candia P, Torri A, Tegnér J, Abrignani S, Rossi RL. Normalization of circulating microRNA expression data obtained by quantitative real-time RT-PCR. Brief Bioinform. 2016;17(2):204-12. doi: 10.1093/bib/bbv056.

Martin A, Ochagavia ME, Rabasa LC, Miranda J, Fernandez-de-Cossio J, Bringas R. BisoGenet: a new tool for gene network building, visualization and analysis. BMC Bioinformatics 2010;11:91. doi: 10.1186/1471-2105-11-91.

Miles GD, Seiler M, Rodriguez L, Rajagopal G, Bhanot G. Identifying microRNA/mRNA dysregulations in ovarian cancer. BMC Res Notes. 2012;5:164. doi: 10.1186/1756-0500-5-164.

Mor M, Nardone S, Sams DS, Elliott E. Hypomethylation of miR-142 promoter and upregulation of microRNAs that target the oxytocin receptor gene in the autism prefrontal cortex. Mol Autism. 2015;6:46. doi: 10.1186/s13229-015-0040-1.

Müller M, Kuiperij HB, Claassen JA, Küsters B, Verbeek MM. MicroRNAs in Alzheimer's disease: differential expression in hippocampus and cell-free cerebrospinal fluid. Neurobiol Aging. 2014;35(1):152-8. doi: 10.1016/j.neurobiolaging.2013.07.005.

Mundalil Vasu M, Anitha A, Thanseem I, Suzuki K, Yamada K, Takahashi T, Wakuda T, Iwata K, Tsujii M, Sugiyama T, Mori N. Serum microRNA profiles in children with autism. Mol Autism. 2014;5:40. doi: 10.1186/2040-2392-5-40.

Munesue T, Yokoyama S, Nakamura K, Anitha A, Yamada K, Hayashi K, Asaka T, Liu HX, Jin D, Koizumi K, Islam MS, Huang JJ, Ma WJ, Kim UH, Kim SJ, Park K, Kim D, Kikuchi M, Ono Y, Nakatani H, Suda S, Miyachi T, Hirai H, Salmina A, Pichugina YA, Soumarokov AA, Takei N, Mori N, Tsujii M, Sugiyama T, Yagi K, Yamagishi M, Sasaki T, Yamasue H, Kato N, Hashimoto R, Taniike M, Hayashi Y, Hamada J, Suzuki S, Ooi A, Noda M, Kamiyama Y, Kido MA, Lopatina O, Hashii M, Amina S, Malavasi F, Huang EJ, Zhang J, Shimizu N, Yoshikawa T, Matsushima A, Minabe Y, Higashida H. Two genetic variants of CD38 in subjects with autism spectrum disorder and controls. Neurosci Res. 2010;67(2):181-91. doi: 10.1016/j.neures.2010.03.004.

Nautiyal J, Christian M, Parker MG. Distinct functions for RIP140 in development, inflammation, and metabolism. Trends Endocrinol Metab. 2013;24(9):451-9. doi: 10.1016/j.tem.2013.05.001.

Nguyen LS, Lepleux M, Makhlouf M, Martin C, Fregeac J, Siquier-Pernet K, Philippe A, Feron F, Gepner B, Rougeulle C, Humeau Y, Colleaux L. Profiling olfactory stem cells from living patients identifies miRNAs relevant for autism pathophysiology. Mol Autism. 2016;7:1. doi: 10.1186/s13229-015-0064-6.

Nogales-Gadea G, Ramos-Fransi A, Suárez-Calvet X, Navas M, Rojas-García R, Mosquera JL, Díaz-Manera J, Querol L, Gallardo E, Illa I. Analysis of serum miRNA profiles of myasthenia gravis patients. PLoS One. 2014;9(3):e91927. doi: 10.1371/journal.pone.0091927.

Pando R, Even-Zohar N, Shtaif B, Edry L, Shomron N, Phillip M, Gat-Yablonski G. MicroRNAs in the growth plate are responsive to nutritional cues: association between miR-140 and SIRT1. J Nutr Biochem. 2012;23(11):1474-81. doi: 10.1016/j.jnutbio.2011.09.010.

Park T, Yi SG, Kang SH, Lee S, Lee YS, Simon R. Evaluation of normalization methods for microarray data. BMC Bioinformatics 2003;4:33. doi: 10.1186/1471-2105-4-33.

Peng JS, Chen SY, Wu CL, Chong HE, Ding YC, Shiau AL, et Wang CR. Amelioration of Experimental Autoimmune Arthritis Through Targeting of Synovial Fibroblasts by Intraarticular Delivery of MicroRNAs 140-3p and 140-5p. Arthritis Rheumatol. 2016;68(2):370-81. doi: 10.1002/art.39446.

Peng X, Yang L, Liu H, Pang S, Chen Y, Fu J, Chen Y, Wen Z, Zhang R, Zhu B, Yu J, Invernizzi P. Identification of Circulating MicroRNAs in Biliary Atresia by Next-Generation Sequencing. J Pediatr Gastroenterol Nutr. 2016;63(5):518-523. doi: 10.1097/MPG.0000000000001194

Perfetti A, Greco S, Bugiardini E, Cardani R, Gaia P, Gaetano C, Meola G, Martelli F. Plasma microRNAs as biomarkers for myotonic dystrophy type 1. Neuromuscul Disord. 2014;24(6):509-15. doi: 10.1016/j.nmd.2014.02.005.

Perfetti A, Greco S, Cardani R, Fossati B, Cuomo G, Valaperta R, Ambrogi F, Cortese A, Botta A, Mignarri A, Santoro M, Gaetano C, Costa E, Dotti MT, Silvestri G, Massa R, Meola G, Martelli F. Validation of plasma microRNAs as biomarkers for myotonic dystrophy type 1. Sci Rep. 2016;6:38174. doi: 10.1038/srep38174.

Piepoli A, Tavano F, Copetti M, Mazza T, Palumbo O, Panza A, di Mola FF, Pazienza V, Mazzoccoli G, Biscaglia G, Gentile A, Mastrodonato N, Carella M, Pellegrini F, di Sebastiano P, Andriulli A. Mirna expression profiles identify drivers in colorectal and pancreatic cancers. PLoS One. 2012;7(3):e33663. doi: 10.1371/journal.pone.0033663.

Poliandri AH, Gamsby JJ, Christian M, Spinella MJ, Loros JJ, Dunlap JC, Parker MG. Modulation of clock gene expression by the transcriptional coregulator receptor interacting protein 140 (RIP140). J Biol Rhythms. 2011;26(3):187-99. doi: 10.1177/0748730411401579.

Quarona V, Zaccarello G, Chillemi A, Brunetti E, Singh VK, Ferrero E, Funaro A, Horenstein AL, Malavasi F. CD38 and CD157: a long journey from activation markers to multifunctional molecules. Cytometry B Clin Cytom. 2013;84(4):207-17. doi: 10.1002/cyto.b.21092.

R Core Team. R: A language and environment for statistical computing. R Foundation for Statistical Computing, Vienna, Austria. 2016.

Ragusa M, Barbagallo D, Purrello M. Exosomes: nanoshuttles to the future of BioMedicine. Cell Cycle. 2015;14(3):289-90. doi: 10.1080/15384101.2015.1006535.

Ragusa M, Bosco P, Tamburello L, Barbagallo C, Condorelli AG, Tornitore M, Spada RS, Barbagallo D, Scalia M, Elia M, Di Pietro C, Purrello M. miRNAs Plasma Profiles in Vascular Dementia: Biomolecular Data and Biomedical Implications. Front Cell Neurosci. 2016;10:51. doi: 10.3389/fncel.2016.00051.

Ragusa M, Statello L, Maugeri M, Barbagallo C, Passanisi R, Alhamdani MS, Li Destri G, Cappellani A, Barbagallo D, Scalia M, Valadi H, Hoheisel JD, Di Pietro C, Purrello M. Highly skewed distribution of miRNAs and proteins between colorectal cancer cells and their exosomes following Cetuximab treatment: biomolecular, genetic and translational implications. Oncoscience. 2014;1(2):132-57. doi: 10.18632/oncoscience.19.

Rakoczy J, Fernandez-Valverde SL, Glazov EA, Wainwright EN, Sato T, Takada S, Combes AN, Korbie DJ, Miller D, Grimmond SM, Little MH, Asahara H, Mattick JS, Taft RJ, Wilhelm D. MicroRNAs-140-5p/140-3p modulate Leydig cell numbers in the developing mouse testis. Biol Reprod. 2013;88(6):143. doi: 10.1095/biolreprod.113.107607.

Rasheed Z, Rasheed N, Al-Shaya O. Epigallocatechin-3-O-gallate modulates global microRNA expression in interleukin-1β-stimulated human osteoarthritis chondrocytes: potential role of EGCG on negative co-regulation of microRNA-140-3p and ADAMTS5. Eur J Nutr. 2017; doi: 10.1007/s00394-016-1375-x.

Reddemann K, Gola D, Schillert A, Knief J, Kuempers C, Ribbat-Idel J, Ber S, Schemme J, Bernard V, Gebauer N, Feller AC, Thorns C. Dysregulation of microRNAs in angioimmunoblastic T-cell lymphoma. Anticancer Res. 2015;35(4):2055-61.

Riebold M, Mankuta D, Lerer E, Israel S, Zhong S, Nemanov L, et al. All-trans retinoic acid upregulates reduced CD38 transcription in lymphoblastoid cell lines from Autism spectrum disorder. Mol Med. 2011;17(7-8):799-806. doi: 10.2119/molmed.2011.00080.

Rizzo R, Ragusa M, Barbagallo C, Sammito M, Gulisano M, Calì PV, Pappalardo C, Barchitta M, Granata M, Condorelli AG, Barbagallo D, Scalia M, Agodi A, Di Pietro C, Purrello M. Circulating miRNAs profiles in Tourette syndrome: molecular data and clinical implications. Mol Brain. 2015;8:44. doi: 10.1186/s13041-015-0133-y.

Robertson MM. A personal 35 year perspective on Gilles de la Tourette syndrome: assessment, investigations, and management. Lancet Psychiatry. 2015; 2(1):88-104. doi: 10.1016/S2215-0366(14)00133-3.

Robertson MM. The Gilles de la Tourette syndrome: the current status. Arch Dis Child Educ Pract Ed. 2012; 97(5):166-75. doi: 10.1136/archdischild-2011-300585.

Romano GL, Platania CBM, Drago F, Salomone S, Ragusa M, Barbagallo C, Di Pietro C, Purrello M, Reibaldi M, Avitabile T, Longo A, Bucolo C. Retinal and Circulating miRNAs in Age-Related Macular Degeneration: An In vivo Animal and Human Study. Front Pharmacol. 2017;8:168. doi: 10.3389/fphar.2017.00168.

Rong H, Liu TB, Yang KJ, Yang HC, Wu DH, Liao CP, Hong F, Yang HZ, Wan F, Ye XY, Xu D, Zhang X, Chao CA, Shen QJ. MicroRNA-134 plasma levels before and after treatment for bipolar mania. J Psychiatr Res. 2011;45(1):92-5. doi: 10.1016/j.jpsychires.2010.04.028.

Salem O, Erdem N, Jung J, Münstermann E, Wörner A, Wilhelm H, Wiemann S, Körner C. The highly expressed 5'isomiR of hsa-miR-140-3p contributes to the tumor-suppressive effects of miR-140 by reducing breast cancer proliferation and migration. BMC Genomics. 2016;17:566. doi: 10.1186/s12864-016-2869-x.

Sand M, Skrygan M, Georgas D, Sand D, Hahn SA, Gambichler T, Altmeyer P, Bechara FG. Microarray analysis of microRNA expression in cutaneous squamous cell carcinoma. J Dermatol Sci. 2012;68(3):119-26. doi: 10.1016/j.jdermsci.2012.09.004.

Sand M, Skrygan M, Sand D, Georgas D, Hahn SA, Gambichler T, Altmeyer P, Bechara FG. Expression of microRNAs in basal cell carcinoma. Br J Dermatol. 2012;167(4):847-55. doi: 10.1111/j.1365-2133.2012.11022.x.

Scardoni G, Tosadori G, Faizan M, Spoto F, Fabbri F, Laudanna C. Biological network analysis with CentiScaPe: centralities and experimental dataset integration. Version 2. F1000Res. 2014; doi: 10.12688/f1000research.4477.2.

Schmittgen TD, Livak KJ. Analyzing real-time PCR data by the comparative C(T) method. Nat Protoc 2008;3(6):1101-8.

Schwarzenbach H, da Silva AM, Calin G, Pantel K. Data Normalization Strategies for MicroRNA Quantification. Clin Chem. 2015;61(11):1333-42. doi: 10.1373/clinchem.2015.239459.

Serrano NA, Xu C, Liu Y, Wang P, Fan W, Upton MP, Houck JR, Lohavanichbutr P, Kao M, Zhao LP, Schwartz SM, Chen C, Méndez E. Integrative analysis in oral squamous cell carcinoma reveals DNA copy number-associated miRNAs dysregulating target genes. Otolaryngol Head Neck Surg. 2012;147(3):501-8. doi: 10.1177/0194599812442490.

Shannon P, Markiel A, Ozier O, Baliga NS, Wang JT, Ramage D, Amin N, Schwikowski B, Ideker T. Cytoscape: a software environment for integrated models of biomolecular interaction networks. Genome Res 2003;13(11):2498-504. doi: 10.1101/gr.1239303.

Shao NY, Hu HY, Yan Z, Xu Y, Hu H, Menzel C, Li N, Chen W, Khaitovich P. Comprehensive survey of human brain microRNA by deep sequencing. BMC Genomics. 2010;11:409. doi: 10.1186/1471-2164-11-409.

Simonoff E, Pickles A, Charman T, Chandler S, Loucas T, Baird G. Psychiatric disorders in children with autism spectrum disorders: prevalence, comorbidity, and associated factors in a population-derived sample. J Am Acad Child Adolesc Psychiatry. 2008;47(8):921-9. doi: 10.1097/CHI.0b013e318179964f.

Tan X, Qin W, Zhang L, Hang J, Li B, Zhang C, Wan J, Zhou F, Shao K, Sun Y, Wu J, Zhang X, Qiu B, Li N, Shi S, Feng X, Zhao S, Wang Z, Zhao X, Chen Z, Mitchelson K, Cheng J, Guo Y, He J. A 5-microRNA signature for lung squamous cell carcinoma diagnosis and hsa-miR-31 for prognosis. Clin Cancer Res. 2011;17(21):6802-11. doi: 10.1158/1078-0432.CCR-11-0419.

Taurino C, Miller WH, McBride MW, McClure JD, Khanin R, Moreno MU, Dymott JA, Delles C, Dominiczak AF. Gene expression profiling in whole blood of patients with coronary artery disease. Clin Sci (Lond). 2010;119(8):335-43. doi: 10.1042/CS20100043.

Vlachos IS, Paraskevopoulou MD, Karagkouni D, Georgakilas G, Vergoulis T, Kanellos I, Anastasopoulos IL, Maniou S, Karathanou K, Kalfakakou D, Fevgas A, Dalamagas T, Hatzigeorgiou AG. DIANA-TarBase v7.0: indexing more than half a million experimentally supported miRNA:mRNA interactions. Nucleic Acids Res 2015;43(Database issue):D153-9. doi: 10.1093/nar/gku1215.

Voineagu I, Eapen V. Converging Pathways in Autism Spectrum Disorders: Interplay between Synaptic Dysfunction and Immune Responses. Front Hum Neurosci. 2013;7:738. doi: 10.3389/fnhum.2013.00738.

Voineagu I, Wang X, Johnston P, Lowe JK, Tian Y, Horvath S, Mill J, Cantor RM, Blencowe BJ, Geschwind DH. Transcriptomic analysis of autistic brain reveals convergent molecular pathology. Nature. 2011;474(7351):380-4. doi: 10.1038/nature10110.

Vorstman JAS, Parr JR, Moreno-De-Luca D, Anney RJL, Nurnberger JI Jr, Hallmayer JF. Autism genetics: opportunities and challenges for clinical translation. Nat Rev Genet. 2017; 18(6):362-376. doi: 10.1038/nrg.2017.4.

Waki T, Lee SY, Niikura T, Iwakura T, Dogaki Y, Okumachi E, Oe K, Kuroda R, Kurosaka M. Profiling microRNA expression during fracture healing. BMC Musculoskelet Disord. 2016;17:83. doi: 10.1186/s12891-016-0931-0.

Wang J, Yu JT, Tan L, Tian Y, Ma J, Tan CC, Wang HF, Liu Y, Tan MS, Jiang T, Tan L. Genome-wide circulating microRNA expression profiling indicates biomarkers for epilepsy. Sci Rep. 2015;5:9522. doi: 10.1038/srep09522.

Weiland M, Gao XH, Zhou L, Mi QS. Small RNAs have a large impact: circulating microRNAs as biomarkers for human diseases. RNA Biol. 2012;9(6):850-9. doi: 10.4161/rna.20378.

Witwer KW. Circulating microRNA biomarker studies: pitfalls and potential solutions. Clin Chem. 2015;61(1):56-63. doi: 10.1373/clinchem.2014.221341.

Xia J, Broadhurst D, Wilson M, Wishart D. Translational biomarker discovery in clinical metabolomics: an introductory tutorial. Metabolomics. 2013; 9(2):280-299. doi: 10.1007/s11306-012-0482-9

Xia J, Wishart DS. Using MetaboAnalyst 3.0 for Comprehensive Metabolomics Data Analysis. Curr Protoc Bioinformatics. 2016; 55:14.10.1-14.10.91. doi: 10.1002/cpbi.11.

Yang Z, Matsumoto A, Nakayama K, Jimbo EF, Kojima K, Nagata K, Iwamoto S, Yamagata T. Circadian-relevant genes are highly polymorphic in autism spectrum disorder patients. Brain Dev. 2016;38(1):91-9. doi: 10.1016/j.braindev.2015.04.006.

Yu G, Wang LG, Han Y, He QY. clusterProfiler: an R package for comparing biological themes among gene clusters. OMICS 2012;16(5):284-7. doi: 10.1089/omi.2011.0118.

Yuan L, Chan GC, Fung KL, Chim CS. RANKL expression in myeloma cells is regulated by a network involving RANKL promoter methylation, DNMT1, microRNA and TNFα in the microenvironment. Biochim Biophys Acta. 2014;1843(9):1834-8. doi: 10.1016/j.bbamcr.2014.05.010.

Zhu J, Ma X, Zhang Y, Ni D, Ai Q, Li H, Zhang X. Establishment of a miRNA-mRNA regulatory network in metastatic renal cell carcinoma and screening of potential therapeutic targets. Tumour Biol. 2016; doi: 10.1007/s13277-016-5135-6.

Zou MX, Huang W, Wang XB, Lv GH, Li J, Deng YW. Identification of miR-140-3p as a marker associated with poor prognosis in spinal chordoma. Int J Clin Exp Pathol. 2014;7(8):4877-85.

Chapter 4. Circulating miRNAs in supernatant saliva from ASD patients

4.1. Abstract

Given its prevalence and social impact, ASD is drawing much interest. Molecular basis of ASD is heterogeneous and only partially known. Saliva represents an easily accessible, rich, and complete source of different types of molecules that could reflect genetic, epigenetic, environmental, metabolic, emotional, and behavioral alterations in ASD. To further investigate ASD etiology and to identify potential biomarkers to support its diagnosis, we used NanoString nCounter technology to profile supernatant saliva circulating miRNAs from 23 ASD patients and 12 NCs. Through validation assays in 54 ASD patients and 28 NCs, we demonstrated that both miR-29a-3p and miR-141-3p are upregulated in ASD saliva compared to NC one (Mann-Whitney test, p-value = 0.001, < 0.0001, respectively). ΔCt values for both miRNAs are correlated with overlapping neuropsychiatric scores evaluating ASD defects in social interaction and verbal communication. Target genes of miR-29a-3p and miR-141-3p, in particular the well-documented ASD susceptibility gene PTEN (phosphatase and tensin homolog), represent main components and regulators of pathways and processes known to be dysregulated in ASD (i.e., PI3K-Akt-mTOR signaling pathway, neuronal differentiation, synaptic function, and methionine metabolism). Biomarker performance evaluation proved that saliva miR-29a-3p and miR-141-3p when used in combination could be useful and non-invasive tools for discriminating ASD patients from NCs (AUC: 0.74; sensitivity: 64.81%; specificity: 67.86%). These findings suggest that these miRNAs could be used as supportive means for the recognition of ASD verbal and social defects and that a further characterization of their potential central role in neurodevelopment is needed.

4.2. Specific background and aims

Recent studies unanimously propose saliva as the ideal body fluid for the potential identification of ASD molecular biomarkers (Galiana-Simal et al., 2018). Saliva is secreted in the mouth by the sublingual, submandibular, and parotid salivary glands, which are under parasympathetic and sympathetic autonomic innervation controlling saliva secretion through the release of various neurotransmitters, such as acetylcholine, noradrenaline, and NPY (Ferreira and Hoffman, 2013). This close relationship between salivary glands and nervous system suggests that saliva could represent a rich pool of biomarkers reflecting, not only the systemic state of the body, but also various normal and pathological conditions

of the nervous system. In fact, in recent years, saliva has been used as a valid source of biomarkers for many neural pathologies, including sleep disorder, BD, schizophrenia, ASD, depression, and neurodegenerative diseases (Farah et al., 2018; Panahi et al., 2016; Wormwood et al., 2015), in addition to head and neck cancers and breast cancer (Aro et al., 2017; Panahi et al., 2016).

The alternative use of this liquid biopsy offers many important advantages (Galiana-Simal et al., 2018): (1) its sampling is painless, quick, and non-invasive; (2) its sampling procedure is easy and it does not need to be performed by professionals with formal medical training; (3) it contains a wide spectrum of stable molecules, easily and inexpensively measurable, (4) many of which are produced by the brain and are specifically related to its physiology and functioning (Lindell et al., 1999). The first two points make saliva the most appropriate body fluid to be sampled from ASD patients (Putnam et al., 2012; Spratt et al., 2012), clinically defined by high sensory reactivity (Lydon et al., 2016; Spratt et al., 2012) and severe behavioral difficulties, especially in stressful and anxiety-provoking social contexts. The last two ones encourage the search for potential saliva biomarkers to be used to support ASD clinical behavior-based diagnosis and to have promising insights about the heterogeneous etiology of this disorder.

Many molecules have been tested and monitored in ASD saliva samples (Galiana-Simal et al., 2018): (i) hormones, like cortisol (Tomarken et al., 2015; Bitsika et al., 2015; Gabriels et al., 2013; Spratt et al., 2012) and sexual steroids; (ii) proteins (Ngounou Wetie et al., 2015), including cytokines, peptide hormones (like OT) (Gordon et al., 2013), peptides, and neurotransmitters; (iii) nucleic acids, as mRNAs (Panahi et al., 2016), miRNAs (Hicks et al., 2016), and DNA. Therefore, saliva represents a rich and complete source of different types of molecules that could give researchers hints at the genetic, epigenetic, environmental, metabolic, emotional, and behavioral levels of ASD investigation. This oral sampling-based approach even gives the opportunity of easily explore the role of the oral microbiota in ASD (Qiao et al., 2018), evaluating how it may in turn affect brain function.

A molecular test for non-syndromic ASD is not available still and diagnosis relies on clinical assessment and confirmation. Considering the clinical variation and etiological heterogeneity of ASD, a precise diagnosis can be very difficult. That is why there is an urgent need for potential ASD biomarkers that could support clinical discrimination of patients. An ideal ASD biomarker should be: differentially observed in ASD patients compared to control general population; detectable in the ASD population at every stage of life; specific and helpful in ASD discrimination from other neurodevelopmental disorders; and correlated with available ASD screening tools, scales, and parameters (Galiana-Simal et al., 2018).

At the moment, only one pilot study has characterized miRNAs in whole saliva from ASD patients through RNA-sequencing (Hicks et al., 2016). We hypothesized that the supernatant saliva profile of circulating miRNAs may contain some specific fingerprints for ASD that could also complement the

discrimination of ASD patients. Aiming to gain more knowledge about ASD biomolecular basis and identify new potential biomarkers for this disorder through an oral sampling-based approach, we exploited NanoString nCounter technology to analyze the expression of circulating miRNAs in saliva from ASD patients and unaffected controls.

We validated saliva circulating miR-29a-3p and miR-141-3p as significantly upregulated in ASD patients compared to NCs. In addition, we demonstrated that their higher saliva expression levels are correlated with neuropsychiatric scores evaluating ASD aberrations in social interaction and verbal communication. Then, we observed that both target genes of miR-29a-3p and those of miR-141-3p, in particular PTEN, represent main components and regulators of pathways and processes that are convergingly dysregulated in ASD (i.e., PI3K-Akt-mTOR signaling pathway, neuronal differentiation, synaptic function, and methionine metabolism). Finally, through biomarker performance evaluation, we proved that saliva miR-29a-3p and miR-141-3p when used in combination could be used as helpful tools for the discrimination of ASD patients.

4.3. Results

4.3.1. Profiling of circulating miRNAs in saliva from ASD patients

Through NanoString nCounter technology, we investigated the expression levels of 827 circulating miRNAs in processed saliva from twenty-three ASD patients and twelve NCs. Data were normalized to the 36 miRNA reporters with the highest counts within the panel.

We identified ten miRNAs (let-7b-5p, miR-16-5p, miR-29a-3p, miR-141-3p, miR-146a-5p, miR-200a-3p, miR-200b-3p, miR-205-5p, miR-451a, and miR-4454 + miR-7975) as DE in ASD saliva compared to NC one (FDR < 0.25) (Figure 4.1, Table 4.1).

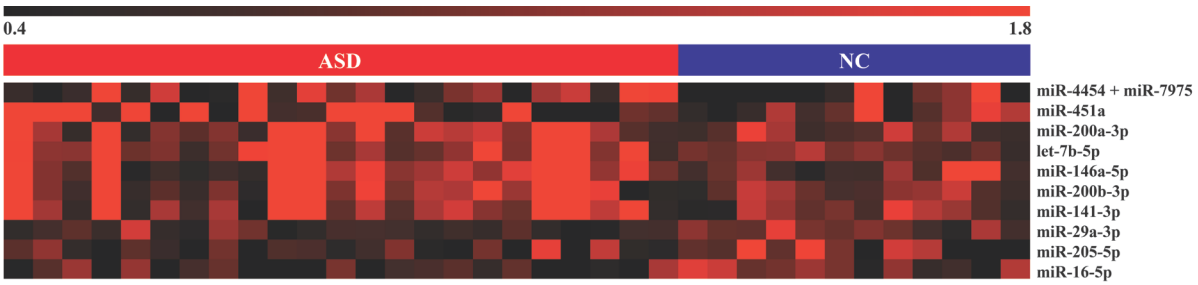

Figure 4. 1. Ten miRNAs are dysregulated in saliva from ASD patients compared to NCs. *Sample group annotations and names of DE miRNAs are reported in columns and rows of this miRNA expression heatmap, respectively. Colored heatmap cells represent expression values of each DE miRNA in every sample of a certain group. Data for each miRNA are shown as ratios of sample-specific normalized count to NC mean normalized count to obtain a better visualization of miRNA expression trends. For more information about miRNA expression trend, see figure legend.*

Table 4. 1. Ten miRNAs are dysregulated in ASD saliva. *Name, mean normalized count in both ASD and NC groups, and expression FC of each DE miRNA are reported. MiRNAs are decreasingly ordered by their FC. Since the same CodeSet probe hybridizes to both miR-4454 and miR-7975, we considered those two miRNAs as just one dysregulated molecule (miR-4454 + miR-7975). DE: differentially expressed; ASD: Autism Spectrum Disorder; NC: Unaffected Control; FC: Fold Change.*

DE miRNA	ASD mean normalized count	NC mean normalized count	ASD vs CTRL FC
miR-4454 + miR-7975	5872.62	1735.37	3.38
miR-451a	341.60	179.77	1.90
miR-200a-3p	136.99	79.12	1.73
let-7b-5p	352.66	206.07	1.71
miR-146a-5p	133.83	81.94	1.63
miR-200b-3p	197.65	121.34	1.63
miR-141-3p	168.21	109.28	1.54
miR-29a-3p	312.97	443.22	-1.42
miR-205-5p	228.21	324.83	-1.42
miR-16-5p	652.25	1026.10	-1.57

4.3.2. Dysregulated expression levels of miR-29a-3p and miR-141-3p in saliva from ASD patients

We selected miR-16-5p, miR-29a-3p, miR-141-3p, miR-146a-5p, and miR-200a-3p for further validation through single TaqMan assays. MiR-21-5p was used as endogenous control in all the analyses carried out.

We found both miR-29a-3p and miR-141-3p as significantly upregulated in saliva from fifty-four ASD patients compared to twenty-eight NCs (Mann-Whitney test, p-value = 0.001 and p-value < 0.0001, respectively) (Figure 4.2). It is worth noting that we did not confirm the expression trend obtained in the profiling analysis for miR-29a-3p: according to the validation analysis on bigger groups, this miRNA is slightly upregulated, rather than downregulated, in ASD saliva (Figure 4.2).

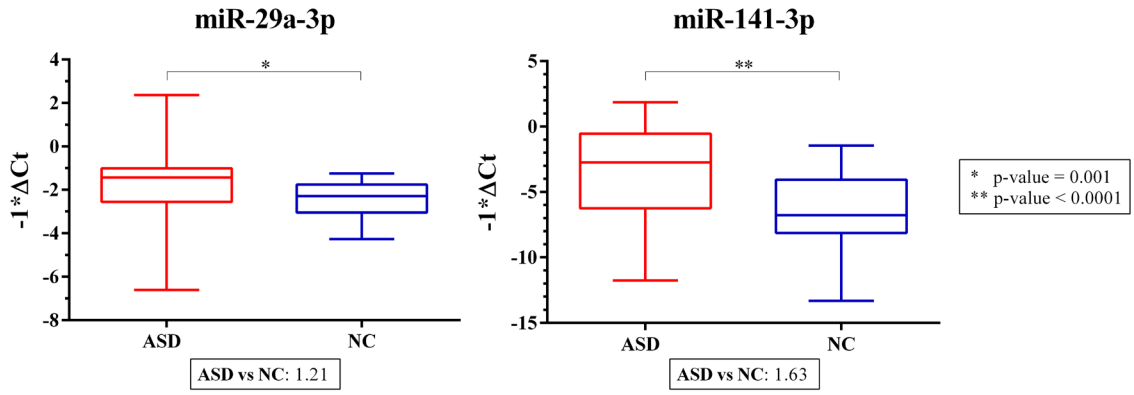

Figure 4. 2. MiR-29a-3p and miR-141-3p are significantly upregulated in saliva from ASD patients. *Single TaqMan assays for miR-29a-3p and miR-141-3p. Box and whiskers plots depicting saliva levels of these two miRNAs in ASD patients and NCs. Y-axes represent the distributions of -1*ΔCt values for miR-29a-3p and miR-141-3p. P-values from Mann-Whitney test are shown in the box next to the plots while expression FC values are shown in the boxes below them.*

We did not observe any expression differences between the two groups for miR-16-5p (Mann-Whitney test, p-value = 0.12), miR-146a-5p (Mann-Whitney test, p-value > 0.99), and miR-200a-3p (Mann-Whitney test, p-value = 0.60). Since the p-value obtained for miR-16-5p was very close to the chosen α for Mann-Whitney test, we repeated the analysis just for this miRNA by stratifying study participants for their age and considering two different subgroups in the validation set of samples, the young (age ≤ 6; 17 ASD patients vs 9 NCs) and old (age ≥ 7; 37 ASD patients vs 19 NCs) ones. We found miR-16-5p as significantly downregulated in ASD saliva only in the old group (Mann-Whitney test, p-value = 0.03), and not in the young one (Mann-Whitney test, p-value = 0.79) (Figure 4.3).

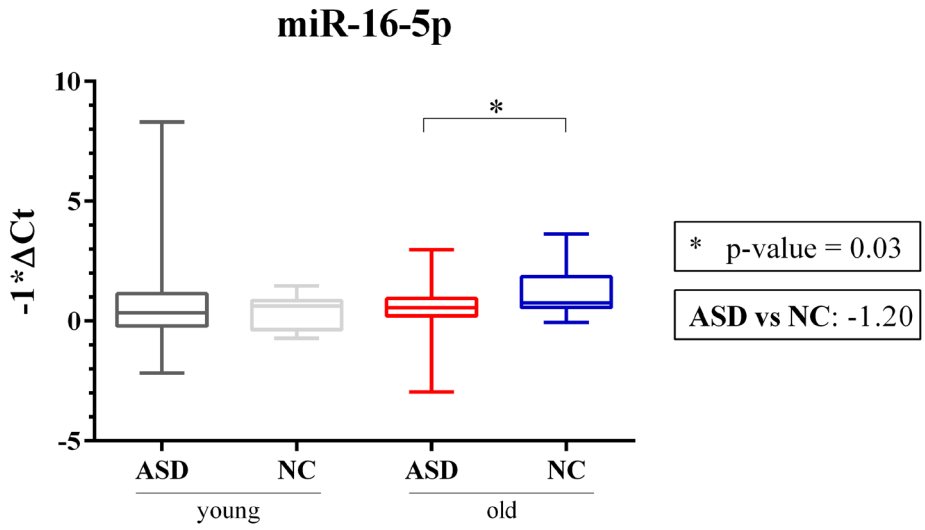

Figure 4. 3. MiR-16-5p is slightly downregulated in saliva between ASD patients and NCs aged seven or older. *Single TaqMan assays for miR-16-5p. Box and whiskers plot depicting saliva levels of miR-16-5p in ASD patients and NCs belonging to either the young or the old subgroup. Y-axis represents the distribution of -1*ΔCt values for miR-16-5p. P-value from Mann-Whitney test and expression FC value for the old subgroup are shown in the boxes next to the plot.*

4.3.3. Correlation between expression levels of dysregulated miRNAs and neuropsychiatric parameters

In order to test if any link existed between saliva expression of these two dysregulated miRNAs and commonly used ASD neuropsychiatric parameters, we computed the correlation between ΔCt values for either miR-29a-3p or miR-141-3p and various neuropsychiatric scores of study participants (Tables 4.2-3).

Table 4. 2. Correlation between miR-29a-3p expression and neuropsychiatric parameters. *We chose IQ (Section 1), ADI-R (Section 2), and ADOS (Section 3) scores as neuropsychiatric parameters for these analyses. Spearman r values from every analysis are reported along with corresponding raw and multiple comparison corrected p-values. Only correlations with a p-value ≤ Bonferroni corrected α were strictly selected as significant ones. Bonferroni corrected α = 0.05/11 = 0.0045. IQ: Intelligence Quotient; VIQ: Verbal Intelligence Quotient; PIQ: Performance Intelligence Quotient; TIQ: Total Intelligence Quotient; ADI-R: Autism Diagnostic Interview-Revised; ADOS: Autism Diagnostic Observation Schedule; 95% CI: 95% Confidence Interval; NC: Not Computed.*

1. IQ and miR-29a-3p			
	ΔCt vs. VIQ	**ΔCt vs. PIQ**	**ΔCt vs. TIQ**
Spearman r	0.33	0.19	0.24
95% CI	0.11 - 0.52	-0.04 - 0.39	0.02 - 0.44
two-sided p-value	0.0027	0.10	0.03
Is p < Bonferroni	Y	N	N

corrected α?				
Bonferroni-Holm corrected p-value	0.01	NC	0.03	
Benjamini-Hochberg adjusted p-value	0.005	NC	0.03	
Number of XY Pairs	80	80	80	
2. ADI-R and miR-29a-3p				
	ΔCt vs. ADI-R Social interaction	**ΔCt vs. ADI-R Communication**	**ΔCt vs. ADI-R Repetitive and restricted behaviors**	**ΔCt vs. ADI-R Developmental abnormalities**
Spearman r	-0.34	-0.40	-0.14	-0.22
95% CI	-0.52 - -0.13	-0.58 - -0.20	-0.35 - 0.09	-0.42 - 0.006
two-sided p-value	0.0017	0.0002	0.23	0.0502
Is p < Bonferroni corrected α?	Y	Y	N	N
Bonferroni-Holm corrected p-value	0.009	0.001	NC	NC
Benjamini-Hochberg adjusted p-value	0.004	0.001	NC	NC
Number of XY Pairs	82	82	82	82
3. ADOS and miR-29a-3p				
	ΔCt vs. ADOS Communication	**ΔCt vs. ADOS Social interaction**	**ΔCt vs. ADOS Imagination**	**ΔCt vs. ADOS Repetitive and restricted behaviors**
Spearman r	-0.39	-0.29	-0.27	-0.15
95% CI	-0.56 - -0.18	-0.48 - -0.07	-0.47 - -0.05	-0.36 - 0.07
two-sided p-value	0.0003	0.009	0.01	0.17
Is p < Bonferroni corrected α?	Y	N	N	N
Bonferroni-Holm corrected p-value	0.002	0.03	NC	NC
Benjamini-Hochberg adjusted p-value	0.001	0.01	NC	NC
Number of XY Pairs	82	82	82	82

Table 4. 3. Correlation between miR-141-3p expression and neuropsychiatric parameters. *We chose IQ (Section 1), ADI-R (Section 2), and ADOS (Section 3) scores as neuropsychiatric parameters for these analyses. Spearman r values from every analysis are reported along with corresponding raw and multiple comparison corrected p-values. Only correlations with a p-value ≤ Bonferroni corrected α were strictly selected as significant ones. Bonferroni corrected α = 0.05/11 = 0.0045. IQ: Intelligence Quotient; VIQ: Verbal Intelligence Quotient; PIQ: Performance Intelligence Quotient; TIQ: Total Intelligence Quotient; ADI-R: Autism Diagnostic Interview-Revised; ADOS: Autism Diagnostic Observation Schedule; 95% CI: 95% Confidence Interval; NC: Not Computed.*

1. IQ and miR-141-3p			
	ΔCt vs. VIQ	**ΔCt vs. PIQ**	**ΔCt vs. TIQ**

Spearman r	0.27	0.19	0.22	
95% CI	0.04 - 0.46	-0.04 - 0.40	-0.01 - 0.42	
two-sided p-value	0.02	0.10	0.053	
Is p < Bonferroni corrected α?	N	N	N	
Bonferroni-Holm corrected p-value	0.04	NC	NC	
Benjamini-Hochberg adjusted p-value	0.02	NC	NC	
Number of XY Pairs	80	80	80	
2. ADI-R and miR-141-3p				
	ΔCt vs. ADI-R Social interaction	**ΔCt vs. ADI-R Communication**	**ΔCt vs. ADI-R Repetitive and restricted behaviors**	**ΔCt vs. ADI-R Developmental abnormalities**
Spearman r	-0.34	-0.41	-0.19	-0.27
95% CI	-0.53 - -0.13	-0.58 - -0.20	-0.39 - 0.04	-0.47 - -0.05
two-sided p-value	0.0015	0.0002	0.0955	0.0126
Is p < Bonferroni corrected α?	Y	Y	N	N
Bonferroni-Holm corrected p-value	0.008	0.002	NC	0.04
Benjamini-Hochberg adjusted p-value	0.003	0.001	NC	0.02
Number of XY Pairs	82	82	82	82
3. ADOS and miR-141-3p				
	ΔCt vs. ADOS Communication	**ΔCt vs. ADOS Social interaction**	**ΔCt vs. ADOS Imagination**	**ΔCt vs. ADOS Repetitive and restricted behaviors**
Spearman r	-0.39	-0.29	-0.37	-0.22
95% CI	-0.56 - -0.18	-0.48 - -0.07	-0.55 - -0.16	-0.42 - 0.001
two-sided p-value	0.0003	0.009	0.0007	0.045
Is p < Bonferroni corrected α?	Y	N	Y	N
Bonferroni-Holm corrected p-value	0.002	0.03	0.004	0.045
Benjamini-Hochberg adjusted p-value	0.001	0.01	0.002	0.045
Number of XY Pairs	82	82	82	82

We found a positive correlation (Spearman r = 0.33; two-sided p-value = 0.0027) and a linear relationship (Table 4.4) between miR-29a-3p expression levels and VIQ scores (Figure 4.4). We could assume that higher saliva levels of miR-29a-3p, which have been observed in ASD patients, are potentially associated with deficits in verbal ability. We also found negative correlations and linear relationships (Table 4.4) between (i) miR-29a-3p expression levels and ADI-R Social interaction item scores (Spearman r = -0.34; two-sided p-value = 0.0017), (ii) miR-29a-3p expression levels and ADI-R

Communication item scores (Spearman r = -0.40; two-sided p-value = 0.0002), and (iii) miR-29a-3p expression levels and ADOS Communication item scores (Spearman r = -0.39; two-sided p-value = 0.0003) (Figure 4.4). We could infer that higher saliva levels of miR-29a-3p, typical of ASD patients, could be linked to aberrations in social interaction and verbal communication.

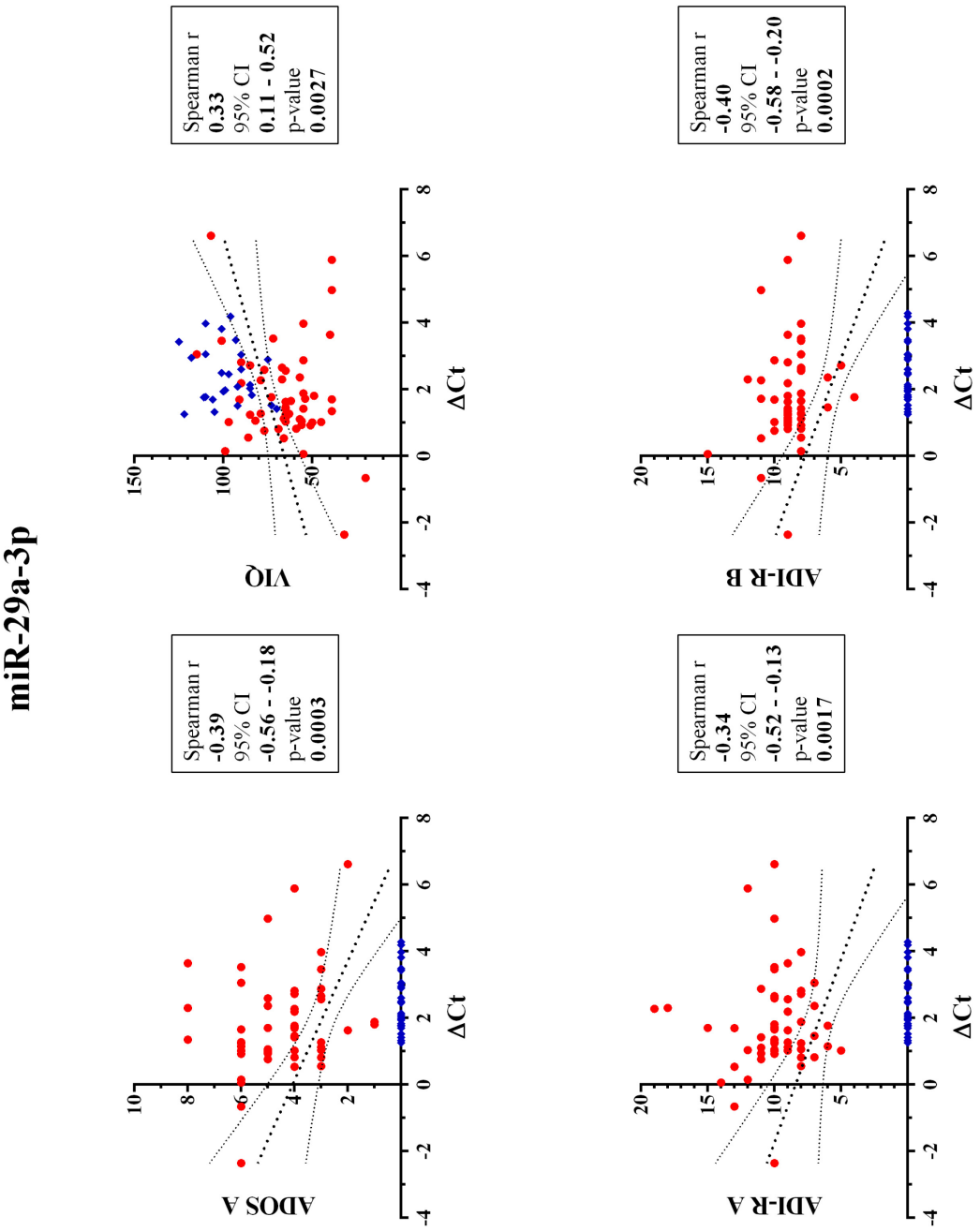

Figure 4. 4. Correlation between saliva levels of miR-29a-3p and ADOS, VIQ, and ADI-R scores. *The scatterplots also report the best-fit lines obtained from linear regression analyses. ADOS A represents the ADOS Communication item; ADI-R A refers to the ADI-R Social interaction item; ADI-R B to the ADI-R Communication one. VIQ: Verbal Intelligence Quotient; ADI-R: Autism Diagnostic Interview-Revised; ADOS: Autism Diagnostic Observation Schedule; 95% CI: 95% Confidence Interval.*

Moreover, we found negative correlations and linear relationships (Table 4.4) between (i) miR-141-3p expression levels and ADI-R Social interaction item scores (Spearman r = -0.34; two-sided p-value = 0.0015), (ii) miR-141-3p expression levels and ADI-R Communication item scores (Spearman r = -0.41;

two-sided p-value = 0.0002), (iii) miR-141-3p expression levels and ADOS Communication item scores (Spearman r = -0.39; two-sided p-value = 0.0003), and (iv) miR-141-3p expression levels and ADOS Imagination item scores (Spearman r = -0.37; two-sided p-value = 0.0007) (Figure 4.5). We could infer that higher saliva levels of even miR-141-3p, that have been observed in ASD patients, could be potentially associated with defects in social interaction and verbal communication, as shown for miR-29a-3p, and with deficient creative skills.

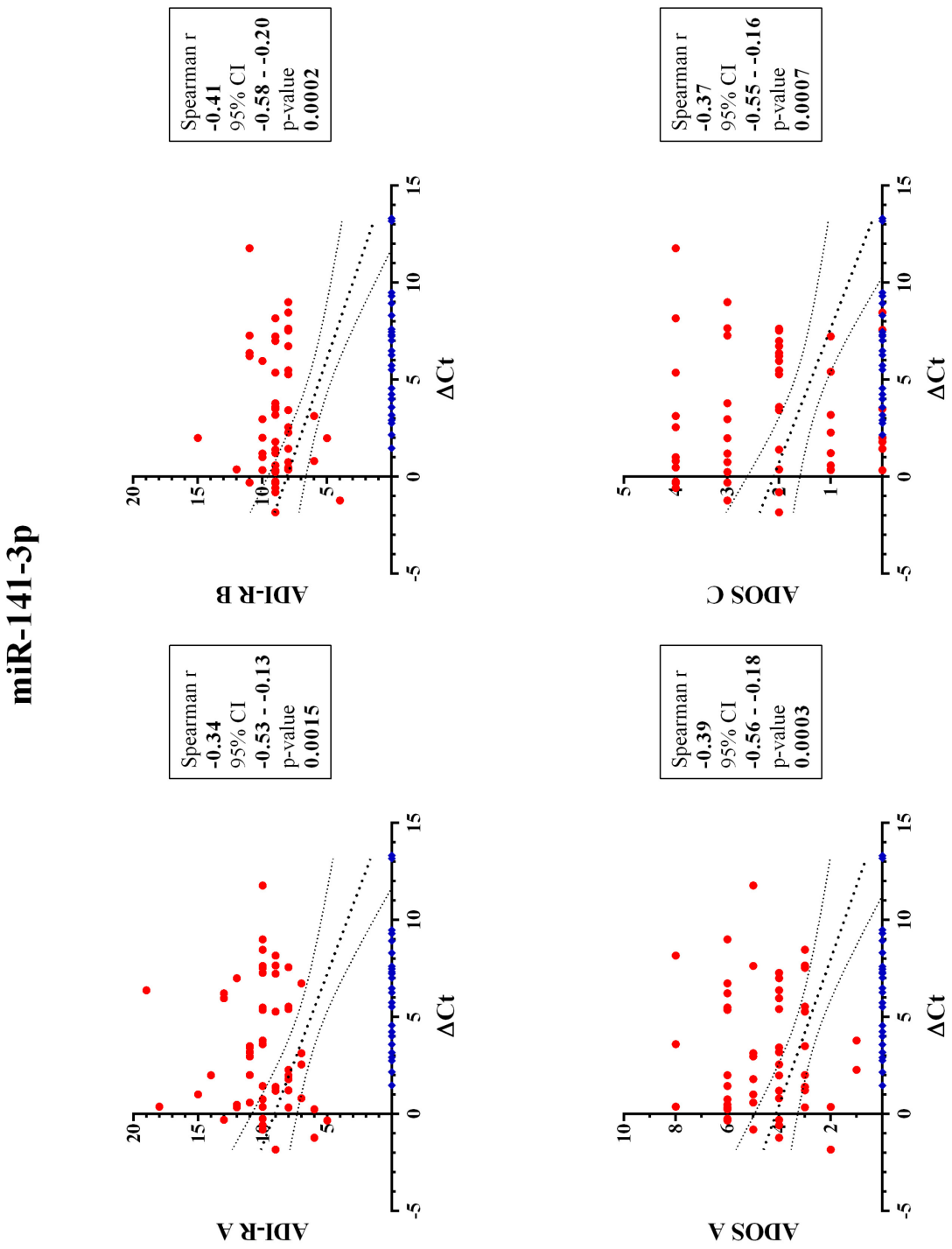

Figure 4. 5. Correlation between saliva levels of miR-141-3p and both ADOS and ADI-R scores. *The scatterplots also report the best-fit lines obtained from linear regression analyses. ADI-R A refers to the ADI-R Social interaction item; ADI-R B to the ADI-R Communication one; ADOS A represents the ADOS Communication item; ADOS C the ADOS Imagination one. VIQ: Verbal Intelligence Quotient; ADI-R: Autism Diagnostic Interview-Revised; ADOS: Autism Diagnostic Observation Schedule; 95% CI: 95% Confidence Interval.*

Table 4. 4. Linear regression analyses performed for the eight significant correlations found between saliva levels of dysregulated miRNAs and some neuropsychiatric parameters. *Bonferroni corrected α = 0.05/4 = 0.0125. VIQ: Verbal Intelligence Quotient; ADI-R: Autism Diagnostic Interview-Revised; ADOS: Autism Diagnostic Observation Schedule.*

	miR-29a-3p			
	ΔCt vs. ADOS Communication	**ΔCt vs. VIQ**	**ΔCt vs. ADI-R Social interaction**	**ΔCt vs. ADI-R Communication**
Best-fit line	y = -0.557x + 4.065	y = 5.189x + 65.91	y = -0.910x + 8.412	y = -0.925x + 7.710
R square	0.090	0.087	0.055	0.078
p-value	0.006	0.008	0.03	0.011
Is p < Bonferroni corrected α?	Y	Y	N	Y
	miR-141-3p			
	ΔCt vs. ADI-R Social interaction	**ΔCt vs. ADI-R Communication**	**ΔCt vs. ADOS Communication**	**ΔCt vs. ADOS Imagination**
Best-fit line	y = -0.565x + 9.088	y = -0.511x + 8.113	y = -0.265x + 4.116	y = -0.145x + 2.107
R square	0.141	0.158	0.136	0.113
p-value	0.0005	0.0002	0.0007	0.002
Is p < Bonferroni corrected α?	Y	Y	Y	Y

This correlation analysis confirmed that saliva expression of both miR-29a-3p and miR-141-3p correlated with crucial traits for the clinical diagnosis of ASD. We assume that these miRNAs could prove to be useful to strengthen the behavior-based diagnosis of ASD, by supporting the recognition of deficits in social interaction and verbal communication.

4.3.4. Functional analyses of validated targets of miR-29a-3p and miR-141-3p

By searching on miRTarBase database for validated targets of the two dysregulated miRNAs in ASD saliva, we retrieved 106 and 58 targets, whose validation was based on strong evidence, for miR-29a-3p and miR-141-3p, respectively (Table 4.5). These miRNAs share two common targets: KEAP1 (kelch like ECH associated protein 1) and PTEN (phosphatase and tensin homolog).

Table 4. 5. Validated targets of miR-29a-3p and miR-141-3p retrieved by miRTarBase database. *Total number and gene names of the validated targets for each differentially expressed miRNA in ASD saliva are reported. Targets in common between the two miRNAs are written in bold type.*

DE miRNA	**Total number of validated targets**	**Gene names of validated targets**
miR-29a-3p	106	ABL1, ADAM12, ADAMTS9, AHR, AKT2, AKT3, ALDH5A1, ATG9A, BACE1, BCL2, BCL7A, CACNA1C, CALCR, CCND1, CCND2, CCNT2, CD276, CD93, CDC42, CDC7,

		CDK2, CDK4, CDK6, CEACAM6, CLDN1, COL10A1, COL1A2, COL3A1, COL4A1, COL4A2, COL5A2, CPEB3, CPEB4, CYP2C19, DICER1, DKK1, DNMT1, DNMT3A, DNMT3B, ELN, FBN1, FGA, FGB, FGG, FOXO3, FSTL1, GLUL, GPR85, GSK3B, HBP1, HMGCR, IFNAR1, IGF1, IMPDH1, ITGA11, ITGA6, ITGB1, ITIH5, KDM5B, **KEAP1**, KLF4, KREMEN2, LAMC2, LOX, LPL, MCL1, MMP2, MUC1, MYC, MYCN, NASP, NAV3, NFIA, NMI, PDGFRB, PER1, PIK3R1, PPM1D, PPP1R13B, **PTEN**, PXDN, QKI, RAN, RASGRP1, RNASEL, ROBO1, S100B, SAPCD2, SERPINB9, SERPINH1, SETDB1, SFRP2, SLC22A7, SPARC, SRGAP2, TDG, TET1, TET2, TET3, TFEB, TNFAIP3, TRAF4, TRIM68, VDAC1, VEGFA, ZFP36
miR-141-3p	58	ACVR2B, BAP1, BRD3, CDC25A, CDC25C, CDYL, CLOCK, CTBP2, DLX5, E2F3, EIF4E, ELMO2, ERBIN, HDGF, HIPK2, HNRNPD, HOXB5, IGF1R, **KEAP1**, KLF11, KLF12, KLF5, KLHL20, MALAT1, MAP4K4, MAPK14, MAPK9, NR0B2, PAPPA, PHLPP1, PHLPP2, PPARA, **PTEN**, PTPRD, RASSF2, RIN2, SEPT7, SFPQ, SHC1, STAT4, STAT5A, STK3, TAZ, TCF7L1, TFDP2, TGFB2, TIAM1, TM4SF1, TRAPPC2B, UBAP1, VAC14, WDR37, YAP1, YWHAG, ZEB1, ZEB2, ZFPM2, ZMPSTE24

In order to investigate the molecular functions and the potential etiological role of these two miRNAs in ASD, we performed functional enrichment analyses of their target genes using GO, DO, and KEGG gene annotation databases.

Interestingly, genes controlled by miR-29a-3p (i) showed some neuronal specific cellular components (i.e., myelin sheath, postsynapse, dendritic spine, and neuron spine; PTEN was one of the targets determining the enrichment for all these terms) (Table 4.6, Figure S4.1C), (ii) were involved in various mechanisms taking place within the nervous system (i.e., dopaminergic neuron differentiation, regulation of neuron apoptotic process, pallium development, myelination, dendritic spine development, axon regeneration, and modulation of chemical synaptic transmission; PTEN was one of the targets determining the enrichment for all these terms except for the first two) (Table 4.6, Figure S4.1A), and (iii) were components of many pathways either crucial for neural development or known to be dysregulated in ASD (i.e., neurotrophin signaling pathway, axon guidance, and PI3K-Akt, Hedgehog, Wnt, and mTOR signaling pathways) (Table 4.6, Figure S4.2A). Also, it is worth noting that Ehlers-Danlos syndrome and methionine degradation were one of the over-represented DO terms and one of the over-represented KEGG modules in this list of target genes, respectively (Table 4.6, Figures S4.2B and S4.3).

Table 4. 6. Over-represented GO, DO, and KEGG terms associated with genes controlled by miR-29a-3p. *Selection of interesting illustrative over-represented terms. For a more complete (but still filtered)*

output see Figures S4.1-3. Term database, ID, and description, corresponding BH adjusted p-value generated by the hypergeometric test, Gene Ratio and Background Ratio values, and list of annotated genes are reported for all the most interesting over-represented terms associated with miR-29a-3p target genes. It is worth noting that PTEN (in bold type) is a target gene shared with miR-141-3p. Gene Ratio: the ratio of number of genes of interest that are annotated with a certain term from the database used to perform the analysis to number of genes of interest that are annotated with terms from the same database. Background Ratio: the ratio of number of genes in the genome that are annotated with a certain term from the database used to perform the analysis to number of genome genes that are annotated with terms from the same database. BH: Benjamini-Hochberg; GO: Gene Ontology; DO: Disease Ontology; BP: Biological Process; CC: Cellular Component; KEGG: Kyoto Encyclopedia of Genes and Genomes.

Annotation Database	Term ID	Term description	BH adjusted p-value	Gene Ratio	Background Ratio	Annotated Target Genes
KEGG Pathway	hsa04151	PI3K-Akt signaling pathway	3.90E-13	25/77	352/7430	CDK6, COL4A2, COL4A1, MCL1, BCL2, PIK3R1, ITGA11, **PTEN**, CCND2, VEGFA, AKT2, CDK2, FOXO3, LAMC2, ITGA6, PDGFRB, CCND1, CDK4, IGF1, AKT3, ITGB1, GSK3B, IFNAR1, MYC, COL1A2
KEGG Module	M00676	PI3K-Akt signaling	1.66E-05	4/16	13/1522	PIK3R1, AKT2, FOXO3, AKT3
KEGG Pathway	hsa04722	Neurotrophin signaling pathway	0.0002	8/77	119/7430	BCL2, PIK3R1, CDC42, ABL1, AKT2, FOXO3, AKT3, GSK3B
KEGG Module	M00035	Methionine degradation	0.0003	3/16	11/1522	DNMT3A, DNMT3B, DNMT1
GO BP	GO:1904338	regulation of dopaminergic neuron differentiation	0.0007	3/106	10/17653	SFRP2, DKK1, GSK3B
GO BP	GO:0021543	pallium development	0.001	7/106	163/17653	CDK6, RAN, **PTEN**, COL3A1, SRGAP2, ROBO1, GSK3B
GO BP	GO:0071542	dopaminergic neuron differentiation	0.001	4/106	37/17653	SFRP2, DKK1, VEGFA, GSK3B
DO	DOID:13359	Ehlers-Danlos syndrome	0.002	3/92	12/8007	COL3A1, COL5A2, COL1A2
KEGG Pathway	hsa04340	Hedgehog signaling pathway	0.004	4/77	47/7430	BCL2, CCND2, CCND1, GSK3B
GO CC	GO:0043209	myelin sheath	0.006	6/106	164/18698	BCL2, GLUL, CDC42, **PTEN**, VDAC1, ITGB1
GO BP	GO:0042552	myelination	0.006	5/106	113/17653	S100B, DICER1, **PTEN**, AKT2, QKI
KEGG Pathway	hsa04360	Axon guidance	0.007	7/77	175/7430	PIK3R1, CDC42, ABL1, SRGAP2,

						ITGB1, ROBO1, GSK3B
GO BP	GO:0031641	regulation of myelination	0.009	3/106	35/17653	S100B, DICER1, **PTEN**
GO CC	GO:0098794	postsynapse	0.011	9/106	450/18698	CPEB3, CPEB4, CDC42, **PTEN**, ABL1, SRGAP2, ITGB1, CACNA1C, GSK3B
KEGG Pathway	hsa04310	Wnt signaling pathway	0.011	6/77	146/7430	SFRP2, DKK1, CCND2, CCND1, GSK3B, MYC
KEGG Pathway	hsa04150	mTOR signaling pathway	0.013	6/77	151/7430	PIK3R1, **PTEN**, AKT2, IGF1, AKT3, GSK3B
GO BP	GO:0060996	dendritic spine development	0.014	4/106	90/17653	CPEB3, CDC42, **PTEN**, SRGAP2
GO BP	GO:0031103	axon regeneration	0.016	3/106	45/17653	BCL2, **PTEN**, KLF4
GO CC	GO:0043197	dendritic spine	0.016	5/106	153/18698	CPEB4, CDC42, **PTEN**, SRGAP2, ITGB1
GO CC	GO:0044309	neuron spine	0.016	5/106	155/18698	CPEB4, CDC42, **PTEN**, SRGAP2, ITGB1
GO BP	GO:0043525	positive regulation of neuron apoptotic process	0.018	3/106	48/17653	MCL1, CDC42, FOXO3
GO BP	GO:0050804	modulation of chemical synaptic transmission	0.022	7/106	335/17653	BACE1, DKK1, S100B, GLUL, CPEB3, **PTEN**, ABL1
GO BP	GO:0048679	regulation of axon regeneration	0.039	2/106	25/17653	**PTEN**, KLF4

Importantly, even genes controlled by miR-141-3p (i) were involved in nervous system's mechanisms (i.e., presynaptic membrane assembly, regulation of neuron projection regeneration and dendrite morphogenesis, hippocampus development; PTEN was one of the targets determining the enrichment for all these terms) (Table 4.7, Figure S4.4A), and (ii) were components of many interconnected crucial pathways (i.e., PI3K-Akt, Wnt, Hippo, JAK-STAT, and FoxO signaling pathways) (Table 4.7, Figures S4.4 and S4.5).

Table 4. 7. Over-represented GO and KEGG terms associated with genes regulated by miR-141-3p. *Selection of interesting illustrative over-represented terms. For a more complete (but still filtered) output see Figures S4.4-5. Term database, ID, and description, corresponding BH adjusted p-value generated by the hypergeometric test, Gene Ratio and Background Ratio values, and list of annotated genes are reported for all the most interesting over-represented terms associated with miR-141-3p target genes. It is worth noting that PTEN (in bold type) is a target gene shared with miR-29a-3p. For*

in-depth description of the column names see Table 4.6 legend. BH: Benjamini-Hochberg; GO: Gene Ontology; BP: Biological Process; KEGG: Kyoto Encyclopedia of Genes and Genomes.

Annotation Database	Term ID	Term description	BH adjusted p-value	Gene Ratio	Background Ratio	Annotated Target Genes
KEGG Pathway	hsa04392	Hippo signaling pathway - multiple species	0.005	3/38	29/7430	STK3, RASSF2, YAP1
KEGG Pathway	hsa04068	FoxO signaling pathway	0.005	5/38	132/7430	TGFB2, **PTEN**, MAPK14, MAPK9, IGF1R
GO BP	GO:0030111	regulation of Wnt signaling pathway	0.008	7/57	344/17653	ZEB2, DLX5, STK3, MAPK14, TCF7L1, YAP1, TIAM1
KEGG Pathway	hsa04390	Hippo signaling pathway	0.009	5/38	154/7430	STK3, TGFB2, YWHAG, TCF7L1, YAP1
GO BP	GO:0097105	presynaptic membrane assembly	0.020	2/57	10/17653	**PTEN**, PTPRD
GO BP	GO:0070571	negative regulation of neuron projection regeneration	0.028	2/57	15/17653	**PTEN**, MAP4K4
KEGG Module	M00683	Hippo signaling	0.037	2/13	16/1522	STK3, YAP1
KEGG Module	M00684	JAK-STAT signaling	0.037	2/13	19/1522	STAT4, STAT5A
GO BP	GO:0021766	hippocampus development	0.040	3/57	75/17653	ZEB2, **PTEN**, PHLPP2
KEGG Pathway	hsa04151	PI3K-Akt signaling pathway	0.044	6/38	352/7430	**PTEN**, EIF4E, YWHAG, PHLPP1, PHLPP2, IGF1R
GO BP	GO:0048814	regulation of dendrite morphogenesis	0.046	3/57	83/17653	**PTEN**, PTPRD, TIAM1

4.3.5. Saliva levels of miR-29a-3p and miR-141-3p in the discrimination of ASD patients

We used ΔCt values for miR-29a-3p and miR-141-3p to perform classical univariate ROC curve analyses. The univariate ROC plots revealed an AUC of 0.72 for miR-29a-3p (p-value = 0.03) and an AUC of 0.77 for miR-141-3p (p-value = 0.00005) (Figure 4.6, Figure S4.6).

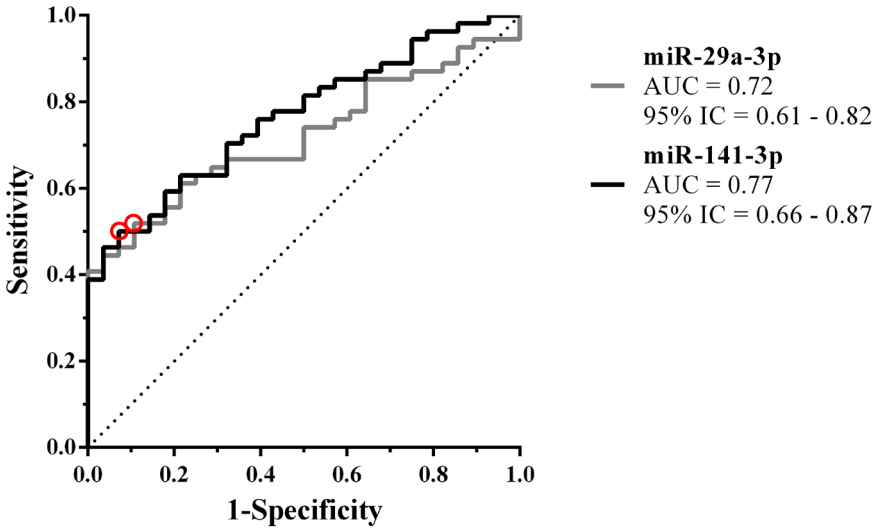

Figure 4. 6. Classical univariate ROC curve analyses for miR-29a-3p and miR-141-3p. *Each point on the ROC curves represents a sensitivity/specificity pair corresponding to a particular decision threshold (ΔCt value cut-off). Red circles on the curves refer to the sensitivity/specificity pairs with the highest Youden index J. AUC: Area under the ROC curve; 95% CI: 95% Confidence Interval.*

We used ΔCt value cut-offs corresponding to the sensitivity/specificity pair with the highest Youden index J for every computed ROC curve to perform a blind diagnosis on all the 82 analyzed samples (Figure 4.7).

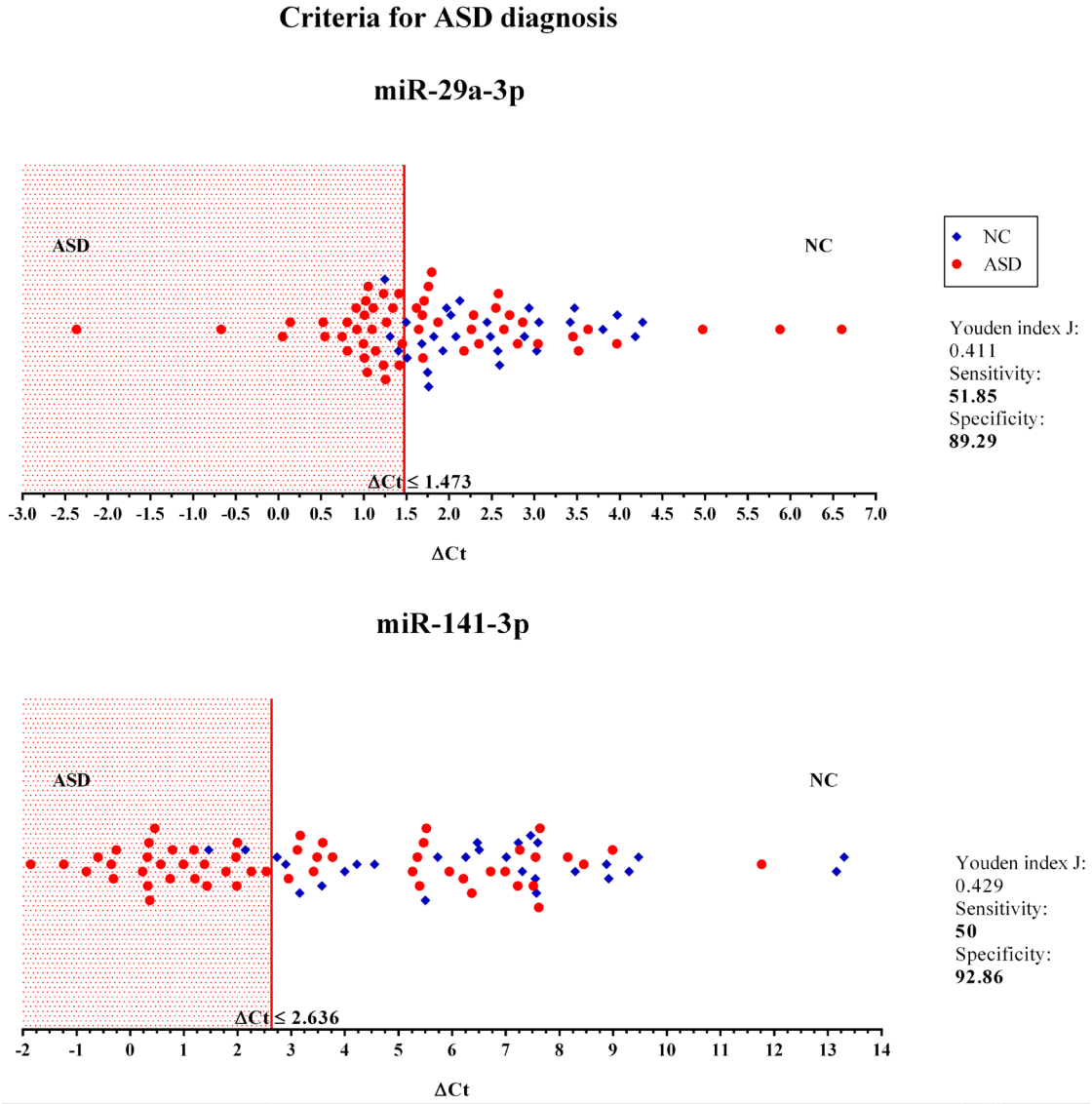

Figure 4. 7. The potential use of saliva miR-29a-3p and miR-141-3p as classifiers for ASD. *The graphs show the distribution of ΔCt values of all the 82 analyzed samples, for which we already had a clinical diagnosis. We used data from classical univariate ROC curve analyses to perform a blind diagnosis of all study participants. As regards miR-29a-3p, the ΔCt ≤ 1.473 criterion divides ASD patients from NCs and determines the correct discrimination of 28/54 ASD patients and 25/28 NCs. As concerns miR-141-3p, the ΔCt ≤ 2.636 criterion divides ASD patients from NCs and determines the correct discrimination of 27/54 ASD patients and 26/28 NCs.*

Then, we built a logistic regression model for both miRNAs and we tested those predictive models through CV and permutation testing. 100-time repeated random sub-sampling CV was used to test the performance of the logistic regression models. MiR-29a-3p performed at a discrete level for the comparison ASD vs NC, with an average AUC of 0.72, a sensitivity of 66.67%, and a specificity of 57.14% (Figure 4.8.1A-B). MiR-141-3p also performed at a good level in discriminating ASD patients, with an average AUC of 0.76, a sensitivity of 62.96%, and a specificity of 67.86% (Figure 4.8.2A-B).

CV results demonstrated the general applicability of these predictive models. 100-time repeated permutation tests on the performance measure AUC were carried out to validate the structure of these models. Permutation testing results were significant and quite stable in different runs for all the models tested (Figure 4.8.1C and .2C).

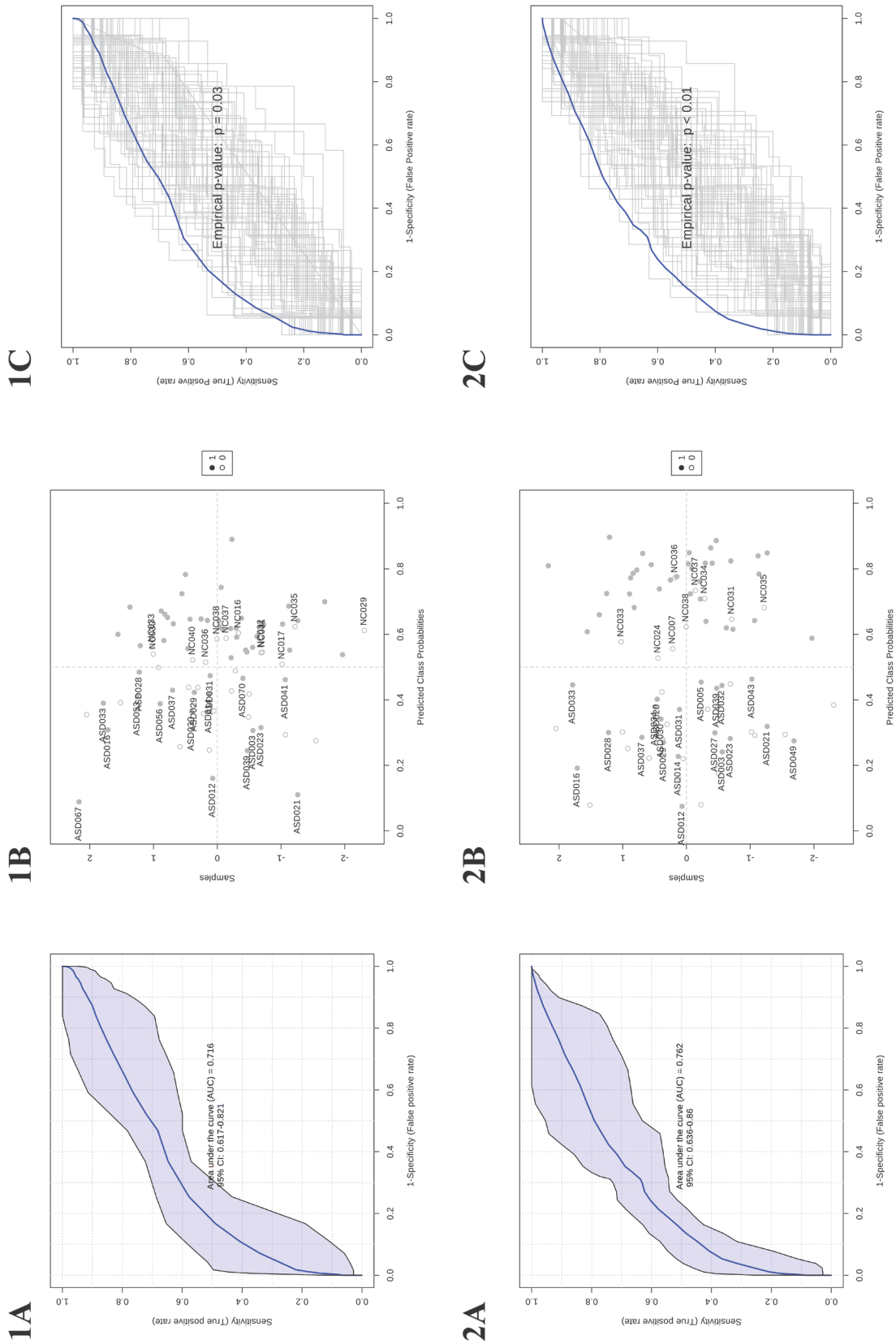

Figure 4. 8. Individual miR-29a-3p and miR-141-3p in the discrimination of ASD patients. *(1) The graphs refer to miR-29a-3p. (2) The graphs refer to miR-141-3p. (A) Average ROC curve from 100-time repeated random sub-sampling CV of the built logistic regression model. (B) Average predicted class*

probabilities (x-axis) of each sample (y-axis) from the 100 CV iterations. Probability scores more than 0.5 belong to the ASD group, those less than 0.5 belong to the NC group. Incorrectly classified subjects are identified by their ID number. (C) Results from the permutation tests on the model performance measure AUC. Average ROC curve and corresponding p-value are reported. AUC: Area under the ROC curve; 95% CI: 95% Confidence Interval.

Finally, to evaluate the performance of these two miRNAs if they were used as combined classifiers for ASD, we built a logistic regression model combining them and we tested it through CV and permutation testing. MiR-29a-3p and miR-141-3p when used in combination performed at a better level than when used individually in the discrimination of ASD patients, with an average AUC of 0.74, a sensitivity of 64.81%, and a specificity of 67.86% (corresponding to a better sensitivity/specificity pair) (Figure 4.9.A-B). Permutation testing results were significant and quite stable in different runs for this combined model (Figure 4.9.C).

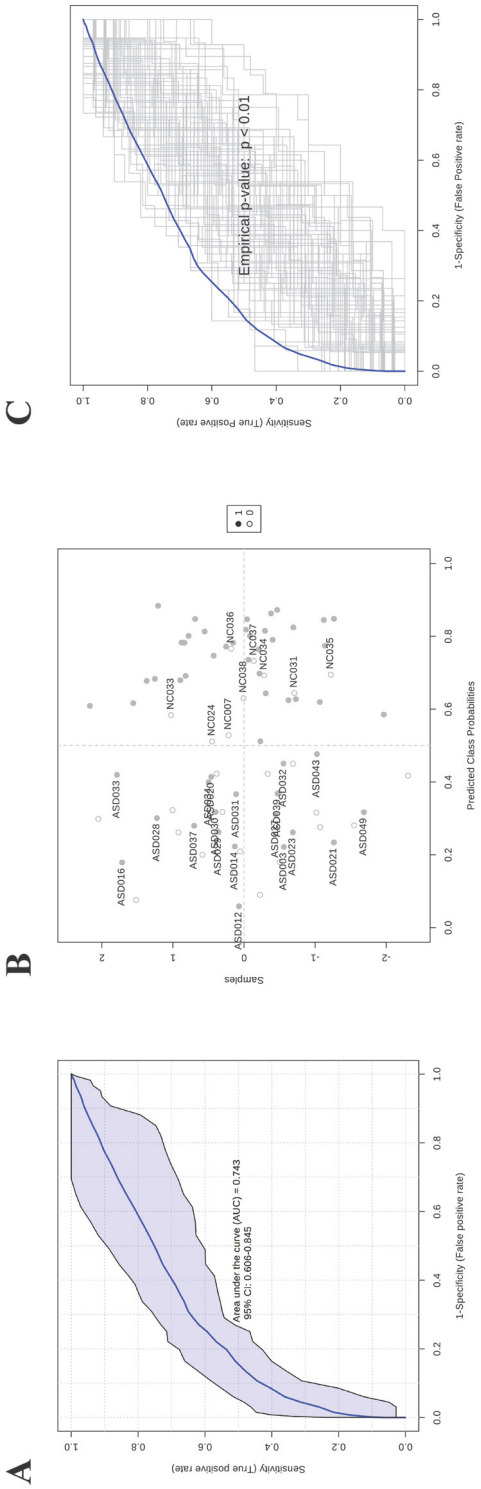

Figure 4. 9. Combined miR-29a-3p and miR-141-3p in the discrimination of ASD patients. *The graphs refer to the combination of two potential classifiers: miR-29a-3p and miR-141-3p. (A) Average ROC curve from 100-time repeated random sub-sampling CV of the built logistic regression model. (B) Average predicted class probabilities (x-axis) of each sample (y-axis) from the 100 CV iterations. Probability scores more than 0.5 belong to the ASD group, those less than 0.5 belong to the NC group. Incorrectly classified subjects are identified by their ID number. (C) Results from the permutation tests on the model performance measure AUC. Average ROC curve and corresponding p-value are reported. AUC: Area under the ROC curve; 95% CI: 95% Confidence Interval.*

These data showed that combined saliva miR-29a-3p and miR-141-3p could be helpful in the discrimination of ASD patients and could support ASD behavior-based diagnostic process.

4.4. Discussion

Recent studies suggest saliva as the ideal body fluid for the identification of potential ASD biomarkers given its easy and comfortable sampling and its richness as a source of different types of molecules (Galiana-Simal et al., 2018). The close relationship between salivary glands and nervous system (Ferreira and Hoffman, 2013) suggests that molecules secreted in saliva may reflect both normal and pathological conditions of the nervous system. Stability, general consistency of expression among individuals, and condition-specific expression profile make circulating miRNAs appropriate diagnostic biomarkers (Weiland et al., 2012; Larrea et al., 2016). We hypothesized that processed saliva profile of circulating miRNAs may contain specific fingerprints for ASD: these could help in the investigation of the molecular basis of ASD and be used as supportive non-invasive means to the clinical behavior-based diagnosis of this disorder.

By using NanoString nCounter technology, we profiled the expression of 827 circulating miRNAs in processed saliva from twenty-three ASD patients and twelve NCs and we selected ten miRNAs as dysregulated in ASD saliva (Figure 4.1, Table 4.1). Through our validation expression analysis on fifty-four ASD patients and twenty-eight NCs, we identified both miR-29a-3p and miR-141-3p as upregulated in saliva from ASD patients compared to NCs (Figure 4.2). Interestingly, contrary to results from profiling analysis, we found miR-29a-3p to be slightly upregulated, rather than downregulated, in ASD saliva: this observation confirmed the importance of data validation in larger cohorts (Witwer, 2015). Moreover, miR-16-5p showed decreased saliva expression levels in ASD compared to NC only in the old subgroup of study participants (Figure 4.3).

None of these miRNAs has ever been observed as dysregulated in either human ASD tissues or body fluids. According to expression data from the Human miRNA Tissue Atlas (Ludwig et al., 2016), miR-29a-3p is highly expressed in brain, meninges (arachnoid mater and dura mater), nerves, spinal cord, muscle, prostate, and thyroid, while miR-141-3p is highly expressed in colon, lung, skin, and thyroid, and just lowly expressed in brain. MiR-16-5p is highly expressed in blood vessels, muscle, and thyroid, whereas it is moderately expressed in brain, nerves, and spinal cord. According to RNA-seq data on miRNAs across the developing human brain (from infancy to adolescence) (Ziats and Rennert, 2014), miR-29a-3p and miR-16-5p are expressed at high read levels (> 1000) in multiple brain regions, including cerebellum, dorsolateral PFC (prefrontal cortex), ventrolateral PFC, medial PFC, orbitofrontal

PFC, and hippocampus, throughout infancy and childhood, while miR-141-3p shows very low read levels (< 1000) in these during developmental time. Moreover, in contrast to miR-29a-3p and miR-16-5p, that are not DE both within and between brain regions over developmental time, miR-141-3p is slightly upregulated in PFC compared to the hippocampus during late childhood and adolescence (Ziats and Rennert, 2014).

MiR-29a-3p function has mainly been investigated in human diseases like cancer (Lian et al., 2018; Cui et al., 2018; Catanzaro et al., 2017; He et al., 2017; Li et al., 2017; Wang et al., 2017), diabetes mellitus and diabetic kidney disease (Snowhite et al., 2017; Widlansky et al., 2018; Assmann et al., 2018), axial spondyloarthritis (Prajzlerová et al., 2017), hypothyroidism (Tokić et al., 2018), and Friedreich's ataxia (Dantham et al., 2018), in studies proving its onco-suppressor, inflammatory, immunoregulatory, and neurodegenerative role. In some of these diseases, its dysregulation has been observed in body fluids, such as either serum or plasma (Lian et al., 2018; Snowhite et al., 2017; Prajzlerová et al., 2017; Dantham et al., 2018). In mice model of ALS (amyotrophic lateral sclerosis), miR-29a-3p expression in brain and spinal cord is high: its in vivo CNS knockdown increases ALS mice lifespan (Nolan et al., 2014). On the contrary, it has been observed that miR-29a/b-1 knockout mice develop a progressive disorder characterized by locomotor impairment and ataxia and show smaller Purkinje cells, with less dendritic arborization and synaptic formation, demonstrating the important role that this miRNA cluster exerts in the brain (Papadopoulou et al., 2015). Moreover, in vivo mice brain-specific knockdown of miR-29a/b-1 determines massive cell death in large regions of the hippocampus and cerebellum and causes an ataxic phenotype, confirming the role of these miRNAs in neuronal survival and their involvement in several neurodegenerative disorders, including AD (Alzheimer's disease), Huntington's disease, and spinocerebellar ataxias, where they are usually downregulated and cannot act as efficient neuroprotectors (Roshan et al., 2014). Finally, miR-29a-3p has been proposed as a promising therapeutic target for CNS injury since its upregulation promotes neuronal differentiation and decreases astrocyte differentiation of neural stem cells derived from rat embryonic cortex via targeting PTEN (Shi et al., 2018). MiR-141-3p function has mainly been investigated in many human diseases and mechanisms, like cancer (Cui et al., 2018; Ishibashi et al., 2018; Zheng et al., 2018; Zhang et al., 2018; Wang et al., 2018; Huang et al., 2017; Ju et al., 2017), renal development (Zhang et al., 2018), age-related macular degeneration (Ayaz and Dinç, 2018), PD (Parkinson's disease) (Tolosa et al., 2018), gut microbiome balance (Moloney et al., 2018), prostatitis (Chen et al., 2018), and diabetic kidney disease (Li et al., 2017). Its dysregulation has been observed in body fluids, such as either serum or plasma, during pregnancy (Chim et al., 2008), in PD (Dong et al., 2016), in primary biliary cirrhosis (Tan et al., 2014), and in many tumors (Wang et al., 2017; Arab et al., 2017; Halvorsen et al., 2017). It has also been proposed as a feces biomarker of microbial fluctuations along with gut pathology in the intestine (Moloney et al., 2018). Moreover, miR-141 has been identified in mouse neural stem cells as a fine-tuning regulator of the expression patterns of FET proteins, a family of RBPs (RNA-binding proteins)

with a well-documented role in neurodegenerative diseases, during the differentiation of neuronal cells, a crucial mechanism for proper cortical development (Svetoni et al., 2017). Finally, middle-aged rats, displaying declined learning ability and increased APP (amyloid precursor protein) and BACE1 (β-secretase) protein expression in the forebrain cortex, typical signs of aging, have higher expression levels of miR-141-3p, a BACE1 modulator, in hippocampus (Che et al., 2014). Interestingly, miR-29a-3p and miR-141-3p exert very similar molecular functions in inflammation, cortical development, and neurodegeneration. Similarly, miR-16-5p has been identified as dysregulated in CSF-derived exosomes of young-onset AD patients, proving a possible involvement of this miRNA in neurodegenerative progression (McKeever et al., 2018). In addition, this miRNA is essential for the regulation of BDNF (brain derived neurotrophic factor)-induced dendritogenesis during neural development (Antoniou et al., 2018) and it can also be released by astrocytes in order to negatively regulate target neurons' synaptic stability and neuronal excitability during neuroinflammation (Chaudhuri et al., 2018). Therefore, there is strong evidence suggesting a potential role for these brain miRNAs even in neurodevelopment. Finally, miR-16-5p has been identified as one of the most abundantly expressed miRNAs in human whole saliva from healthy donors (Patel et al., 2011). Intriguingly, we confirmed this miRNA as downregulated in ASD compared to NC only in the old subgroup of study participants: however, this promising result needs to be validated on larger groups of samples.

We found the expression levels of both miR-29a-3p and miR-141-3p to be correlated with neuropsychiatric parameters that are clinically used to evaluate young ASD patients for their verbal, communicative, and social abilities (Figures 4.4-5). Higher saliva levels of these miRNAs, which we observed in ASD samples belonging to the validation set, could be potentially associated with defects in verbal communication and social interaction. These findings show that saliva expression analysis of both miR-29a-3p and miR-141-3p could strengthen the clinical diagnostic process of ASD, especially when assessing ASD symptoms and deficits in the domain of social communication and social interaction or when observing simultaneous language impairment in young patients.

Intriguingly, in a rat study investigating the effect of social isolation on oral mucosal healing, socially isolated rats persistently exhibit higher levels of miR-29 family members in their oral tissues (Yang et al., 2013). Interestingly, in a mouse study investigating the effect of social isolation on recovery after stroke, miR-141-3p levels are increased in frontal cortex from post-stroke isolated animals: post-stroke inhibition of this miRNA improves mortality and neurological deficits, and decreases infarct volumes, being particularly effective in aged mice (Verma et al., 2018). These two studies confirm an interesting potential link between defected social interaction and overexpression of both miR-29a-3p and miR-141-3p.

Through functional analyses on validated target genes of these two dysregulated miRNAs, we observed that both genes controlled by miR-29a-3p and those regulated by miR-141-3p partly exert a role in

maintaining the structural and functional integrity of the nervous system and in regulating its development; in addition, they act as components of many pathways both linked to neural development and associated to ASD (Tables 4.6-7). In particular, PTEN, one of the two shared targets between miR-29a-3p and miR-141-3p (Table 4.5), is directly involved in pallium and hippocampus development, axon regeneration, myelination, dendrite morphogenesis, and synaptic function, and it is a central unit in PI3K-Akt, mTOR, and FoxO signaling pathways (Tables 4.6-7).

The human PTEN gene encodes a lipid phosphatase with specificity towards PIP3 (phosphatidylinositol-3,4,5- triphosphate), inhibiting PI3K (phosphoinositide-3-kinase) and downstream AKT (protein kinase B) signaling pathways and acting as a negative regulator of cell proliferation. PTEN has been established as an ASD susceptibility gene. Germline mutation frequently occurs in this gene in patients diagnosed with PTEN Hamartoma Tumor Syndrome (PHTS). PHTS individuals show macrocephaly, benign growth of multiple tissues, and increased tumor risk (Hansen-Kiss et al., 2017). Intriguingly, autistic features are found in PHTS individuals with macrocephaly and carrying germline PTEN mutations reducing protein stability and activity (Hansen-Kiss et al., 2017; Wong et al., 2018). Similarly, patients with macrocephaly and developmental delay and/or ASD also show mutations in MTOR (mechanistic target of rapamycin kinase), PIK3CA (phosphatidylinositol-4,5-bisphosphate 3-kinase catalytic subunit alpha), and PPP2R5D (protein phosphatase 2 regulatory subunit B', delta) genes, confirming the role of the whole PI3K-AKT-mTOR pathway in these dysmorphic features and neurodevelopmental issues (Yeung et al., 2017). Knock-in mouse models carrying PTEN mutations altering its function and subcellular localization show increased brain weight, cell number, neuronal hypertrophy, and behavioral deficits associated with ASD: it has been demonstrated that nuclear wild-type PTEN alone is sufficient to regulate soma size and rescue the neuronal hypertrophy (Fricano-Kugler et al., 2017). Recent evidence has revealed that PTEN acts as a synaptic player during plasticity events, in addition to controlling cell proliferation and neuronal growth during development (Knafo and Esteban, 2017). Imbalance in excitation/inhibition (E/I imbalance), changes in intrinsic neuronal excitability, local hyper connectivity, and alterations in synaptic plasticity are the most common neuronal phenotypes seen in mice lacking PTEN, consistently with dysfunctional synapses or networks associated with ASD (Knafo and Esteban, 2017). Finally, FOXO (forkhead box proteins O) proteins, that have been found to also regulate neuronal polarization and positioning, synaptic function, and memory consolidation, are downstream effectors of the PI3K-Akt pathway. FOXO has been predicted to be one of the transcriptional factors responsible for transcriptional changes observed in neural progenitors and neurons obtained from multiple lines of iPSCs (induced pluripotent stem cells) derived from patients suffering from Timothy syndrome, a monogenic condition with high penetrance for ASD (Tian et al., 2014). Therefore, all these findings prove that we have identified two dysregulated miRNAs in ASD saliva that could indirectly control crucial mechanisms and pathways for this disorder.

Interestingly, we found Ehlers-Danlos syndrome (EDS) and methionine degradation as one of the over-represented DO terms and one of the over-represented KEGG modules in the list of miR-29a-3p target genes, respectively (Table 4.6).

EDS is the name used to refer to a rather large and heterogeneous group of inherited disorders affecting the connective tissue and characterized by joint hypermobility (GJH, Generalized Joint Hypermobility), myalgia, skin problems, sleep apnea, pneumothorax, and cardiovascular disease. In a Swedish nationwide population-based matched cohort study, it has been observed that EDS individuals are at increased risks of being diagnosed with psychiatric disorders, with ASD having the highest risk ratio among all of the tested disorders (Cederlöf et al., 2016). In addition, EDS individuals often present with immune- and endocrine-mediated conditions and both immune and endocrine dysregulation seem to have a role in the etiology of ASD. A recent study demonstrated that women suffering from both ASD and GJH, a major feature of EDS, manifest more immune- and endocrine-mediated conditions than those just affected by ASD, showing a potential etiological relationship between ASD, GJH, and EDS (Casanova et al., 2018).

Abnormal metabolism of methionine and homocysteine has already been associated with ASD by many studies. ASD children have significantly lower baseline plasma concentrations of methionine, SAM (S-adenosylmethionine), homocysteine, cystathionine, cysteine, and total glutathione, and significantly higher concentrations of SAH (S-adenosylhomocysteine), adenosine, and oxidized glutathione; this metabolic profile is consistent with impaired capacity for methylation and increased vulnerability to oxidative stress in these patients (James et al., 2004). Moreover, ASD patients show higher levels of homocysteine in urine that are positively correlated with deficits in communication (Puig-Alcaraz et al., 2015) and lower urinary levels of methionine (Li et al., 2018). To sum up, convincing evidence suggests that miR-29a-3p could indirectly play a role in ASD immune, endocrine, and metabolic impairments.

Through ROC curve analyses, we proved that saliva levels of both miR-29a-3p and miR-141-3p could be used in the discrimination of ASD patients from NCs because of their very high specificity (Figures 4.6-7). In particular, these curves indicated miR-141-3p to have the best discriminating potential as ASD biomarker (Figure 4.6). However, it was essential to evaluate the actual performance of the corresponding predictive models of these two miRNAs through CV and permutation testing (Figure 4.8). In fact, through these analyses, we showed that the two models based on the individual expression of the saliva dysregulated miRNAs would perform at a very similar level and would have a less optimistic specificity in discriminating ASD patients. Finally, we evaluated the performance of miR-29a-3p and miR-141-3p when used as combined classifiers for ASD by building a logistic regression model based on their combined expression levels in saliva: we demonstrated that, when used in combination, miR-29a-3p and miR-141-3p performed at a better level than when used individually in the discrimination of ASD patients (Figure 4.9). These results, together with those from the correlation

analyses, make us suggest that saliva miR-29a-3p and miR-141-3p could serve as potential non-invasive biomarkers to support the behavior-based diagnosis of ASD. However, further studies on larger cohorts and on participants of lower age would be necessary in order to better test the discriminatory power of these two miRNAs and prove their value in supporting early diagnosis of ASD.

Our study has some limitations that are typical of those proposing circulating miRNAs as biomarkers. The first one regards diagnostic specificity. As reported above, both circulating miR-29a-3p and miR-141-3p have already been associated with multiple pathological conditions. The second issue is reproducibility. There is little overlap between circulating miRNAs reported as biomarkers from independent investigators and this challenges their clinical utility. For example, just two miRNAs (miR-27a-3p in Mundalil Vasu et al., 2014 and Hicks et al., 2016; miR-140-3p in Hicks et al., 2016 and Cirnigliaro et al., 2017) were found as consistently dysregulated in independent studies on body fluids from ASD patients. None of the three other independent studies on miRNA expression in human ASD liquid biopsies (discussed below) is consistent with this saliva one. That highlights the importance of data validation in larger cohorts and standardization of experimental conditions (Witwer, 2015).

Our study is the fourth high-throughput one profiling miRNAs in a body fluid from ASD patients in order to discover some potential biomarkers. It is also the first one characterizing circulating miRNAs in supernatant saliva from ASD patients, validating profiling data by TaqMan assay, a probe-based system designed to specifically detect the expression of miRNAs of interests.

The first study (Mundalil Vasu et al., 2014) was carried out on serum from a Japanese cohort of 55 ASD patients and 55 unaffected controls. The authors identified and validated 13 circulating miRNAs as dysregulated in serum from ASD patients and showed the accurate predictive power of 5 of them in discriminating ASD patients (Mundalil Vasu et al., 2014). Our ASD and NC sample size is slightly smaller than the one from this work, but we have used a hybridization-based technology that allowed us to profile the expression of many more miRNAs than the 139 that the authors analyzed. None of circulating miRNAs from this study matches those from our saliva profile. However, functional enrichment analyses from both studies (Mundalil Vasu et al., 2014; this chapter) demonstrated over-representation of the same neurological pathways, such as axon guidance, Hedgehog signaling, Wnt signaling, and mTOR signaling, observed for miR-29a-3p target genes, and MAPK signaling and ErbB signaling, observed for miR-141-3p target genes. This observation suggests that discrepancies can be explained with differences in pre-analytic variables, such as genetic structure of studied populations, cohort composition, type of sample used, sample processing, validation technique, and data normalization (Witwer, 2015). In particular, ethnicity of participants, cohort size, and miRNA panel and intercalating dye-based system used may have determined the inconsistencies observed. However, these can mainly be explained with the fact that the studies (Mundalil Vasu et al., 2014; this chapter) investigated two different human biofluids (processed serum and processed saliva, respectively).

The second paper (Hicks et al., 2016) describes a pilot study on whole saliva from a US cohort of 24 ASD patients and 21 unaffected controls. By RNA-sequencing, the authors identified 14 miRNAs as dysregulated in saliva from ASD patients and showed the discriminative accuracy of this molecular signature (Hicks et al., 2016). Our ASD and NC sample size is much bigger than the one from this work. In addition, sequencing data from it have not been validated through miRNA-specific qPCR assays. None of dysregulated miRNAs from this study matches those from our supernatant saliva profile. Nevertheless, consistently with our results, their functional enrichment analysis detected significant over-representation of target genes related to neuron and axon projection and transcriptional activation, observed for both miR-29a-3p and miR-141-3p target genes (Hicks et al., 2016; this chapter). Discrepancies between this work and our study can mainly be explained, other than with all the factors listed above, with the fact that they investigated two different types of saliva samples, whole and processed ones, and therefore, they looked at incomparable compartments, with or without a cellular contribution, respectively.

The third study (Cirnigliaro et al., 2017, or Chapter 3), that was also carried by our research group, analyzed serum samples from a Caucasian cohort of 30 ASD patients and 25 unaffected controls. In that study, through single TaqMan assays, we validated miR-140-3p as upregulated in serum from ASD patients compared to NCs. None of circulating miRNAs from that serum study matches those from this saliva profile. However, functional enrichment analyses from both studies (Cirnigliaro et al., 2017, or Chapter 3; this chapter) demonstrated over-representation of the same neurological biological processes and pathways, such as regulation of synaptic function, neuron differentiation, dendrite development, and Wnt signaling, observed for both miR-29a-3p and miR-141-3p target genes, and response to nerve growth factors, observed for miR-29a-3p target genes. These two studies used two different profiling approaches and sample sizes, whereas genetic structure of studied populations, cohort composition, sample processing, validation technique, and data normalization were very similar and comparable. Therefore, discrepancies between our two studies can mainly be explained with the fact that we investigated two different human body fluids (processed serum and processed saliva).

4.5. Summary and conclusions

This study identifies miR-29a-3p and miR-141-3p, two miRNAs exerting an important role in brain development, as potential non-invasive biomarkers for ASD, easily measurable in saliva samples, and suggests that these could be used as supportive means for the recognition of ASD verbal and social defects. Moreover, both target genes of miR-29a-3p and those of miR-141-3p are main components and regulators of pathways and processes that are convergingly dysregulated in ASD: this observation confirms the importance of their further characterization in tissues from ASD patients in order to investigate their potential central role in neurodevelopmental disorders.

This study led us to conclusions similar to those of the serum paper (Chapter 3) about our approach for the investigation of ASD. Despite some preliminary weak evidence about these (Hicks et al., 2016; Cirnigliaro et al., 2017, Chapter 3), we could (i) neither identify promising overlapping patterns and mechanisms of miRNA secretion between the two different human body fluids analyzed (ii) nor suggest interesting potential links between body fluids and diseased tissues.

4.6. Materials and methods

4.6.1. Patient selection

From the patient database of the Section of Child and Adolescent Psychiatry from University of Catania, seventy-seven Caucasian ASD patients, aged 3-9 years and from varying socio-economic contexts [mean age: 7.0 (SD: 1.5); M:F 63:14], were randomly recruited and studied from September 2017 to July 2018. They were compared to a control group composed of forty, randomly selected, neurologically intact unaffected NCs, aged 4-13 years and recruited from local schools [mean age: 6.9 (SD: 1.8); M:F 29:11], without any history of either chronic diseases or psychiatric disorders.

Each of the two groups of study participants was randomly divided in two subgroups, to be used as parts of the discovery and validation sets of samples, respectively. The discovery set of samples, used for miRNA profiling analysis, included saliva samples from twenty-three ASD patients [mean age: 6.7 (SD: 1.4); M:F 21:2] and twelve NCs [mean age: 6.8 (SD: 1.3); M:F 10:2]. We performed both gender and age (young: age ≤ 6; old: age ≥ 7) control analyses to check if group compositions in the discovery set of samples were equivalent. Neither gender nor age distribution are different between ASD and NC (Fisher's exact test, two-sided p-value = 0.59, p-value = 1.00, respectively). The validation set of samples, analyzed for miRNA profiling data validation, consisted of saliva samples from fifty-four ASD patients [mean age: 7.1 (SD: 1.6); M:F 42:12] and twenty-eight NCs [mean age: 6.9 (SD: 2.0); M:F 19:9]. We performed both gender and age (young: age ≤ 6; old: age ≥ 7) control analyses to check if group compositions in the validation set of samples were equivalent. Neither gender nor age distribution are different between ASD and NC (Fisher's exact test, two-sided p-value = 0.42, p-value = 1.00, respectively).

The study was approved by the local Ethics Committee. All parents gave written informed consent.

Diagnosis of ASD was made according to both DSM-IV-TR (Diagnostic and Statistical Manual of Mental Disorders, IV edition – Text Revision) and DSM-5 criteria by a child neurologist (Professor Renata Rizzo). All study participants were evaluated at the University Hospital Policlinico-Vittorio Emanuele of Catania. They were assessed through the ADOS and ADI-R schedules in order to evaluate

ASD symptoms and through the WISC-III and WPSSI-IV (Weschler Preschool and Primary Scale of Intelligence) scales, used by a psychologist, to estimate both IQ and cognitive functioning. Neuropsychological features of participants are summarized in Table 4.8.

Table 4. 8. Clinical and neuropsychological features of study participants. *Data are shown as means and standard deviations between parentheses. ASD: Autism Spectrum Disorder; NC: Unaffected Control; TIQ: Total Intelligence Quotient; ADI-R: Autism Diagnostic Interview-Revised; ADOS: Autism Diagnostic Observation Schedule.*

	TIQ	ADI-R				ADOS			
		Social interaction	Commu-nication	Repetitive and restricted behaviors	Developmental abnormalities	Commu-nication	Social interaction	Imagination	Repetitive and restricted behaviors
ASD	68.9 (19.7)	10.9 (3.7)	9.4 (2.4)	5.9 (2.8)	3.2 (1.3)	4.6 (1.9)	7.8 (2.4)	2.2 (1.2)	2.6 (1.3)
NC	96.6 (11.9)	0	0	0	0	0	0	0	0

4.6.2. Saliva sample processing

Saliva samples were taken in the morning by inviting young participants to collect saliva in their oral cavities and then, release it into 50 ml tubes that were kept at 4°C and processed within an hour from sampling (Cheng et al., 2011). Study participants were without food for at least three hours and had a good oral hygienical condition at the moment of saliva collection (Cheng et al., 2011). Saliva was separated from eukaryotic cellular components and eventual prokaryotic cells through centrifugation at 10000 rpm in a Beckman J2-21 Centrifuge, at 4°C for 15 minutes. Supernatant saliva was isolated and stored at -80°C until analysis.

4.6.3. RNA extraction and precipitation

Total RNA to be used for miRNA profiling analysis was isolated from 800 µl saliva samples by using Qiagen miRNeasy Mini Kit (Qiagen), according to Qiagen Supplementary Protocol for purification of RNA (including small RNAs) from serum or plasma. RNA was eluted in a 200 µl volume of RNAse-free water and subsequently subjected to precipitation by adding 20 µg of glycogen, 0.1 volume of 3 M sodium acetate, and 2.5 volumes of ice cold 100% ethanol (Walker and Lorsch, 2013). After incubation at -80°C overnight, RNA was centrifuged, washed twice in a 500 µl volume of ice cold 75% ethanol, and dissolved in a final 7 µl volume of RNAse-free water. Total RNA to be used for miRNA profiling data validation was extracted from 400 µl saliva samples by using the same kit and protocol. It was eluted in a final 45 µl volume of RNase-free water (with two consecutive steps of elution performed in the same collection tube) and it was not subjected to precipitation (Cirnigliaro et al., 2017). RNA was quantified and assessed for its purity by using the NanoDrop Spectrophotometer.

4.6.4. MiRNA profiling through NanoString nCounter technology

The saliva expression of 827 circulating miRNAs from 23 ASD patients and 12 NCs (discovery set) was profiled through NanoString nCounter technology by using three nCounter Human miRNA Expression Assay Kits (NanoString Technologies) and a nCounter Analysis System with FLEX configuration (Prep Station and Digital Analyzer) (NanoString Technologies), according to manufacturer's instructions (Momen-Heravi et al., 2014). We used a 3 µl (corresponding to approximately 300 ng) volume of total RNA for sample preparation (Momen-Heravi et al., 2014). We performed three individual runs of 12 samples each. NanoString Technologies nCounter assays, in combination with nCounter Analysis System, provides a sensitive, reproducible, and highly multiplexed method for direct and precise detection of targets through molecular barcodes, without the use of (and following bias introduced by) either reverse transcription or amplification.

We carried out data analysis using both nSolver 3.0 (Momen-Heravi et al., 2014) and MeV software. All the following steps were performed on nSolver 3.0. First, we assessed imaging quality control metrics for each sample run. At this point, we neither subtracted a background count level from each of the miRNA probes nor normalized miRNA counts using the internal positive controls present in each CodeSet. To normalize data prior to comparing them between hybridizations, we rather preferred a global normalization method which utilized miRNA reporters with the highest counts (36 ones with mean counts across samples higher than 100) to generate geometric mean-based sample-specific normalization factors. Moreover, since one of the three kits came from a different production lot, we used a reference sample that we prepared with kits from both lots and that we run twice to perform batch calibration, correcting counts by computing miRNA-specific calibration factors. Once we obtained a matrix (miRNAs in rows, samples in columns) containing normalized calibrated counts, we filtered it by keeping only those miRNAs (45 ones) whose counts were higher than 50 in at least 30 of the samples analyzed. DE circulating miRNAs in saliva from ASD patients compared to NCs were obtained performing SAM statistical analysis on this filtered matrix with MeV software. We used a two-class unpaired test, based on at least 100 permutations per miRNA, with a FDR cut-off of 0.25, in order to detect dysregulated miRNAs. This statistical analysis identified 25 DE miRNAs for the comparison ASD vs NC. However, we strictly selected just 10 out of these 25 miRNAs as DE (Figure 4.1, Table 4.1), since these showed the most marked and reproducible expression differences between the two groups. In addition, we used raw p-values for these 10 DE miRNAs from unpaired t-test as an additional criterion to elect miRNAs for further validation in order to investigate only the most promising ones. It is worth noting that the same CodeSet probe hybridizes to both miR-4454 and miR-7975 and therefore, we only could observe the combined and cumulative expression levels of these two miRNAs and consider them as just one dysregulated molecule (miR-4454 + miR-7975). We chose miR-21-5p as an appropriate housekeeping miRNA to use for validation assays, since (i) sample-specific normalization

factors based on its counts were highly correlated with those generated in the analysis performed on nSolver 3.0 and (ii), as a consequence, when normalizing raw counts to sample-specific normalization factors based on it, we were able to reproduce the expression differences observed in the original analysis between the two groups.

4.6.5. MiRNA profiling data validation

We used RNA from saliva of fifty-four ASD patients and twenty-eight NCs (validation set) to perform miRNA-specific reverse transcription reactions producing miRNA-specific cDNAs for real-time PCRs. These RT-PCR analyses were performed using TaqMan MicroRNA Assays (Applied Biosystems) specific for the 5 most promising DE miRNAs, miR-16-5p, miR-29a-3p, miR-141-3p, miR-146a-5p, and miR-200a-3p, and for the selected endogenous control, miR-21-5p. All the following analyses were performed with GraphPad Prism for Windows v6.01. D'Agostino-Pearson omnibus K2 test and Shapiro-Wilk test were performed to check if data from the two groups were normally distributed. Mann-Whitney test was used to test the differential expression of those miRNAs between the two groups. Statistical significance was established at a p-value ≤ 0.05. Expression FC values of miRNAs were calculated by applying the $2^{-\Delta\Delta Ct}$ method (Schmittgen and Livak, 2008).

Since the p-value obtained for miR-16-5p was very close to the chosen α for Mann-Whitney test, we repeated the analysis just for this miRNA by stratifying study participants for their age and considering two different subgroups in the validation set of samples, the young (age ≤ 6; 17 ASD patients vs 9 NCs) and old (age ≥ 7; 37 ASD patients vs 19 NCs) ones. We performed gender control analyses on both subgroups to check if subgroup compositions were equivalent. Gender distributions are not different between ASD and NC for both the young and the old groups (Fisher's exact test, two-sided p-value = 1.00, p-value = 0.19, respectively). We also performed gender control analyses between the two ASD subgroups and the two NC subgroups, individually. Gender distribution is not different between young ASD and old ASD subgroups (Fisher's exact test, two-sided p-value = 0.48). Moreover, gender distribution is not different between young NC and old NC subgroups (Fisher's exact test, two-sided p-value = 0.67). These last analyses made us conclude that gender is not responsible for the expression differences for miR-16-5p observed in the old subgroup.

4.6.6. Correlation between expression levels of dysregulated miRNAs and neuropsychiatric parameters

We analyzed correlation between ΔCt values for either miR-29a-3p or miR-141-3p, obtained from the normalization to miR-21-5p, and neuropsychiatric parameters. IQ (Verbal, Performance, and Total), ADI-R items concerning social interaction, communication, repetitive and restricted behaviors, and developmental abnormalities (ADI-R items A-D), and ADOS items regarding communication, social interaction, imagination, and repetitive and restricted behaviors (ADOS items A-D) were the

neuropsychiatric parameters chosen for these analyses. Spearman correlation was computed on GraphPad Prism software when analyzing these not normally distributed data. Two-sided p-values from these correlation analyses that were ≤ 0.05 were further corrected for multiple comparisons by using three different approaches: Bonferroni correction, Holm-Bonferroni correction, and BH FDR procedure. Statistical significance was established at a p-value ≤ Bonferroni corrected $\alpha = 0.05/11 = 0.0045$, at a Holm-Bonferroni corrected p-value ≤ 0.05, and at a BH FDR adjusted p-value ≤ 0.05. However, we strictly selected only correlations with a p-value ≤ Bonferroni corrected α as significant ones. Linear regression analyses were also carried out on GraphPad Prism software only for the eight significant correlations. Statistical significance was established at a p-value ≤ 0.05. We also corrected these p-values for multiple comparisons by using Bonferroni correction and statistical significance was established at a p-value ≤ Bonferroni corrected $\alpha = 0.05/4 = 0.0125$.

4.6.7. Functional analyses of validated targets of miR-29a-3p and miR-141-3p

miR-29a-3p and miR-141-3p targets whose validation was based on strong evidence were retrieved by miRTarBase (Release 7.0) database (Chou et al., 2016). clusterProfiler v3.8.1 R package (Yu et al., 2012) was used to perform individual functional enrichment analyses on validated targets of miR-29a-3p and miR-141-3p in R v3.5.0 (R Core Team, 2016). We searched for the gene annotation terms from the GO, DO, and KEGG databases that were over-represented in these two lists of targets compared to the entire genome. Statistical significance for the hypergeometric test was established at a BH adjusted p-value ≤ 0.05. gofilter() and simplify() functions in clusterProfiler were employed in order to select level-specific GO terms and to remove the most redundant ones, respectively.

4.6.8. ROC curve analyses and biomarkers' performance evaluations

ΔCt values for miR-29a-3p and miR-141-3p, obtained from the normalization to miR-21-5p, served as input data to perform classical univariate ROC curve analyses for each miRNA on the server Metaboanalyst 3.0 (Xia and Wishart, 2016). An appropriate ΔCt cut-off point maximizing both sensitivity and specificity was found for each curve by calculating the maximum Youden index J. GraphPad Prism software was used to create Figure 4.6 and 4.7. The true positive rate (y-axis) was plotted in function of the false positive rate (x-axis), for different ΔCt cut-off points.

Since these ROC curves were based on miRNAs already identified as differentially expressed between ASD and NC, they should be considered just as indicators of the discriminating potential of the two miRNAs, not of their actual performance as biomarkers. Therefore, we also built corresponding logistic regression models for both miR-29a-3p and miR-141-3p expression and we tested them through CV and permutation testing, once again, by using the server Metaboanalyst 3.0. For more details about this procedure see Section 3.6.8. Finally, we built a logistic regression model combining these two miRNAs

and we tested it through CV and permutation testing on Metaboanalyst 3.0, to evaluate their performance if they were used as combined classifiers for ASD.

4.7. Supplementary Figures

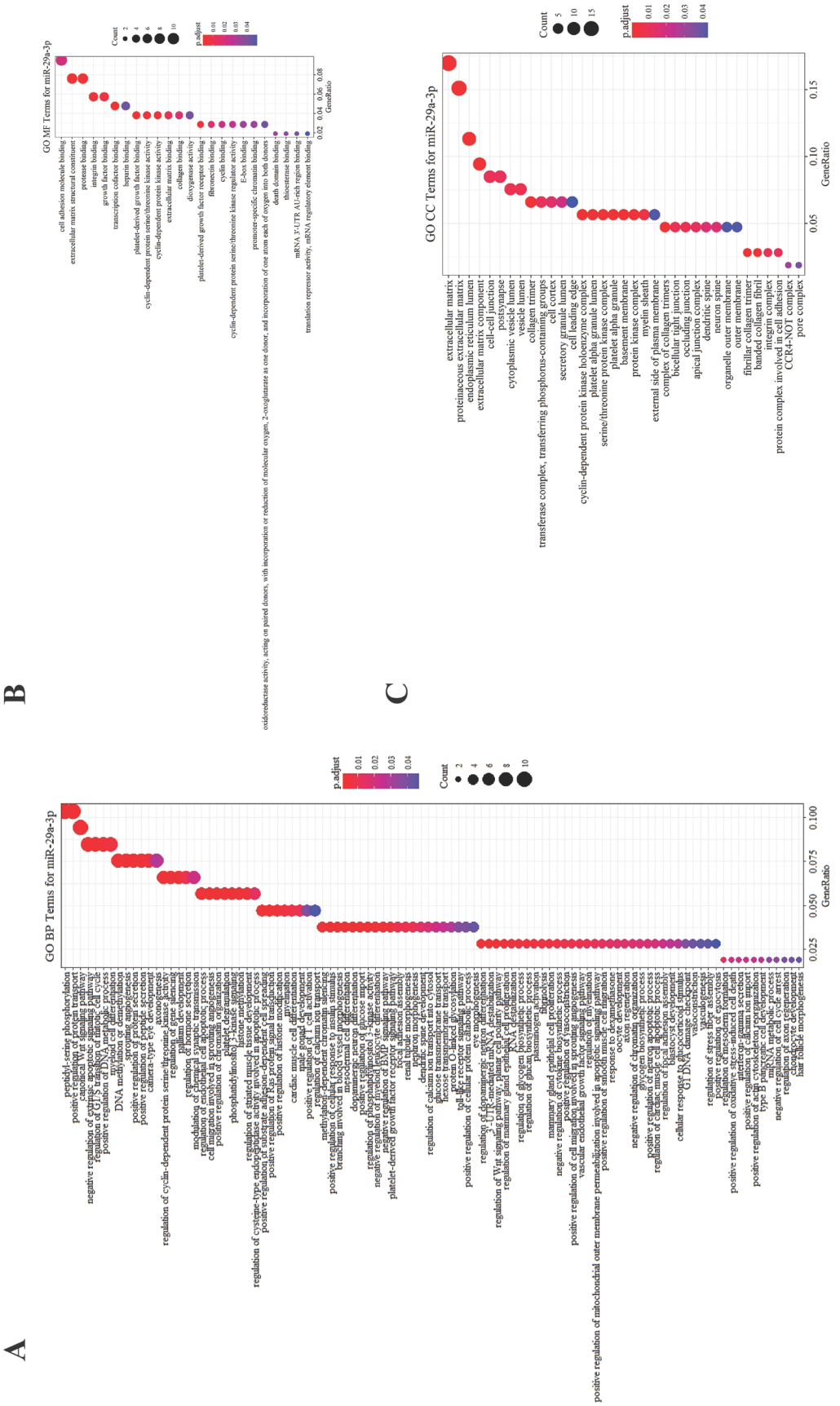

Figure S4. 1. Over-represented GO terms in the list of target genes controlled by miR-29a-3p compared to the entire genome. *(A) Dot plot for GO BP terms. This dot plot shows only 98 of the 819 significantly over-represented GO BP terms. These were the left terms after two subsequent steps of filtering: (i) selection of level 9 BP terms and (ii) removal of terms that were similar for at least the 70% (only the term with the lowest Benjamini-Hochberg adjusted p-value in each group of redundant ones was kept). (B) Dot plot for GO Molecular Function terms. (C) Dot plot for GO Cellular Component terms. Each circle in the plots symbolizes an over-represented term: its x-axis coordinate reflects the Gene Ratio value; its size is directly proportional to the Count value; its color represents the Benjamini-Hochberg adjusted p-value generated by the hypergeometric test. Gene Ratio: the ratio of number of genes of interest that are annotated with a certain term from the database used to perform the analysis to number of genes of interest that are annotated with terms from the same database. Count: number of node genes within the network that are annotated with a certain term. GO: Gene Ontology; BP: Biological Process; MF: Molecular Function; CC: Cellular Component.*

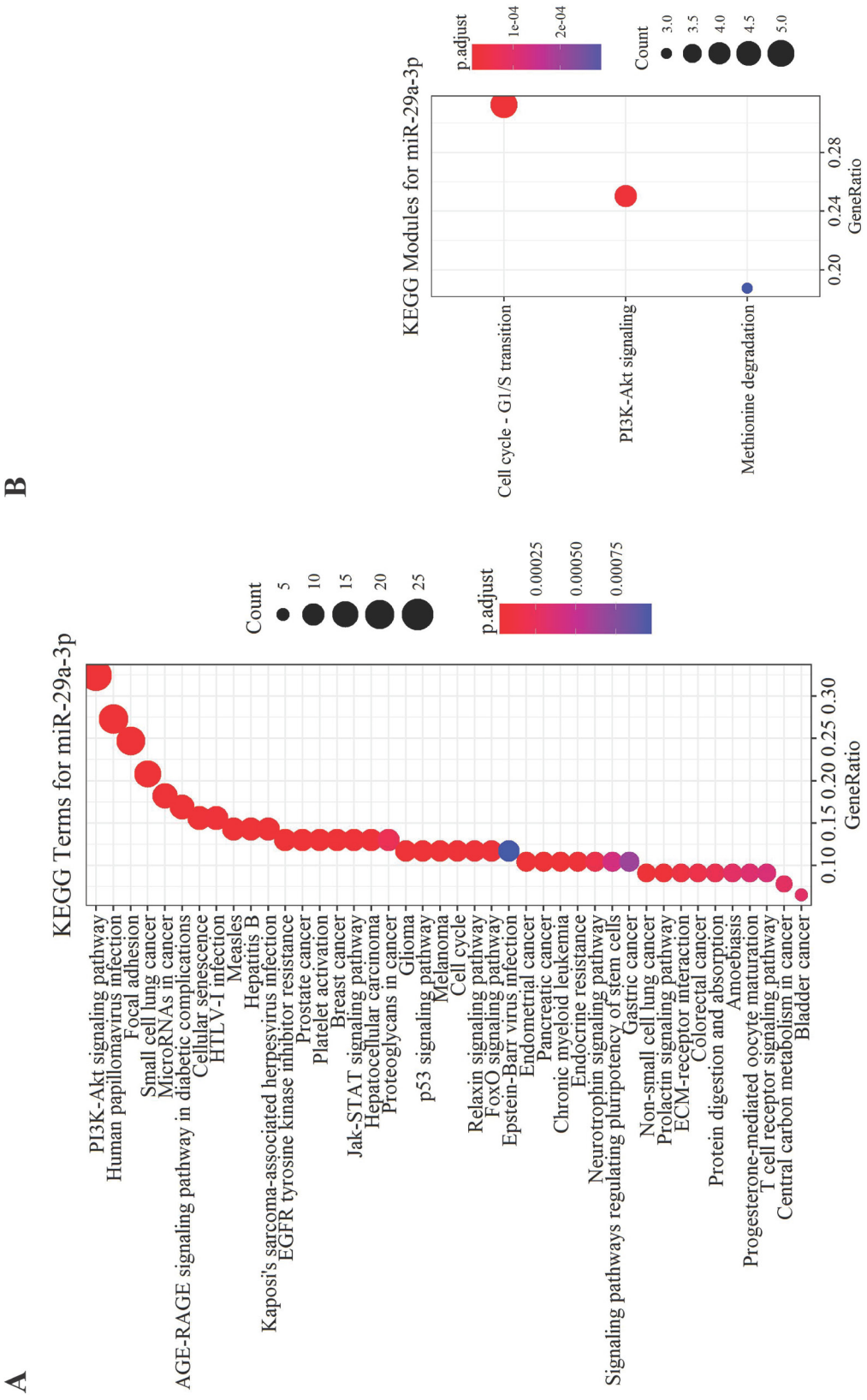

Figure S4. 2. Over-represented KEGG Pathway terms and Module terms in the list of target genes controlled by miR-29a-3p compared to the entire genome. *(A) Dot plot for KEGG Pathway terms. This dot plot shows only 42 of the 88 significantly over-represented KEGG Pathway terms. These were the terms with a Benjamini-Hochberg adjusted p-value ≤ 0.001. (B) Dot plot for KEGG Module terms. For*

in-depth description of the plots see Figure S4.1 legend. KEGG: Kyoto Encyclopedia of Genes and Genomes.

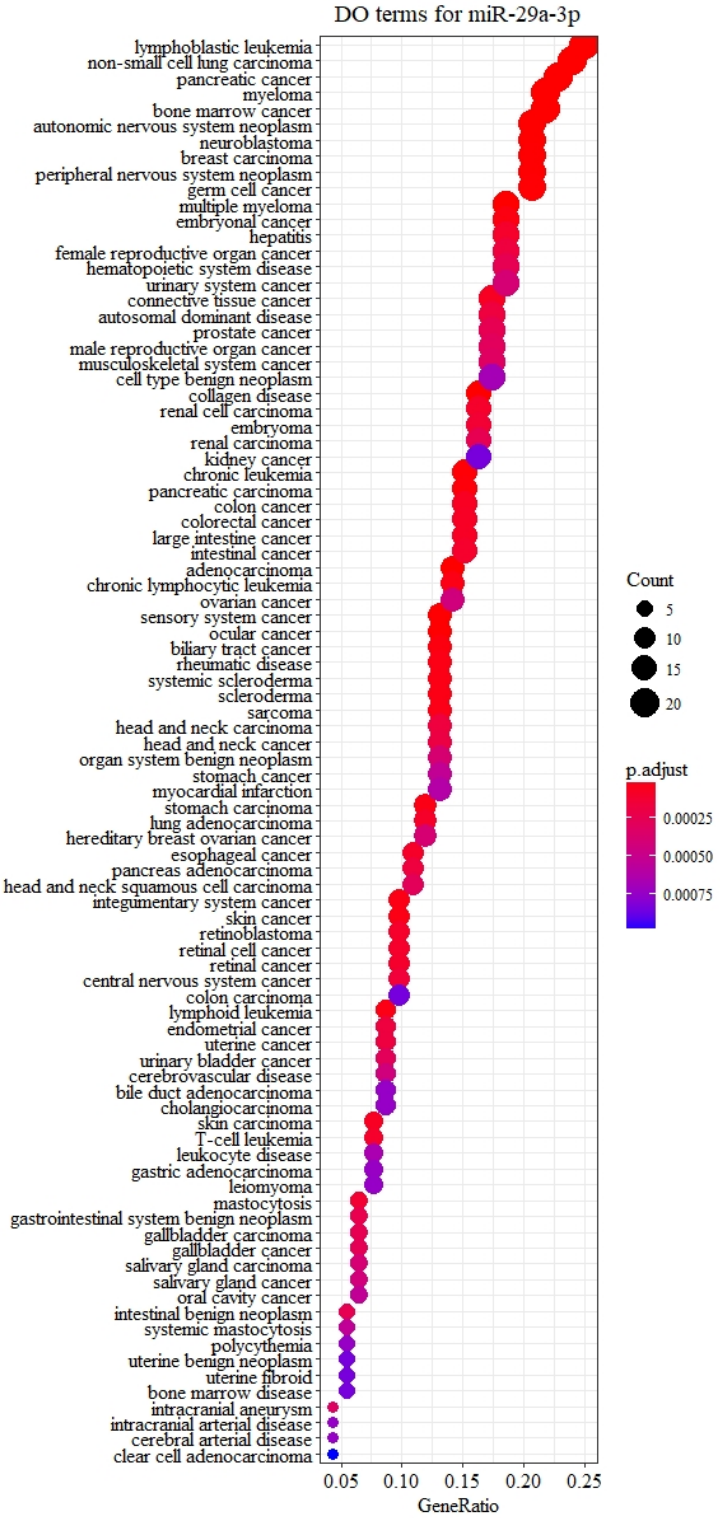

Figure S4. 3. Over-represented DO terms in the list of target genes controlled by miR-29a-3p compared to the entire genome. *Dot plot for DO terms. This dot plot shows only 90 of the 219 significantly over-represented DO terms. These were the terms with a Benjamini-Hochberg adjusted p-value ≤ 0.001. For in-depth description of the plot see Figure S4.1 legend. DO: Disease Ontology.*

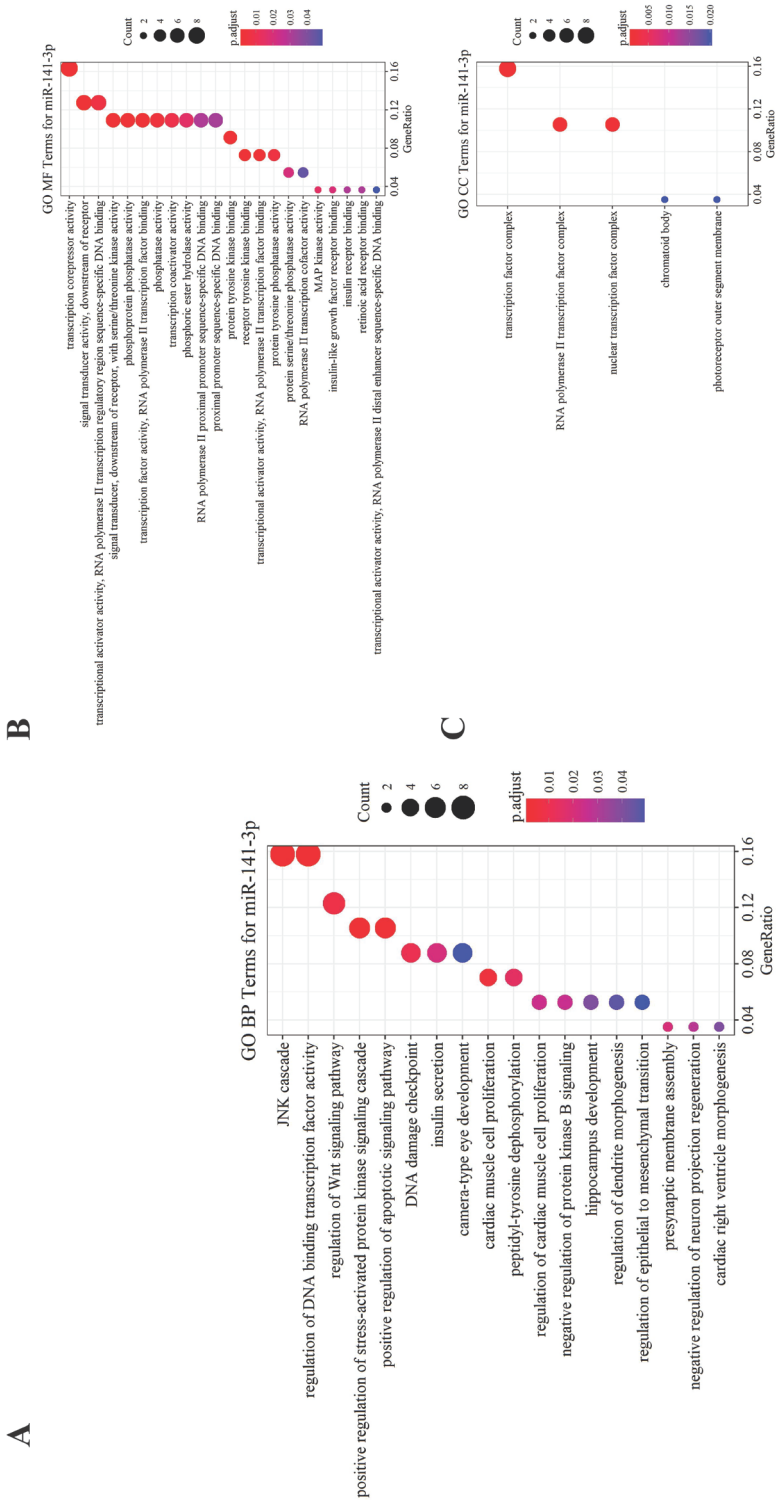

Figure S4. 4. Over-represented GO terms in the list of target genes controlled by miR-141-3p compared to the entire genome. *(A) Dot plot for GO BP terms. This dot plot shows only 18 of the 103 significantly over-represented GO BP terms. These were the left terms after two subsequent steps of filtering: (i) selection of level 9 BP terms and (ii) removal of terms that were similar for at least the 70% (only the term with the lowest Benjamini-Hochberg adjusted p-value in each group of redundant ones was kept). (B) Dot plot for GO Molecular Function terms. (C) Dot plot for GO Cellular Component terms. For in-depth description of the plot see Figure S4.1 legend. GO: Gene Ontology; BP: Biological Process; MF: Molecular Function; CC: Cellular Component.*

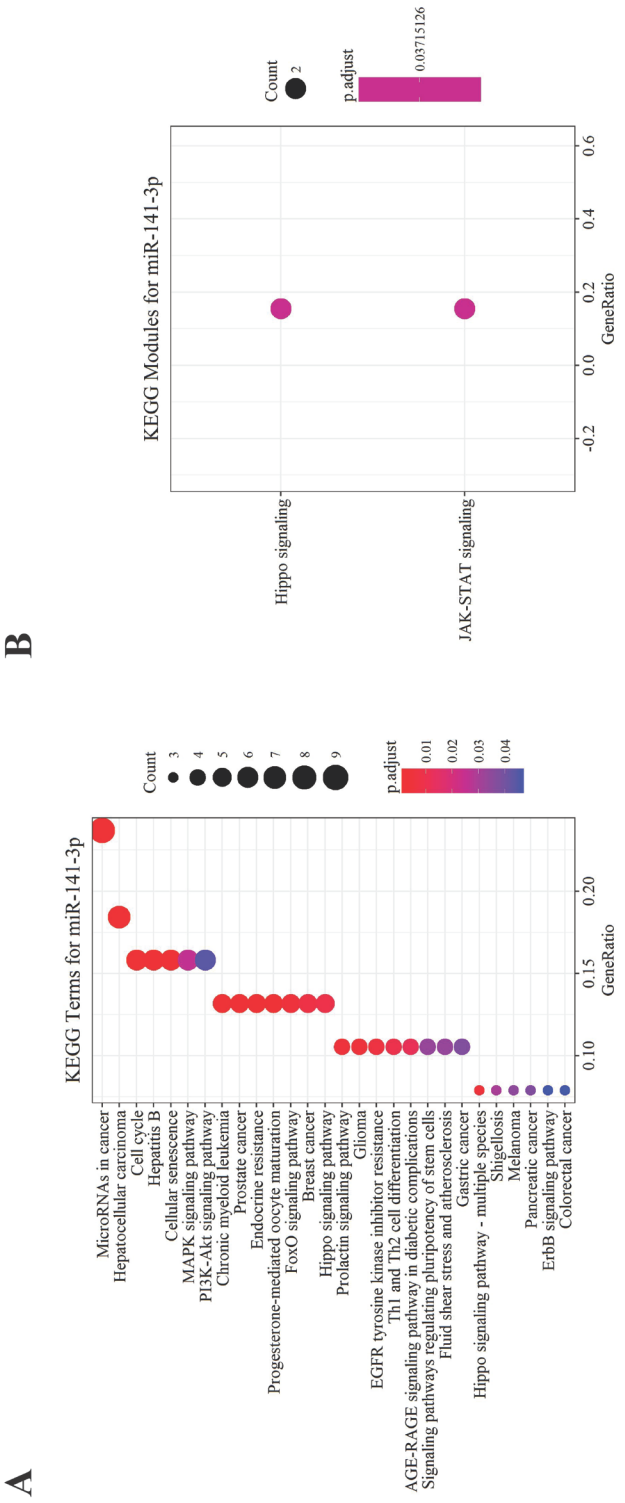

Figure S4. 5. Over-represented KEGG Pathway terms and Module terms in the list of target genes controlled by miR-141-3p compared to the entire genome. *(A) Dot plot for KEGG Pathway terms. (B) Dot plot for KEGG Module terms. For in-depth description of the plots see Figure S4.1 legend. KEGG: Kyoto Encyclopedia of Genes and Genomes.*

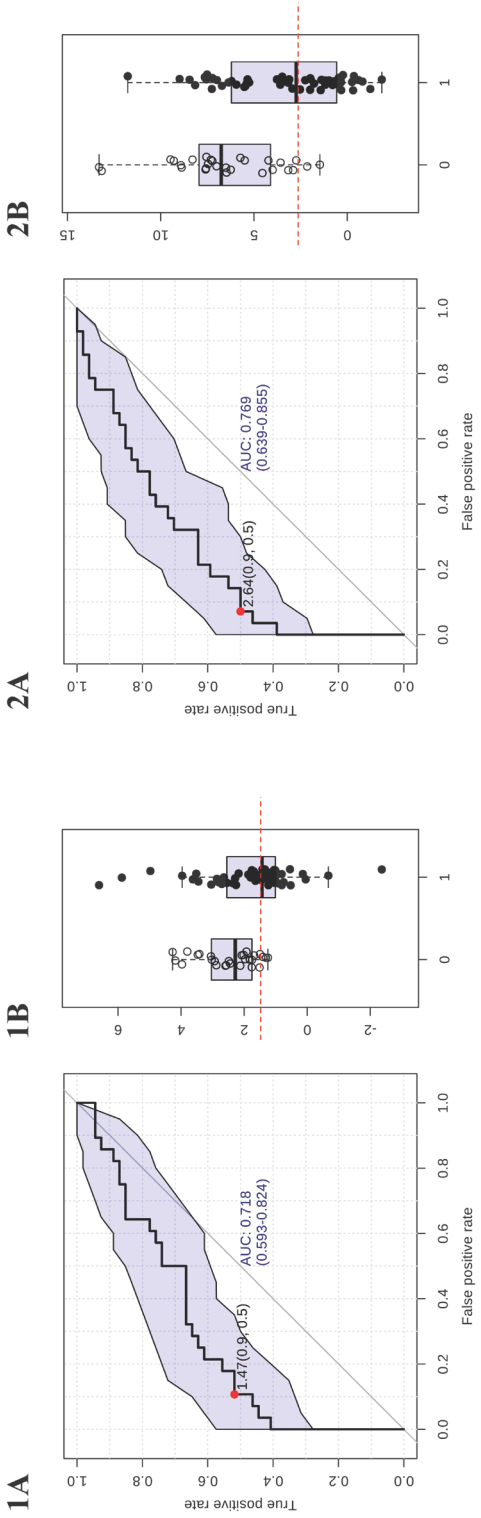

Figure S4. 6. Classical univariate ROC curve analyses for saliva miR-29a-3p and miR-141-3p. *(1) The graphs refer to miR-29a-3p. (2) The graphs refer to miR-141-3p. (A) Classical univariate ROC curve analysis. The red dot represents the sensitivity/specificity pair with the highest Youden index J. (B) Boxplot depicting the distribution of ΔCt values in the two groups. The red line represents the ΔCt value cut-off corresponding to the red dot on the curve in (A). The label 1 refers to the ASD group, 0 to the NC group.*

4.8. References

Antoniou A, Khudayberdiev S, Idziak A, Bicker S, Jacob R, Schratt G. The dynamic recruitment of TRBP to neuronal membranes mediates dendritogenesis during development. EMBO Rep. 2018;19(3). pii: e44853. doi: 10.15252/embr.201744853.

Arab A, Karimipoor M, Irani S, Kiani A, Zeinali S, Tafsiri E, Sheikhy K. Potential circulating miRNA signature for early detection of NSCLC. Cancer Genet. 2017;216-217:150-158. doi: 10.1016/j.cancergen.2017.07.006.

Aro K, Wei F, Wong DT, Tu M. Saliva Liquid Biopsy for Point-of-Care Applications. Front Public Health. 2017;5:77. doi: 10.3389/fpubh.2017.00077.

Assmann TS, Recamonde-Mendoza M, de Souza BM, Bauer AC, Crispim D. MicroRNAs and diabetic kidney disease: Systematic review and bioinformatic analysis. Mol Cell Endocrinol. 2018. pii: S0303-7207(18)30191-6. doi: 10.1016/j.mce.2018.06.005.

Ayaz L, Dinç E. Evaluation of microRNA responses in ARPE-19 cells against the oxidative stress. Cutan Ocul Toxicol. 2018;37(2):121-126. doi: 10.1080/15569527.2017.1355314.

Bitsika V, Sharpley CF, Agnew LL, Andronicos NM. Age-related differences in the association between stereotypic behavior and salivary cortisol in young males with an Autism Spectrum Disorder. Physiol Behav. 2015;152(Pt A):238-43. doi: 10.1016/j.physbeh.2015.10.010.

Casanova EL, Sharp JL, Edelson SM, Kelly DP, Casanova MF. A Cohort Study Comparing Women with Autism Spectrum Disorder with and without Generalized Joint Hypermobility. Behav Sci (Basel). 2018;8(3). pii: E35. doi: 10.3390/bs8030035.

Catanzaro G, Sabato C, Russo M, Rosa A, Abballe L, Besharat ZM, Po A, Miele E, Bellavia D, Chiacchiarini M, Gessi M, Peruzzi G, Napolitano M, Antonelli M, Mastronuzzi A, Giangaspero F, Locatelli F, Screpanti I, Vacca A, Ferretti E. Loss of miR-107, miR-181c and miR-29a-3p Promote Activation of Notch2 Signaling in Pediatric High-Grade Gliomas (pHGGs). Int J Mol Sci. 2017;18(12). pii: E2742. doi: 10.3390/ijms18122742.

Cederlöf M, Larsson H, Lichtenstein P, Almqvist C, Serlachius E, Ludvigsson JF. Nationwide population-based cohort study of psychiatric disorders in individuals with Ehlers-Danlos syndrome or hypermobility syndrome and their siblings. BMC Psychiatry. 2016;16:207. doi: 10.1186/s12888-016-0922-6.

Chaudhuri AD, Dastgheyb RM, Yoo SW, Trout A, Talbot CC Jr, Hao H, Witwer KW, Haughey NJ. TNFα and IL-1β modify the miRNA cargo of astrocyte shed extracellular vesicles to regulate neurotrophic signaling in neurons. Cell Death Dis. 2018;9(3):363. doi: 10.1038/s41419-018-0369-4.

Che H, Sun LH, Guo F, Niu HF, Su XL, Bao YN, Fu ZD, Liu HL, Hou X, Yang BF, Ai J. Expression of amyloid-associated miRNAs in both the forebrain cortex and hippocampus of middle-aged rat. Cell Physiol Biochem. 2014;33(1):11-22. doi: 10.1159/000356646.

Chen Y, Chen S, Zhang J, Wang Y, Jia Z, Zhang X, Han X, Guo X, Sun X, Shao C, Wang J, Lan T. Expression profile of microRNAs in expressed prostatic secretion of healthy men and patients with IIIA chronic prostatitis/chronic pelvic pain syndrome. Oncotarget. 2018;9(15):12186-12200. doi: 10.18632/oncotarget.24069.

Cheng YS, Rees T, Jordan L, Oxford L, O'Brien J, Chen HS, Wong D. Salivary endothelin-1 potential for detecting oral cancer in patients with oral lichen planus or oral cancer in remission. Oral Oncol. 2011;47(12):1122-6. doi: 10.1016/j.oraloncology.2011.07.032.

Chim SS, Shing TK, Hung EC, Leung TY, Lau TK, Chiu RW, Lo YM. Detection and characterization of placental microRNAs in maternal plasma. Clin Chem. 2008;54(3):482-90. doi: 10.1373/clinchem.2007.097972.

Chou CH, Chang NW, Shrestha S, Hsu SD, Lin YL, Lee WH, Yang CD, Hong HC, Wei TY, Tu SJ, Tsai TR, Ho SY, Jian TY, Wu HY, Chen PR, Lin NC, Huang HT, Yang TL, Pai CY, Tai CS, Chen WL, Huang CY, Liu CC, Weng SL, Liao KW, Hsu WL, Huang HD. miRTarBase 2016: updates to the experimentally validated miRNA-target interactions database. Nucleic Acids Res. 2016;44(D1):D239-47. doi: 10.1093/nar/gkv1258.

Cirnigliaro M, Barbagallo C, Gulisano M, Domini CN, Barone R, Barbagallo D, Ragusa M, Di Pietro C, Rizzo R, Purrello M. Expression and Regulatory Network Analysis of miR-140-3p, a New Potential Serum Biomarker for Autism Spectrum Disorder. Front Mol Neurosci. 2017;10:250. doi:10.3389/fnmol.2017.00250.

Cui Y, Liu Y, Wang D, Liu Y, Liu L, Fang B. Comparative Analysis of miRNA Expression Profiles of Multiple Myeloma with 1q21 Gains and Normal FISH. Acta Haematol. 2018;139(2):96-100. doi: 10.1159/000486662.

Cui Z, An X, Li J, Liu Q, Liu W. LncRNA MIR22HG negatively regulates miR-141-3p to enhance DAPK1 expression and inhibits endometrial carcinoma cells proliferation. Biomed Pharmacother. 2018;104:223-228. doi: 10.1016/j.biopha.2018.05.046.

Dantham S, Srivastava AK, Gulati S, Rajeswari MR. Differentially Regulated Cell-Free MicroRNAs in the Plasma of Friedreich's Ataxia Patients and Their Association with Disease Pathology. Neuropediatrics. 2018;49(1):35-43. doi: 10.1055/s-0037-1607279.

Dong H, Wang C, Lu S, Yu C, Huang L, Feng W, Xu H, Chen X, Zen K, Yan Q, Liu W, Zhang C, Zhang CY. A panel of four decreased serum microRNAs as a novel biomarker for early Parkinson's disease. Biomarkers. 2016;21(2):129-37. doi: 10.3109/1354750X.2015.1118544.

Farah R, Haraty H, Salame Z, Fares Y, Ojcius DM, Said Sadier N. Salivary biomarkers for the diagnosis and monitoring of neurological diseases. Biomed J. 2018;41(2):63-87. doi: 10.1016/j.bj.2018.03.004.

Ferreira JN, Hoffman MP. Interactions between developing nerves and salivary glands. Organogenesis. 2013;9(3):199-205. doi: 10.4161/org.25224.

Fricano-Kugler CJ, Getz SA, Williams MR, Zurawel AA, DeSpenza T Jr, Frazel PW, Li M, O'Malley AJ, Moen EL, Luikart BW. Nuclear Excluded Autism-Associated Phosphatase and Tensin Homolog Mutations Dysregulate Neuronal Growth. Biol Psychiatry. 2017. pii: S0006-3223(17)32243-6. doi: 10.1016/j.biopsych.2017.11.025.

Gabriels RL, Agnew JA, Pan Z, Holt KD, Reynolds A, Laudenslager ML. Elevated repetitive behaviors are associated with lower diurnal salivary cortisol levels in autism spectrum disorder. Biol Psychol. 2013;93(2):262-8. doi: 10.1016/j.biopsycho.2013.02.017.

Galiana-Simal A, Muñoz-Martinez V, Calero-Bueno P, Vela-Romero M, Beato-Fernandez L. Towards a future molecular diagnosis of autism: Recent advances in biomarkers research from saliva samples. Int J Dev Neurosci. 2018;67:1-5. doi: 10.1016/j.ijdevneu.2018.03.004.

Gordon I, Vander Wyk BC, Bennett RH, Cordeaux C, Lucas MV, Eilbott JA, Zagoory-Sharon O, Leckman JF, Feldman R, Pelphrey KA. Oxytocin enhances brain function in children with autism. Proc Natl Acad Sci U S A. 2013;110(52):20953-8. doi: 10.1073/pnas.1312857110.

Halvorsen AR, Kristensen G, Embleton A, Adusei C, Barretina-Ginesta MP, Beale P, Helland Å. Evaluation of Prognostic and Predictive Significance of Circulating MicroRNAs in Ovarian Cancer Patients. Dis Markers. 2017;2017:3098542. doi: 10.1155/2017/3098542.

Hansen-Kiss E, Beinkampen S, Adler B, Frazier T4, Prior T, Erdman S, Eng C, Herman G. A retrospective chart review of the features of PTEN hamartoma tumour syndrome in children. J Med Genet. 2017;54(7):471-478. doi: 10.1136/jmedgenet-2016-104484.

He H, Wang N, Yi X, Tang C, Wang D. Long non-coding RNA H19 regulates E2F1 expression by competitively sponging endogenous miR-29a-3p in clear cell renal cell carcinoma. Cell Biosci. 2017;7:65. doi: 10.1186/s13578-017-0193-z.

Hicks SD, Ignacio C, Gentile K, Middleton FA. Salivary miRNA profiles identify children with autism spectrum disorder, correlate with adaptive behavior, and implicate ASD candidate genes involved in neurodevelopment. BMC Pediatr. 2016;16:52. doi: 10.1186/s12887-016-0586-x.

Huang S, Wa Q, Pan J, Peng X, Ren D, Huang Y, Chen X, Tang Y. Downregulation of miR-141-3p promotes bone metastasis via activating NF-κB signaling in prostate cancer. J Exp Clin Cancer Res. 2017;36(1):173. doi: 10.1186/s13046-017-0645-7.

Ishibashi O, Akagi I, Ogawa Y, Inui T. MiR-141-3p is upregulated in esophageal squamous cell carcinoma and targets pleckstrin homology domain leucine-rich repeat protein phosphatase-2, a negative regulator of the PI3K/AKT pathway. Biochem Biophys Res Commun. 2018;501(2):507-513. doi: 10.1016/j.bbrc.2018.05.025.

James SJ, Cutler P, Melnyk S, Jernigan S, Janak L, Gaylor DW, Neubrander JA. Metabolic biomarkers of increased oxidative stress and impaired methylation capacity in children with autism. Am J Clin Nutr. 2004;80(6):1611-7.

Ju L, Han M, Li X, Zhao C. MicroRNA Signature of Lung Adenocarcinoma with EGFR Exon 19 Deletion. J Cancer. 2017;8(7):1311-1318. doi: 10.7150/jca.17817.

Knafo S, Esteban J. PTEN: Local and Global Modulation of Neuronal Function in Health and Disease. Trends Neurosci. 2017;40(2):83-91. doi: 10.1016/j.tins.2016.11.008.

Larrea E, Sole C, Manterola L, Goicoechea I, Armesto M, Arestin M, Caffarel MM, Araujo AM, Araiz M, Fernandez-Mercado M, Lawrie CH. New Concepts in Cancer Biomarkers: Circulating miRNAs in Liquid Biopsies. Int J Mol Sci. 2016;17(5). doi: 10.3390/ijms17050627.

Li C, Shen K, Chu L, Liu P, Song Y, Kang X. Decreased levels of urinary free amino acids in children with autism spectrum disorder. J Clin Neurosci. 2018. pii: S0967-5868(17)30468-X. doi: 10.1016/j.jocn.2018.05.001.

Li XY, Wang SS, Han Z, Han F, Chang YP, Yang Y, Xue M, Sun B, Chen LM. Triptolide Restores Autophagy to Alleviate Diabetic Renal Fibrosis through the miR-141-3p/PTEN/Akt/mTOR Pathway. Mol Ther Nucleic Acids. 2017;9:48-56. doi: 10.1016/j.omtn.2017.08.011.

Li Y, Wang K, Wei Y, Yao Q, Zhang Q, Qu H, Zhu G. lncRNA-MIAT regulates cell biological behaviors in gastric cancer through a mechanism involving the miR-29a-3p/HDAC4 axis. Oncol Rep. 2017;38(6):3465-3472. doi: 10.3892/or.2017.6020.

Lian J, Lin SH, Ye Y, Chang DW, Huang M, Dinney CP, Wu X. Serum microRNAs as predictors of risk for non-muscle invasive bladder cancer. Oncotarget. 2018 Feb 12;9(19):14895-14908. doi:10.18632/oncotarget.24473.

Lindell SG, Suomi SJ, Shoaf S, Linnoila M, Higley JD. Salivary prolactin as a marker for central serotonin turnover. Biol Psychiatry. 1999;46(4):568-72.

Lydon S, Healy O, Reed P, Mulhern T, Hughes BM, Goodwin MS. A systematic review of physiological reactivity to stimuli in autism. Dev Neurorehabil. 2016;19(6):335-355. Epub 2014 Oct 30.

McKeever PM, Schneider R, Taghdiri F, Weichert A, Multani N, Brown RA, Boxer AL, Karydas A, Miller B, Robertson J, Tartaglia MC. MicroRNA Expression Levels Are Altered in the Cerebrospinal Fluid of Patients with Young-Onset Alzheimer's Disease. Mol Neurobiol. 2018. doi: 10.1007/s12035-018-1032-x.

Moloney GM, Viola MF, Hoban AE, Dinan TG, Cryan JF. Faecal microRNAs: indicators of imbalance at the host-microbe interface? Benef Microbes. 2018;9(2):175-183. doi: 10.3920/BM2017.0013.

Momen-Heravi F, Trachtenberg AJ, Kuo WP, Cheng YS. Genomewide study of salivary microRNAs for detection of oral cancer. J Dent Res. 2014;93(7 Suppl):86S-93S. doi: 10.1177/0022034514531018.

Mundalil Vasu M, Anitha A, Thanseem I, Suzuki K, Yamada K, Takahashi T, Wakuda T, Iwata K, Tsujii M, Sugiyama T, Mori N. Serum microRNA profiles in children with autism. Mol Autism. 2014;5:40. doi: 10.1186/2040-2392-5-40.

Ngounou Wetie AG, Wormwood KL, Russell S, Ryan JP, Darie CC, Woods AG. A Pilot Proteomic Analysis of Salivary Biomarkers in Autism Spectrum Disorder. Autism Res. 2015;8(3):338-50. doi: 10.1002/aur.1450.

Nolan K, Mitchem MR, Jimenez-Mateos EM, Henshall DC, Concannon CG, Prehn JH. Increased expression of microRNA-29a in ALS mice: functional analysis of its inhibition. J Mol Neurosci. 2014;53(2):231-41. doi: 10.1007/s12031-014-0290-y.

Panahi Y, Salasar Moghaddam F, Ghasemi Z, Hadi Jafari M, Shervin Badv R, Eskandari MR, Pedram M. Selection of Suitable Reference Genes for Analysis of Salivary Transcriptome in Non-Syndromic Autistic Male Children. Int J Mol Sci. 2016 Oct;17(10). pii: E1711.

Papadopoulou AS, Serneels L, Achsel T, Mandemakers W, Callaerts-Vegh Z, Dooley J, Lau P, Ayoubi T, Radaelli E, Spinazzi M, Neumann M, Hébert SS, Silahtaroglu A, Liston A, D'Hooge R, Glatzel M, De Strooper B. Deficiency of the miR-29a/b-1 cluster leads to ataxic features and cerebellar alterations in mice. Neurobiol Dis. 2015;73:275-88. doi: 10.1016/j.nbd.2014.10.006.

Patel RS, Jakymiw A, Yao B, Pauley BA, Carcamo WC, Katz J, Cheng JQ, Chan EK. High resolution of microRNA signatures in human whole saliva. Arch Oral Biol. 2011;56(12):1506-13. doi: 10.1016/j.archoralbio.2011.05.015.

Prajzlerová K, Grobelná K, Hušáková M, Forejtová Š, Jüngel A, Gay S, Vencovský J, Pavelka K, Šenolt L, Filková M. Association between circulating miRNAs and spinal involvement in patients with axial spondyloarthritis. PLoS One. 2017;12(9):e0185323. doi: 10.1371/journal.pone.0185323.

Puig-Alcaraz C, Fuentes-Albero M, Calderón J, Garrote D, Cauli O. Increased homocysteine levels correlate with the communication deficit in children with autism spectrum disorder. Psychiatry Res. 2015;229(3):1031-7. doi: 10.1016/j.psychres.2015.05.021.

Putnam SK, Lopata C, Fox JD, Thomeer ML, Rodgers JD, Volker MA, Lee GK, Neilans EG, Werth J. Comparison of saliva collection methods in children with high-functioning autism spectrum disorders: acceptability and recovery of cortisol. Child Psychiatry Hum Dev. 2012;43(4):560-73. doi: 10.1007/s10578-012-0284-3.

Qiao Y, Wu M, Feng Y, Zhou Z, Chen L, Chen F. Alterations of oral microbiota distinguish children with autism spectrum disorders from healthy controls. Sci Rep. 2018;8(1):1597. doi: 10.1038/s41598-018-19982-y.

R Core Team (2016). R: A Language and Environment for Statistical Computing. Vienna: R Foundation for Statistical Computing.

Roshan R, Shridhar S, Sarangdhar MA, Banik A, Chawla M, Garg M, Singh VP, Pillai B. Brain-specific knockdown of miR-29 results in neuronal cell death and ataxia in mice. RNA. 2014;20(8):1287-97. doi: 10.1261/rna.044008.113.

Schmittgen TD, Livak KJ. Analyzing real-time PCR data by the comparative C(T) method. Nat Protoc. 2008;3(6):1101-8. doi: 10.1038/nprot.2008.73.

Shi Z, Zhou H, Lu L, Pan B, Wei Z, Liu J, Li J, Yuan S, Kang Y, Liu L, Yao X, Kong X, Feng S. MicroRNA-29a regulates neural stem cell neuronal differentiation by targeting PTEN. J Cell Biochem. 2018;119(7):5813-5820. doi: 10.1002/jcb.26768.

Snowhite IV, Allende G, Sosenko J, Pastori RL, Messinger Cayetano S, Pugliese A. Association of serum microRNAs with islet autoimmunity, disease progression and metabolic impairment in relatives at risk of type 1 diabetes. Diabetologia. 2017;60(8):1409-1422. doi: 10.1007/s00125-017-4294-3.

Spratt EG, Nicholas JS, Brady KT, Carpenter LA, Hatcher CR, Meekins KA, Furlanetto RW, Charles JM. Enhanced cortisol response to stress in children in autism. J Autism Dev Disord. 2012;42(1):75-81. doi: 10.1007/s10803-011-1214-0.

Svetoni F, De Paola E, La Rosa P, Mercatelli N, Caporossi D, Sette C, Paronetto MP. Post-transcriptional regulation of FUS and EWS protein expression by miR-141 during neural differentiation. Hum Mol Genet. 2017;26(14):2732-2746. doi: 10.1093/hmg/ddx160.

Tan Y, Pan T, Ye Y, Ge G, Chen L, Wen D, Zou S. Serum microRNAs as potential biomarkers of primary biliary cirrhosis. PLoS One. 2014;9(10):e111424. doi: 10.1371/journal.pone.0111424.

Tian Y, Voineagu I, Paşca SP, Won H, Chandran V, Horvath S, Dolmetsch RE, Geschwind DH. Alteration in basal and depolarization induced transcriptional network in iPSC derived neurons from Timothy syndrome. Genome Med. 2014;6(10):75. doi: 10.1186/s13073-014-0075-5.

Tokić S, Štefanić M, Glavaš-Obrovac L, Kishore A, Navratilova Z, Petrek M. miR-29a-3p/T-bet Regulatory Circuit Is Altered in T Cells of Patients With Hashimoto's Thyroiditis. Front Endocrinol (Lausanne). 2018;9:264. doi: 10.3389/fendo.2018.00264.

Tolosa E, Botta-Orfila T, Morató X, Calatayud C, Ferrer-Lorente R, Martí MJ, Fernández M, Gaig C, Raya Á, Consiglio A, Ezquerra M, Fernández-Santiago R. MicroRNA alterations in iPSC-derived dopaminergic neurons from Parkinson disease patients. Neurobiol Aging. 2018;69:283-291. doi: 10.1016/j.neurobiolaging.2018.05.032.

Tomarken AJ, Han GT, Corbett BA. Temporal patterns, heterogeneity, and stability of diurnal cortisol rhythms in children with autism spectrum disorder. Psychoneuroendocrinology. 2015;62:217-26. doi: 10.1016/j.psyneuen.2015.08.016.

Verma R, Ritzel RM, Harris NM, Lee J, Kim T, Pandi G, Vemuganti R, McCullough LD. Inhibition of miR-141-3p Ameliorates the Negative Effects of Poststroke Social Isolation in Aged Mice. Stroke. 2018;49(7):1701-1707. doi: 10.1161/STROKEAHA.118.020627.

Walker SE, Lorsch J. RNA purification--precipitation methods. Methods Enzymol. 2013;530:337-43. doi: 10.1016/B978-0-12-420037-1.00019-1.

Wang N, Li P, Liu W, Wang N, Lu Z, Feng J, Zeng X, Yang J, Wang Y, Zhao W. miR-141-3p suppresses proliferation and promotes apoptosis by targeting GLI2 in osteosarcoma cells. Oncol Rep. 2018;39(2):747-754. doi: 10.3892/or.2017.6150.

Wang X, Liu S, Cao L, Zhang T, Yue D, Wang L, Ping Y, He Q, Zhang C, Wang M, Chen X, Gao Q, Wang D, Zhang Z, Wang F, Yang L, Li J, Huang L, Zhang B, Zhang Y. miR-29a-3p suppresses cell proliferation and migration by downregulating IGF1R in hepatocellular carcinoma. Oncotarget. 2017;8(49):86592-86603. doi: 10.18632/oncotarget.21246.

Wang YN, Chen ZH, Chen WC. Novel circulating microRNAs expression profile in colon cancer: a pilot study. Eur J Med Res. 2017;22(1):51. doi: 10.1186/s40001-017-0294-5.

Weiland M, Gao XH, Zhou L, Mi QS. Small RNAs have a large impact: circulating microRNAs as biomarkers for human diseases. RNA Biol. 2012;9(6):850-9. doi: 10.4161/rna.20378.

Widlansky ME, Jensen DM, Wang J, Liu Y, Geurts AM, Kriegel AJ, Liu P, Ying R, Zhang G, Casati M, Chu C, Malik M, Branum A, Tanner MJ, Tyagi S, Usa K, Liang M. miR-29 contributes to normal endothelial function and can restore it in cardiometabolic disorders. EMBO Mol Med. 2018. pii: e8046. doi: 10.15252/emmm.201708046.

Witwer KW. Circulating microRNA biomarker studies: pitfalls and potential solutions. Clin Chem. 2015;61(1):56-63. doi: 10.1373/clinchem.2014.221341.

Wong CW, Or PMY, Wang Y, Li L, Li J, Yan M, Cao Y, Luk HM, Tong TMF, Leslie NR, Lo IF, Choy KW, Chan AML. Identification of a PTEN mutation with reduced protein stability, phosphatase activity, and nuclear localization in Hong Kong patients with autistic features, neurodevelopmental delays, and macrocephaly. Autism Res. 2018. doi: 10.1002/aur.1950.

Wormwood KL, Aslebagh R, Channaveerappa D, Dupree EJ, Borland MM, Ryan JP, Darie CC, Woods AG. Salivary proteomics and biomarkers in neurology and psychiatry. Proteomics Clin Appl. 2015;9(9-10):899-906. doi: 10.1002/prca.201400153.

Xia J, Wishart DS. Using metaboanalyst 3.0 for comprehensive metabolomics data analysis. Curr Protoc Bioinformatics. 2016;55:14.10.1-14.10.91. doi: 10.1002/cpbi.11.

Yang L, Engeland CG, Cheng B. Social isolation impairs oral palatal wound healing in sprague-dawley rats: a role for miR-29 and miR-203 via VEGF suppression. PLoS One. 2013;8(8):e72359. doi: 10.1371/journal.pone.0072359.

Yeung KS, Tso WWY, Ip JJK, Mak CCY, Leung GKC, Tsang MHY, Ying D, Pei SLC, Lee SL, Yang W, Chung BH. Identification of mutations in the PI3K-AKT-mTOR signalling pathway in patients with macrocephaly and developmental delay and/or autism. Mol Autism. 2017;8:66. doi: 10.1186/s13229-017-0182-4.

Yu G, Wang LG, Han Y, He QY. clusterProfiler: an R package for comparing biological themes among gene clusters. OMICS. 2012;16(5):284-7. doi: 10.1089/omi.2011.0118.

Zhang L, Qi M, Feng T, Hu J, Wang L, Li X, Gao W, Liu H, Jiao M, Wu Z, Bai X, Bie Y, Liu L, Han B. IDH1R132H Promotes Malignant Transformation of Benign Prostatic Epithelium by Dysregulating MicroRNAs: Involvement of IGF1R-AKT/STAT3 Signaling Pathway. Neoplasia. 2018;20(2):207-217. doi: 10.1016/j.neo.2017.12.001.

Zhang MN, Tang QY, Li RM, Song MG. MicroRNA-141-3p/200a-3p target and may be involved in post-transcriptional repression of RNA decapping enzyme Dcp2 during renal development. Biosci Biotechnol Biochem. 2018:1-9. doi: 10.1080/09168451.2018.1486176.

Zheng L, Xu M, Xu J, Wu K, Fang Q, Liang Y, Zhou S, Cen D, Ji L, Han W, Cai X. ELF3 promotes epithelial-mesenchymal transition by protecting ZEB1 from miR-141-3p-mediated silencing in hepatocellular carcinoma. Cell Death Dis. 2018;9(3):387. doi: 10.1038/s41419-018-0399-y.

Ziats MN, Rennert OM. Identification of differentially expressed microRNAs across the developing human brain. Mol Psychiatry. 2014;19(7):848-52. doi: 10.1038/mp.2013.93.

Chapter 5. General discussion and conclusions

My PhD research project includes two studies, profiling circulating miRNAs in serum and saliva from ASD patients, respectively. To date, these two series of experiments specifically represent the third and fourth high-throughput studies profiling miRNAs in a body fluid from ASD patients.

We hypothesized that the expression analysis of circulating miRNAs in serum and saliva could represent an easy and innovative approach to address important biomedical needs related to ASD, such as the lack of diagnostic molecular biomarkers and the incompleteness of ASD etiology understanding. Indeed, we also exploited this liquid biopsy-based investigation approach to propose to the scientific community new potentially intriguing pathological mechanisms and corresponding molecules with a crucial role in them. This could represent a particularly valuable option when investigating neurodevelopmental disorders, like ASD, for which preferable tissue biopsies are not easily accessible to researchers.

Ideal ASD biomarkers should be (i) differentially observed in ASD patients compared to healthy controls, (ii) detectable in the ASD population at every stage of life, and preferably at the earliest one possible, (iii) specific and helpful in ASD discrimination from other (even comorbid) neurodevelopmental disorders, and (iv) correlated with commonly used ASD screening tools. Intriguingly, this project led to the identification of serum miR-140-3p and supernatant saliva miR-29a-3p and miR-141-3p as potential non-invasive supportive means for ASD differential diagnosis (Chapter 3) and recognition of ASD defects in social interaction and verbal communication (Chapter 4), respectively.

Our experimental use of two different miRNA profiling technologies, both an amplification-based method and a hybridization-based one, confirmed the importance of validating data from high-throughput approaches with more specific assays in a larger set of samples. In both studies, we verified only few profiling candidate miRNAs (1 out of 4 in Chapter 3 and 2 out of 5 in Chapter 4) as dysregulated in the validation set of samples: also, either extent or sign of differential expression often differed (see miR-29a-3p as an illustrative case). The need for further validation becomes even stronger when proposing the relative quantification of these molecules as a discriminative molecular test: their true predictive performance as biomarkers has to be established on wider and younger cohorts of patients.

Profiling a large number of genes gives the opportunity to screen the specific analyzed samples for more suitable and accurate endogenous controls and represents a good normalization strategy when others are missing in the literature. At the moment, accurately described normalization approaches and validated reference genes for serum and supernatant saliva miRNAs in ASD patients lack. We selected miR-146a

(Chapter 3) and miR-21-5p (Chapter 4) as the most appropriate and accurate reference genes for our two extracellular systems. Both of these miRNAs have been identified as either dysregulated in human ASD tissues or associated to inflammation and immune response observed in neurodegenerative and neurological disorders: however, this neither discourages their use as reference miRNAs in our datasets nor affects the applicability of our results. Nevertheless, in our saliva study we did not confirm miR-146-5p as upregulated in ASD (the expression trend that we found in the profiling data analysis), further proving its appropriate use as endogenous control in the serum one. Moreover, this project actually offers good normalization references to future similar studies.

In our saliva study we observed that, when used in combination, miR-29a-3p and miR-141-3p perform at a better level than when used individually in the discrimination of ASD patients. However, their combined predictive performance showed to be very similar to the one of miR-140-3p alone observed for the comparison ASD vs NC in our serum study: this suggests that a combination of biomarkers is not always to be preferred to a single one. The main limits for the applicability of this project results are the diagnostic specificity and the reproducibility issues related to the use of circulating miRNAs as biomarkers. All of the dysregulated circulating miRNAs proposed as potential biomarkers in this project have already been associated with other pathologies and suggested as disease markers in other contexts, mainly cancer and (neuro)degenerative, inflammatory, and metabolic diseases. One explanation for these observations could be that these miRNAs are simply indicative of a general disease state (i.e., inflammation and response to stress). Interestingly, the non-specific spectrum of associated diseases for each miRNA mostly overlaps with that of the other two dysregulated ones: it could be possible that they are all similarly involved in neuronal and inflammatory pathways and processes in common between the associated pathologies, some of which are also known to be altered in ASD. Finally, it is worth mentioning once again the already identified association of blood miR-140-3p to both bipolar disorder and major depression. Although (i) there is little reproducibility between current studies on biological fluids from ASD patients and results from this project and (ii) we could not even identify promising overlapping patterns and mechanisms of miRNA secretion between serum and saliva, still functional analysis results from all of these independent investigations match and are consistent with the first proposed molecular neuropathological basis for ASD, relying on neuronal down-modulation and immune-glial up-modulation (Chapter 1).

This once again confirms the value of our computational analyses used to reconstruct the potential intracellular context of dysregulated circulating miRNAs as an approach to gain further insight into the molecular basis of neurodevelopmental disorders like ASD. In fact, overall, our computational analysis findings confirmed the validity, appropriateness, and applicability of this alternative research use of liquid biopsies, since we were able to identify, at the same time, already known (i.e., synaptic plasticity and function, immune response, CD38, and PTEN) and completely new (i.e., regulation of circadian

rhythms by NRIP1 and RORA) processes and molecules with a (possible) role in ASD. Importantly, miR-140-3p, miR-29a-3p, and miR-141-3p and their targets are all crucially involved in inflammation, synaptic function and plasticity, neuronal differentiation and morphogenesis, and nervous system development. Finally, miR-140-3p and miR-29a-3p are highly expressed in the brain, where they are crucial for cortical development: this suggests for them a potential central role in neurodevelopmental disorders that is worth further investigating.